A STUDY OF AN OPTIMUM PARABOLIC TROUGH CONCENTRATOR DESIGN FOR POSSIBLE POWER GENERATION IN MALAYSIA

by

BALBIR SINGH A/L MAHINDER SINGH

Thesis submitted in fulfilment of the requirements for the degree of Doctor of Philosophy

June 2004

ACKNOWLEDGEMENT

This research project was conducted over a number of years, where the involvement of certain individuals and organisations made it possible to be completed. First of all, I would like to express my greatest gratitude to Associate Professor Dr. Fauziah Sulaiman, who is my excellent academic supervisor and mentor. Her perceptive guidance, supervision, encouragement, constructive comments and suggestions certainly made it possible for this research to be completed. I have benefited in numerous ways from her close supervision and a short-term Universiti Sains Malaysia grant. Thanks a million.

I am indebted to my employer, Universiti Teknologi PETRONAS for providing me a generous scholarship for a period of one year, which was enough for this thesis to be completed and also for financing the Advanced MATLAB Programming Training. I would also like to extend my gratitude to all the staff of School of Physics and Institute of Postgraduate Studies, Universiti Sains Malaysia for their kind assistance and support that enabled the completion of this thesis.

I am also extremely grateful to my father Mr. Mahinder Singh, for his assistance and support during the experimental stage and not forgetting my mother, Pn. Harbans Kaur for her prayers and confidence in me. I thank my beloved wife, Pn. Jasbeer Kaur Dhillon for her support, understanding and patience. My sincerest thanks to our two lovely sons, Melvinder Singh and Neshvinder Singh for all the inspirations and challenges that helped me retain my sanity in the process of writing this thesis. Finally, I would also extend my gratitude to those not specifically mentioned here, especially my sister and brother and all the other family members.

BALBIR SINGH
JUNE 2004.

PAGE

PAGE

LIST OF TABLES

LIST OF FIGURES

NOMENCLATURE

A	Parabolic constant
A_c	Total area of the concentrator
A_{CS}	Cross-sectional area of parabola
A_e	Edge area
A_{eff}	Effective aperture area
A_{eff}	Effective area for the concentrator
A_i	Total surface area
A_R	Total area of the receiver
C_B	Bond conductance
C_G	Geometrical Concentration Ratio
C_G	Concentration ratio
C_o	Optical concentration ratio
C_p	Specific heat capacity of the fluid flowing in the tube
C_{trough}	Maximum concentration ratio of a parabolic trough
d	Depth of parabolic trough concentrator
D	Diameter
D_{ci}	Inner diameter of the receiver's cover
D_{co}	Outer diameter of the receiver's cover
D_{CTi}	Inner diameter of the back tubes
D_{CTi}	Concentrator's back tubes inner diamete
D_i	Receiver's inner diameter
D_o	Outer diameter of the receiver tube
D_R	Diameter of the receiver
F	Focus line
f	Friction factor
F_C	Concentrator's heat removal factor
F_{CE}	Concentrator's efficiency factor
F_i	Heat removal factor
F_R	Receiver's heat removal factor
F_{RE}	Receiver's efficiency factor
G_C	Dimensionless collector capacitance rate for the concentrator
G_R	Dimensionless collector capacitance rate for the receiver
H	Monthly average global radiation received by horizontal surface
h_{cc}	Convictive heat transfer coefficient inside the back tubes

h_{cc}	Convective heat transfer coefficients for fluid flowing in the back tubes
h_{CR}	Convective heat transfer coefficient inside the receiver
h_{cr}	Convective heat transfer coefficients for receiver's conduit tube
H_d	Ratio of diffuse radiation received by a horizontal surface
H_{FACTOR}	Temperature dependent factor to evaluate convictive heat transfer coefficient
h_{fg}	Enthalpy of evaporation at operating temperature
H_O	Monthly mean of the daily extraterrestrial solar radiation
h_w	Receiver's heat transfer coefficient
h_{wc}	Concentrator's wind heat transfer coefficient
I_{bT}	Beam radiations received on a tilted surface
I_{dT}	Diffuse radiations received on a tilted surface
I_{ET}	Extraterrestrial solar radiation
I_G	Hourly global radiation
I_{SC}	Solar constant
I_T	Global radiation on a tilted surface
J	Mass flow rate
J_C	Mass flow rate in the back tubes
J_R	Mass flow rate in the receiver
k	Thermal conductivity of the receiver tube
K_{AIR}	Temperature dependent factor to evaluate thermal conductivity of air
k_c	Thermal conductivity of the concentrator's absorbing plate
k_f	Working fluid's thermal conductivity
K_{FACTOR}	Temperature dependent factor to evaluate convictive heat transfer coefficient
k_i	Insulator's thermal conductivity
K_i	Polynomial coefficient to evaluate K_{AIR}
L	Length of concentrator or receiver
L_b	Back insulation thickness
L_{ct}	Concentrator thickness
L_{ct}	Thickness
L_e	Edge insulation thickness
m	Day number counted from 1st January
m_b	Mass flow rate from the back tubes
m_s	Steam's mass flow rate
m_s	Steam's mass flow rate

n	Number of resultant standard deviations
Nu	Nusselt number
Nu_W	Nusselt number to evaluate wind heat transfer coefficient
Output_Temp1	Outlet fluid temperature from back tubes correlated with solar insolation.
Output_Temp2	Outlet fluid temperature from receiver correlated with solar insolation.
Output_Temp3	Outlet fluid temperature without back tubes correlated with the inlet fluid temperature
Pr	Prandlt number
Q_{BC}	Rate of heat loss to the back
Q_c	Concentrator's energy balance equation
$Q_{conv, cover}$	Rate of convictive heat loss from the cover
$Q_{conv, fluid}$	Rate of convictive heat loss from the fluid
$Q_{conv, tube}$	Rate of convictive heat loss from the tube
Q_{EC}	Rate of heat loss to the edge
Q_g	Rate of useful energy gained
Q_i	Rate of useful energy leaving the absorber
Q_{LC}	Rate of total heat loss from the concentrator
Q_{loss}	Rate of thermal energy loss from the absorber
Q_{LR}	Total heat loss from the receiver
Q_R	Receiver's energy balance equation
$Q_{rad, cover}$	Rate of radiative heat loss from the cover
$Q_{rad, tube}$	Rate of radiative heat loss from the tube
Q_{TC}	Rate of heat loss to the top
Q_u	Power gained
r_a	Receiver's radius
R_{AIR}	Temperature dependent factor to evaluate Reynolds number
R_b	Ratio of beam radiation on a tilted surface to the radiation on a horizontal surface
R_b	Ratio factor of beam radiation on a tilted surface to the radiation on a horizontal surface
R_d	Ratio of diffuse radiation on a tilted surface to diffuse radiation on a horizontal surface
R_d	Ratio factor of diffuse radiation on a tilted surface to diffuse radiation on a horizontal surface
Re	Reynolds number
R_{FACTOR}	Temperature dependent factor to evaluate Reynolds number
R_i	Polynomial coefficient to evaluate R_{AIR}

R_r	Rim radius
R_S	Radius of the sun
R_{SE}	Distance of the sun from earth
S_A	Rate of absorbed solar radiation
S_{arc}	Arc length of parabolic concentrator
S_C	Amount of solar radiation absorbed by the concentrator
S_i	Absorbed solar radiation
Sp_vol	Specific volume
S_R	Absorbed solar radiation energy
t_1	Time in hours
t_2	Time in minutes
T_a	Ambient temperature
T_c	Cover temperature
T_{ci}	Fluid inlet temperature
T_{co}	Fluid outlet temperature from the back tubes
T_o	Outlet temperature
T_{pm}	Concentrator's absorber plate mean temperature
T_{rm}	Receiver's mean temperature
T_{RO}	Fluid outlet temperature from the receiver tubes
U_{BC}	Back loss coefficient
U_{EC}	Edge loss coefficient
U_{LC}	Overall heat loss coefficient for the concentrator
U_{LR}	Overall heat loss coefficient for the receiver
U_{TC}	Top loss coefficient
V	Mean flow velocity
V_m	Mean velocity
V_T	Volume of parabolic trough concentrator
V_t	Volume flowrate
W	Width of parabolic trough concentrator
W_s	Spacing of the back tubes
X	Horizontal displacement
Y	Vertical displacement

Greek

δ	Angle of declination
θ	Angle of incidence

ω	Hour angle
γ	Surface azimuth angle
β	Slope angle
ϕ	Latitude
ν	Kinematic viscosity
μ	Dynamic viscosity
σ	Stefan-Boltzmann's constant.
ρ	Density of the fluid flowing
σ_1	Error due to σ_{sensor}, σ_{drive}, σ_{slope}, σ_{rec}
σ_2	Error due to σ_{sun}, σ_{refl}, θ
θ_c	Acceptance half-angle
ε_c	Emitance of the cover
σ_{drive}	Motor error
η_E	Experimental efficiency
$\bar{H}$	Monthly mean of the daily global solar radiation
$\bar{H}_d$	Monthly mean of the daily diffuse radiation
$\bar{I}_b$	Hourly mean beam solar radiation
$\bar{I}_d$	Desired hourly mean diffuse solar radiation
$\bar{I}_G$	Measured hourly mean horizontal global radiation
$\bar{K}_T$	Monthly average clearness index
ε_p	Emitance of the receiver tube
ΔP	Pressure drop
ϕ_R	Rim angle
σ_R	Resultant standard deviation
σ_{rec}	Receiver's position error
σ_{refl}	Non-specular reflectance error
ω_s	Sunset hour angle
γ_s	Intercept factor
ε_s	Emissivity of the absorber plate
σ_{sensor}	Tracking mechanism's sensor
σ_{slope}	Reflective surface's slope error
σ_{sun}	Angular width error of the sun
η_T	Theoretical efficiency
θ_Z	Zenith angle

ABSTRACT

The aim of this research work is to design an optimum parabolic trough concentrator, where the optimum design parameters are identified by using simulation method. A new parabolic trough concentrator model was proposed. The new model, based on a standard model of a parabolic trough concentrator, has back copper tubes attached to the parabolic concentrator. The back copper tubes are expected to pick up the surplus heat on the iron concentrator due to incoming solar radiation that is not reflected. Simulations were carried out by using software programmed specifically for this research work and by using the outcomes from simulation, an experimental new model was fabricated based on optimum design parameters. The optimisers that were identified by simulations are the rim angle, concentration ratio, acceptance half-angle and receiver's absorber tube size. The optimum value for rim angle is 90° and concentration ratio is 10. The acceptance half-angles falls in the range between 1.55° and 1.72°, where the optimum diameter for the receiver's absorber tube range between 27 mm and 30 mm. A rim angle of 90° can be obtained when the parabolic depth becomes equal to the focus point. The receiver's absorber tube diameter size was 30 mm, where for the concentration ratio to be 10, the width was calculated as 1.0 m and depth and focus point was set at 0.25 m. The length of the concentrator at 1.83 m was determined by using the thermal module simulation and was also subjected to the budget availability. The simulation software was used to evaluate the performance of the new design with the optimum parameters by using the meteorological data for Bayan Lepas, Ipoh,

Cameron Highlands, Kuantan and Senai. The maximum instantaneous simulated outlet fluid temperature achieved is 133.8 °C for Ipoh. The maximum instantaneous experimental outlet temperature achieved on the 6th July 2003 by using the prototype model was (143.8 ± 0.5) °C, at an average direct and diffuse solar insolation of 2.57 MJ/m^2 and 0.81 MJ/m^2 respectively, with a mass flowrate of 0.01 kg/s and ambient temperature of (31.3 ± 0.5) °C. The performance of the model with and without the back tubes was compared where the difference between average values was (11.8 ± 4.0)°C, which was approximately (14.0 ± 5.0) % increase in the outlet fluid temperature. The working fluid used in this research work is saturated water.

ABSTRAK

KAJIAN REKABENTUK PENGUMPUL SURIA PENUMPU LURAH PARABOLA YANG OPTIMUM BAGI KEMUNGKINAN PENJANAAN KUASA DI MALAYSIA

Tujuan kajian ini dijalankan adalah untuk mereka bentuk sebuah pengumpul suria penumpu lurah parabola yang optimum. Parameter-parameter reka bentuk optimum dikenalpasti dengan menggunakan kaedah simulasi. Reka bentuk pengumpul suria lurah parabola yang baru diperkenalkan, di mana tiub-tiub tambahan kuprum dikimpalkan ke bahagian belakang penumpu parabola. Tiub-tiub kuprum ini dijangka akan mengumpul haba yang mengalir ke belakang penumpu parabola, hasil daripada sinaran suria yang tidak terpantul. Hasil kajian daripada simulasi digunakan untuk menghasilkan model prototaip optimum bagi tujuan eksperimen. Faktor-faktor optimum yang digunakan adalah sudut rim, nisbah kepadatan, sudut separuh-penerima dan diameter tiub penerima utama. Nilai-nilai optimum yang diperolehi bagi sudut rim adalah 90°, nisbah kepadatan ialah 10, sudut separuh penerima di antara 1.55° and 1.72°, di mana diameter tiub penerima utama terletak di antara 27 mm and 30 mm. Nilai-nilai parameter yang lain yang ditentukan adalah penetapan nilai diameter tiub penerima utama pada 30 mm, lebar lurah parabola sebagai 1.0 m, kedalaman lurah dan fokus pada nilai 0.25 m. Nilai panjang lurah penumpu ditetapkan pada 1.83 m, berdasarkan kepada simulasi modul terma dan factor kewangan. Perisian simulasi digunakan untuk menilaikan prestasi model baru ini dengan menggunakan data meteorologi bagi Bayan Lepas, Ipoh, Cameron Highlands, Kuantan and Senai. Nilai simulasi maksimum seketika suhu air

yang keluar daripada tiub penerima utama adalah 133.8 °C bagi Ipoh. Nilai eksperimen maksimum seketika suhu air yang dicapai pada 6^{hb} Julai 2003 dengan menggunakan model prototaip ialah (143.8 ± 0.5) °C pada nilai purata 2.57 MJ/m^2 bagi sinaran suria terus and nilai purata 0.81 MJ/m^2 bagi sinaran suria serakan, di mana kadar pengaliran jisim air adalah 0.01 kg/s dan nilai suhu ambien adalah (31.3 ± 0.5) °C. Prestasi model prototaip dengan dan tanpa tiub-tiub belakang memberikan perbezaan purata suhu keluar air daripada penerima utama sebanyak (11.8 ± 4.0)°C, yang dianggarkan sebagai penambahan sebanyak (14.0 ± 5.0) % suhu air yang mengalir keluar daripada penerima utama. Bendalir yang digunakan di dalam kajian ini adalah air tepu.

CHAPTER 1

INTRODUCTION

Ever since oil was discovered, man has become totally dependent on this reliable source of energy. The dramatic change that followed has thrust us into this new century, with modern civilization, promising a good future and a better quality of life. However, improper use of fossil fuels has led to negative imbalances in the natural environment and energy crisis such as the oil embargo in 1973 which, affected economies around the world. Malaysia too was not spared during the energy crisis in 1973 and chaos in the country due to the shortage should have been taken as a good signal to start looking for new alternatives. The fact that oil, natural gas and coal might deplete someday has never been given any due priority until recently, according to a report by the Ministry of Energy, Communication and Multimedia Malaysia (2001).

Although the use of fossil fuels have given us the flexibility and reliability, but continuous efforts in diversifying other resources are inevitable. In this research, the focus is set on utilising solar energy, which is part of the nation's fifth fuel strategy in generating electrical power. It is projected under the Eight Malaysian Plan (2001), that peak load electricity demand will increase from 10,673 MW in year 2000 to 16,834 MW in year 2005 and 5 % of it is projected by the use of renewable energy technologies by the year 2005. The National Energy Policy, introduced in 1979 aims to have an efficient, secure and environmentally sustainable supply of energy, which is parallel with the global efforts. Three primary objectives in relation to the supply, utilization and environment were formulated, according to a report by the Ministry of Energy, Communication and Multimedia Malaysia (2002). The development plans for using both non-renewable and

renewable energy resources were taken to be the main intend and utilization objectives outlined the need to use energy efficiently. The immediate use of renewable energy technologies will be to supplement the conventional sources of energy (Hong, 2002). The prioritisation of renewable energy development is crucial and the expansion of the Four-Fuel Diversification Policy of oil, gas, coal and hydroelectric power to incorporate renewable energy, with emphasis given to biomass, biogas, municipal waste and solar energy to provide adequate, clean and affordable energy mix for future sustainable economic development (Jaafar *et al.*, 2003). The policy intends to reduce the over reliance on oil and aims for a balanced energy mix.

1.1 MALAYSIA'S PRESENT AND FUTURE ENERGY MIX

One of the main energy utilisation in Malaysia is to generate electrical power. As mentioned in the previous section, the Malaysian Government devised a Four-Fuel Policy, where emphasis was placed on oil, gas, coal and hydroelectric power. However, in May 2001 the Four-Fuel policy was changed to a Five-Fuel Policy with an addition of renewable energy as the fifth fuel. The emphasis on the fifth fuel is to generate 5% of the country's electricity from renewable sources by the year 2005, according to a report from the Economic Planning Unit Malaysia (1999). In order to achieve this, Small Renewable Energy Power Programme (SREP) has been announced (Jaafar *et al.*, 2003), where the utilisation of all types of renewable energy is encouraged, including biomass, biogas, solar, mini hydro and wind. The prioritisation of renewable energy development is crucial, and the Economic Planning Unit's energy division has identified the following three renewable energy resources that will be given priority; biomass, solar energy and municipal waste. The plan to carry out testing and data collection activities has been initiated under the Eight Malaysian Plan (2001).

The data compiled by Economic Planning Unit is presented in Table 1.1, where percentages from the total of energy demand and supply for the years 1980, 1990, 1998, 2000 and 2005 are given. It can be observed from Table 1.1, that the dependence on petroleum is projected to be reduced, both in the demand and supply, but at the same time, the demand and supply for natural gas increases. The other interesting statistics provided are the increase in the use of coal and coke and the decline for hydropower, although the need for electricity increases. This is due to the abundant availability of coal in Malaysia and the clean technology associated in its utilization.

Table 1.1 The percentage from the total of energy demand and supply data for Malaysia between the years 1980 and 2005. *Source: Eight Malaysia Plan (2001-2005),Mid-term Review of the Seventh Malaysia Plan (1996-2000) and National Energy Balance, Malaysia (1980-1997).*

	Energy Demand					Energy Supply				
Source / Year	Petroluem products (%)	Natural Gas (%)	Electricity (%)	Coal & Coke (%)	Total (%)	Petroluem products (%)	Natural Gas (%)	Hydropower (%)	Coal & Coke (%)	Total (%)
1980	86.90	0.60	11.70	0.80	100.00	87.90	7.50	4.10	0.50	100.00
1990	74.80	8.30	13.00	3.90	100.00	71.40	15.70	5.30	7.60	100.00
1998	69.20	9.70	17.90	3.20	100.00	55.60	34.80	4.10	5.50	100.00
2000	68.90	10.30	17.60	3.20	100.00	53.10	37.10	4.40	5.40	100.00
2005	67.00	10.90	18.80	3.30	100.00	50.80	39.90	3.40	5.90	100.00

Figure 1.1 and Figure 1.2 graphically show the data given in Table 1.1 and it can be seen that by the year 2005, although there is a significant reduction in demand for the use of oil, but the total reduction for all sources is only 7.1 % in the demand and 0.7 % in the supply as compared to the base year 1980. Although renewable energy is listed as the fifth fuel, the contribution expected by the year 2005 is still insignificant compared to the other energy sources and this is shown in Figure 1.3. Another interesting finding in Figure 1.3 is the dependence on hydropower is reduced from the year 1990, till the year 2005, although

the demand for electricity increases. It is obvious that the dependence on energy from the conventional sources is increased, despite the sharp fall in the use of oil.

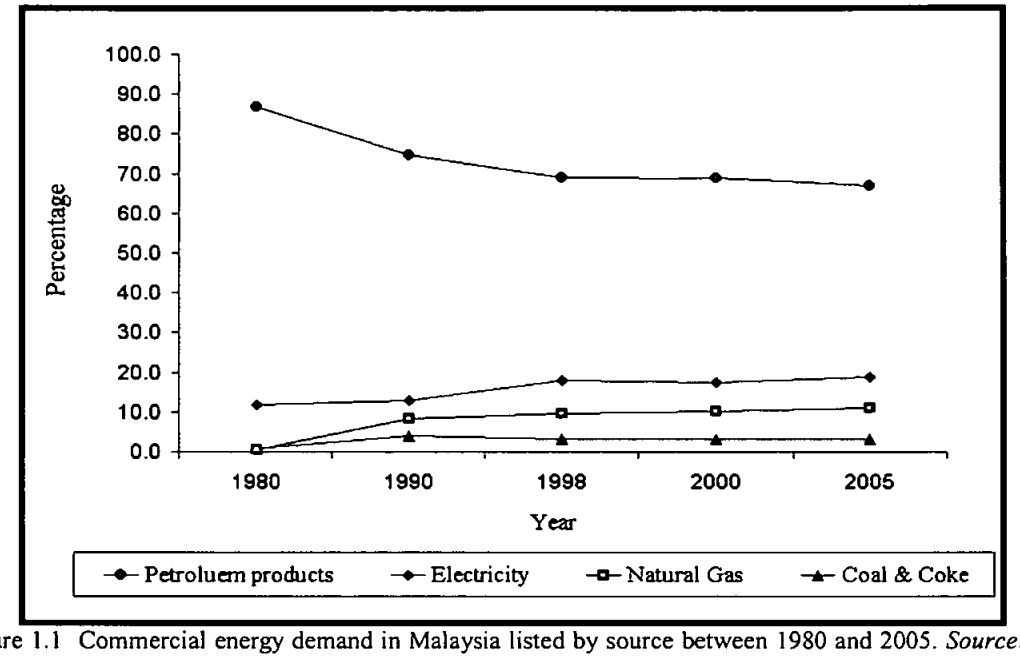

Figure 1.1 Commercial energy demand in Malaysia listed by source between 1980 and 2005. *Source: Eight Malaysia Plan (2001-2005), Mid-term Review of the Seventh Malaysia Plan (1996-2000) and National Energy Balance, Malaysia (1980-1997).*

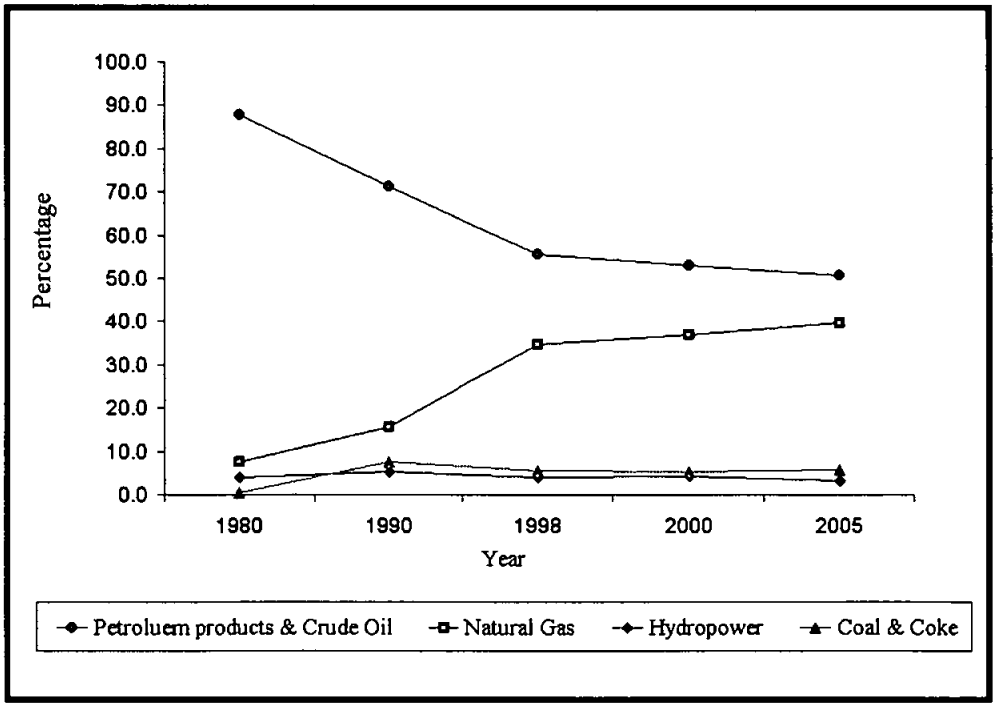

Figure 1.2 Commercial energy supply in Malaysia listed by source between 1980 and 2005. *Source: Eight Malaysia Plan (2001-2005),Mid-term Review of the Seventh Malaysia Plan (1996-2000) and National Energy Balance, Malaysia (1980-1997).*

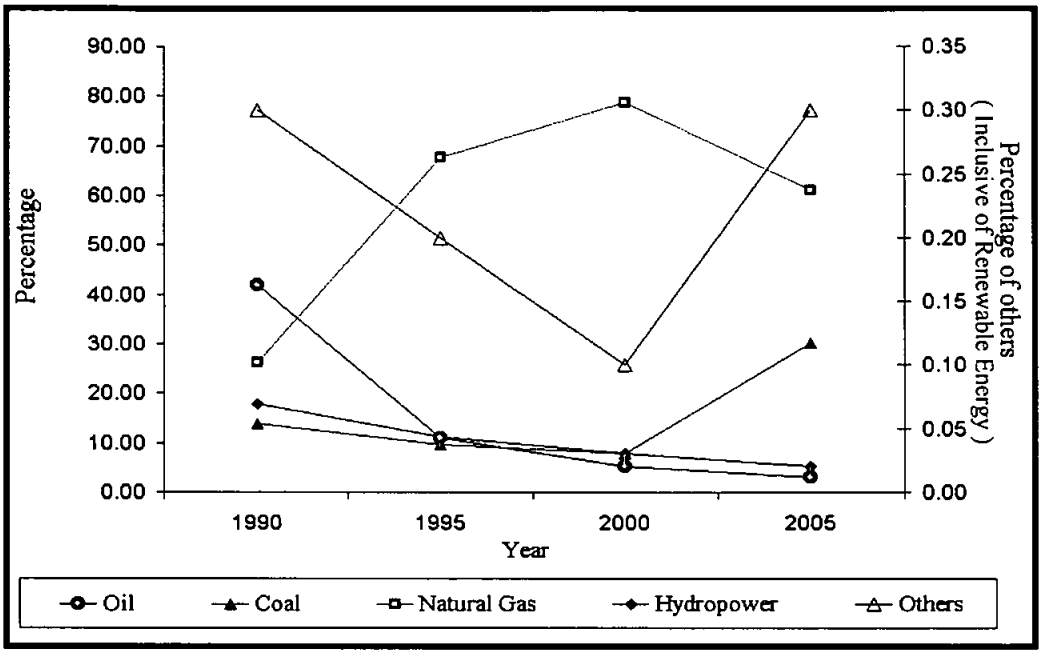

Figure 1.3 The use of various source of fuels to generate electricity in Malaysia, between 1980 and 2005. *Source: Eight Malaysia Plan (2001-2005) and Seventh Malaysia Plan (1996-2000).*

Based on these findings, it is interest to embark on a project that involves the use of solar energy, particularly to study the potential of generating electrical power that will be useful for a country like Malaysia which is blessed with 12 hours of sunshine per day. Since two-biomass related power plants are already being planned and launched, it is timely to exploit the next potential renewable energy source. In view of all these, Malaysia should embark on the journey of exploring the use of solar energy to supplement the use of conventional sources of energy. Solar energy is essentially an inexhaustible source, potentially capable of meeting our country's future energy needs with a minimum adverse effect on the environment.

1.1.1 BIOMASS RESOURCE POTENTIAL

Biomass is a versatile energy source. Organic matter that is used as a source includes trees, timber wastes, wood chips, corn, rice hulls, peanut shells, sugar cane, grass clippings,

leaves, manure, and municipal solid waste. In brief, biomass is made up mainly of the carbon and hydrogen elements and there are technologies that exist to free the energy from chemical compounds made up of these elements. Commercial and industrial facilities can use biomass to produce electricity, where one of the technologies that can be applied is the biomass cogeneration (Duval, 2001). Biomass accounts for about 15 % of the world energy use and 38 % of the total energy utilised in the developing countries (Hall *et al.*, 1993).

Being a nation that supports the global environment policies (Sayigh, 1999), Malaysia has embarked on using electrical power generation technologies that are related to renewable energy, with two renewable energy based plants currently setting up their plants. The companies are Bumibiopower Sdn Bhd and Jana Landfill Sdn Bhd. Bumibiopower's renewable energy plant will make use of oil palm waste such as empty fruit bunches and palm kernel shells as biomass fuel (Susta & Huat, 2002). The plant located in Pantai Remis Perak, has a capacity of generating 5.2 MW of electricity. The cost of building the plant is estimated to be RM 26.6 million and the project is supposed to have been completed towards the end of year 2003. Jana Landfill Sdn. Bhd. on the other hand will be erecting their RM 10 million renewable energy plant at the Ayer Hitam Sanitary Landfill in Puchong, Selangor. The plant will have a capability of supplying 2 MW of electricity and will operate using the landfill gas produced by the natural decomposition process of municipal waste at the landfill (Yean, 2001).

The palm oil mills in Malaysia have been operating using cogeneration systems for quite sometime now, where biomass residue such as fibre and shells from the palm oil fruits are used as the boiler's fuel. The boilers installed at the palm oil mills can produce steam at high temperatures and pressures. The high-pressure steam that is produced is supplied to the steam turbine with enough electrical power generated for the internal needs of the mill. The exhaust steam from the turbine is collected in an accumulator and the steam is then

utilised to carry out a variety of processes in the mill. The cogeneration system employed in the palm oil mills is a good proven method, where it is sustainable as long as there is supply of palm fruit (Husain *et al.*, 2003).

1.1.2 SOLAR ENERGY RESOURCE POTENTIAL

The government has identified the need to include solar energy as part of the nation's present and future energy resource. This is a motivation to the present and future undertakings in solar energy related research works. The various solar energy research groups have the responsibility of carrying out research activities to gauge the performance of all types of solar energy related technologies as its utilisation is achieved through the implementation of these technologies.

The Solar Energy Research Group from Universiti Kebangsaan Malaysia designed a solar assisted dryer for palm oil fronds (Supranto *et al.*, 1999). The choice of designing a solar dryer to assist the drying of fronds is useful, as Malaysia is the largest producer of palm oil. Fronds are the waste product of palm oil, which can be made into pellets and exported as animal feedstock. The method of drying the fronds by directly exposing them to sunlight may produce sub-standard and contaminated processed product. Since each palm oil tree is estimated to produce 100 kg of fronds per year and with moisture content of about 60 %, the use of double-pass solar collector with an estimated temperature rise in the range of 25 °C to 30 °C certainly seems like a good alternative to protect and produce a high quality export commodity.

Flat plate solar thermal collector is a popular solar thermal energy related technology in Malaysia (Kannan, 1999). Flat plate solar thermal collectors are normally used to produce hot water for domestic and industrial purposes. There are various types of flat plate solar

thermal collectors that are now available in the market and it is a common sight to see them on rooftops. Flat plate solar thermal collectors are used to produce hot water at relatively low temperatures between 60 °C to 75 °C. Researchers from Universiti Kebangsaan Malaysia and Universiti Sains Malaysia have carried out substantial amount of work related to flat plate solar thermal collectors (Balbir, 1996).

Photovoltaic (PV) cell is a device that can generate electricity without any moving parts and operate silently without any emissions of dangerous gases (Green, 2002). PV cell uses semiconductor technology to capture the energy in the sunlight and convert it to electricity directly. PV technology can be used to overcome problems to provide electricity in the rural areas (Kannan, 1999), where extending the utility's electricity grid is expensive or impossible. One such case was reported in the local newspaper, where Tenaga Nasional Berhad installed PV panels on a kampung house located at Bukit Apit Felcra settlement in Malacca, at a cost of RM 5,000. The solar kit used had a battery, which provided up to eight power points. Similar facility was also extended to provide electricity to 49 orang asli houses in Kampung Bukit Panjang, Melekek, also in Malacca (Yatim, 2000).

1.2 HYBRID POWER GENERATION

Under the fifth fuel plan, energy efficiency is employed as part of a solution to conserve energy. The decision to use renewable energy is wise and will definitely spur research activities. Solar energy is essentially an inexhaustible source, potentially capable of meeting part of the country's future energy needs with a minimum adverse effect on the environment (Scheer, 1999). Although solar thermal technologies have made noteworthy technical and economic progress, they still encounter a serious competitive threat from natural gas. Due to the lower price of natural gas, it is difficult for any solar related electrical technology to match the cost of gas-fired electrical generating plants in supplying

power to the electric transmission grid. The reason to shift to solar thermal electrical technologies cannot be based on cost alone, but justifications should be focussed towards their essential role in meeting environmental goals (Mahlia, 2002). Natural gas on the other hand, is usually not portrayed as a serious threat to the environment, unlike coal (Hasanen *et al.*, 1986).

Natural gas pollutes too, but it offers clear environmental advantages over other fuels, especially with almost zero emission of sulphur dioxide SO_2 that contributes to acid rain and harms human health (Verkhivker & Yantovskim, 2001) and this is shown in Figure 1.4. The pollutants released through gas combustion are oxides of nitrogen, NO_x and it is reported by Dockery (1994) that pollution from NO_x caused over 50,000 deaths per year in the United States.

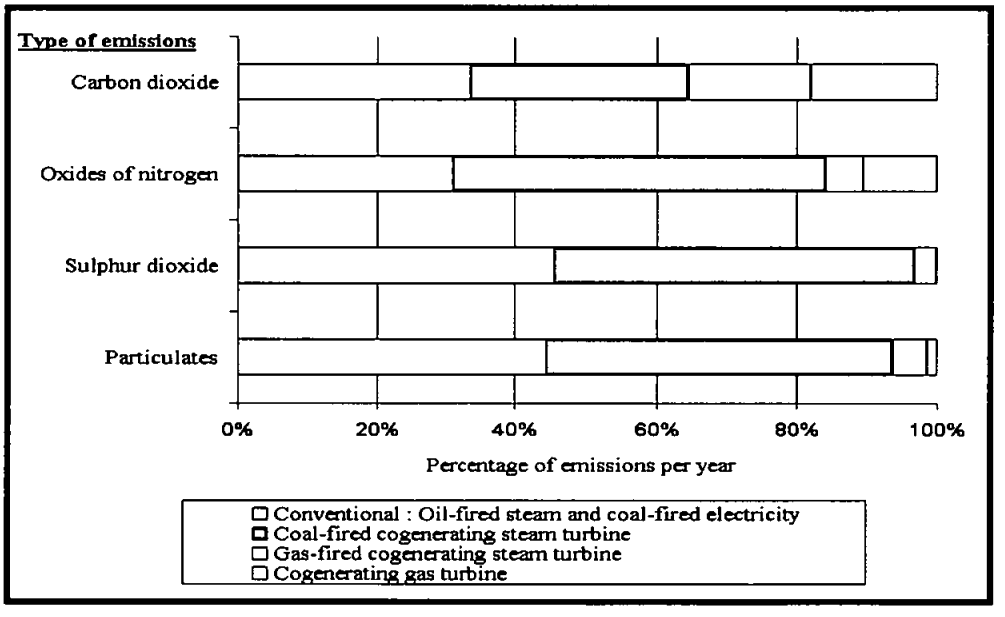

Figure 1.4 Graph shows the comparison of annual emissions of 11.0 MW co-generation plant with a conventional system. Data is compiled from a discussion paper presented by Homer (1993).

The role supposed to be played by solar thermal technologies seems obvious. Natural gas has to play the role of bridging the present where environmental benefits of solar thermal technologies are limited by the small amount of global energy derived, with the future

where environmental necessities may require the solar thermal or renewable sources to satisfy most of the world's energy needs (Flavin and Lenssen, 1994). The bridge between the electrical power generating systems that use natural gas and solar thermal energy can to be considered, as natural gas pollutes less than oil or coal. Although the supply of gas will deplete some day, but for at least the next few decades, natural gas can continue to generate electricity more than all the renewable energy technologies combined (Serchuk & Means, 1997). As the bridging idea provides a logical solution, the efficient use of energy would lead to Malaysia's plan to succeed on the five-fuel strategy.

In Malaysia, we can benefit from the proposed hybrid system as PETRONAS has a comprehensive network of natural gas transmission and distribution pipelines, which starts from Kertih, Terengganu and stretches all the way to Segamat, Johor where the southern line passes through Pasir Gudang, Johor to Singapore and the northern line all the way to Perlis, with a total length of 1753 km. The total length of domestic transmission and distribution pipelines in the neighbouring countries such as Indonesia, Myanmar, Brunei Darussalam, Thailand and Vietnam are around 7013 km, as of March 2000, where the total length of gas pipelines span across Southeast Asia is projected to be about 13,000 km by the year 2005, via Trans-ASEAN Gas Pipeline (Yokobori, 2000). The network of gas pipelines is important, as natural gas cannot be transported economically by truck or rail, as compared to the use of gas pipelines.

PETRONAS has developed a network of natural gas pipelines in Malaysia and some of the independent power producers such as the 1,303 MW Loji Janakuasa Lumut in Segari, Perak which started its commercialised operations in 1996 has already benefited from its supply by using natural gas fired steam turbines. A renewable energy based plant, which consist of biomass, and parabolic solar thermal power plants can be built in the vicinity of one of the natural gas based power stations, with funding from the government and the

private sector. Some of the countries in Asia have already started their effort to move towards using Solar Electricity Generating Systems (SEGS) and Integrated Solar Combined Cycle Sytems (ISCCS) to meet their present and future power demands, besides enjoying the benefit of clean energy that ensures good health of the people. According to Aringhoff (2001), there is a 135 MW ISCCS power plant in India that is capable of harnessing 35 MW through a parabolic trough solar field and the 140 MW ISCCS plant in Egypt also uses its parabolic trough solar field to produce approximately 30 MW to 80 MW of solar electricity. A brief discussion on SEGS and ISCCS will be included in the next section.

1.3 EXISTING SOLAR ELECTRICITY GENERATING SYSTEMS

The parabolic trough power plant is not a new concept, where one of the significant early appearances was recorded in the year 1912. During this time, Frank Schumann and C.V. Boys of the United States constructed a 45 KW solar steam-pumping plant for pumping irrigation water from the Nile, in Meadi, Egypt, which covered an area of 1,200 m^2 (Smith, 1995). The plant was operated successfully until 1915, before it was forced to shut down partially due to the onset of World War I and also cheaper fossil fuel prices. Interest in reviving parabolic trough power plant technology was initiated in the early 1970s, which resulted with a solar electric parabolic trough facility being constructed at the International Energy Agency test site in Tabernas, Spain in 1981 (Grasse, 1985). The test facility was named as Small Solar Power Systems Project / Distributed Collector System (SSPS/DCS), consisting of two solar fields with a total reflector area of 7,602 m^2, a steam generation system and a conventional steam-turbine cycle power system connected to the grid.

The first commercial thermal Solar Electric Generating Systems (SEGS) project initiated by the Luz Company commenced in 1984 and in California USA, as a private investor-

owned power plant supplied electricity to the Southern California Edison Company's grid. The Luz Company operated for 7 years with 9 SEGS plants, and in the late 1991 filed for bankruptcy due to the US laws and not due to the technology that almost achieved a near cost competitiveness with conventional power plants. According to Lotker (1991), who was the vice-president of Business Development section of Luz International Limited, the significant decline in the fossil energy prices in the 1980s, which occurred in parallel with marked reductions in regulatory and financial incentives such as tax credits, created a difficult market environment in the United States for capital-intensive renewable technologies. The cost of constructing and operating the SEGS plants fell considerably, where the installation cost in 1984 was reduced from US$5,979 per kWh to US$3,011 per kWh in 1990. The performance levels also improved and as a result, the electricity supplied by Luz reduced by 70 % from US$0.265 per kWh to US$0.089 per kWh (Kearney *et al.* 1991).

It is important to note that all of the nine Luz's SEGS plants that were completed continued their operations in 1992 (Price & Kistner, 1999) and their first SEGS is currently in its 18th year of operation. It can be observed that from an operational perspective, the SEGS I till IX plants have been very successful and their size range from 14 MW to 80 MW and make up a total of 354 MW of installed electricity generating capacity. The plants have demonstrated the industrial nature of the parabolic trough collector technology. The Luz's SEGS plants are hybrid fossil fuel-solar plants, so when insufficient sunlight is available, the turbine can be operated up to full load with natural gas, where on an annual basis, 75 % or more of the energy to the plant comes from solar energy, with natural gas providing the balance (Cable, 1997).

The Luz's next project is geared towards using direct steam generation technology. With the direct steam generation concept, there is no need for expensive oil-based heat transfer

fluid and oil-heated steam generators (Laquil III *et al.*, 1993). Since oil-based heat transfer fluid is not being used, the solar field's operating temperature is lowered but however it will not really affect the temperature of the steam to the turbine and this will be helpful in reducing the thermal losses. Furthermore, the degradation of synthetic oil can cause loss of heat transfer efficiency and increase in viscosity that would increase pumping costs and can also damage the equipment (Odeh *et al.*, 1998). Synthetic oils are flammable and also toxic, where leakages may lead to hazards of the environment.

The schematic diagram shown in Figure 1.5 explains the direct steam generation concept in one of the Luz's SEGS hybrid plant, where the reheat Rankine cycle is used. A steam flow is introduced to the steam turbine and is reheated halfway through the expansion process. The reheating improves the thermal efficiency of the ideal cycle and also the dryness of the turbine exhaust, which reduces the problem of erosion of the turbine blade (Nakanishi, 1999).

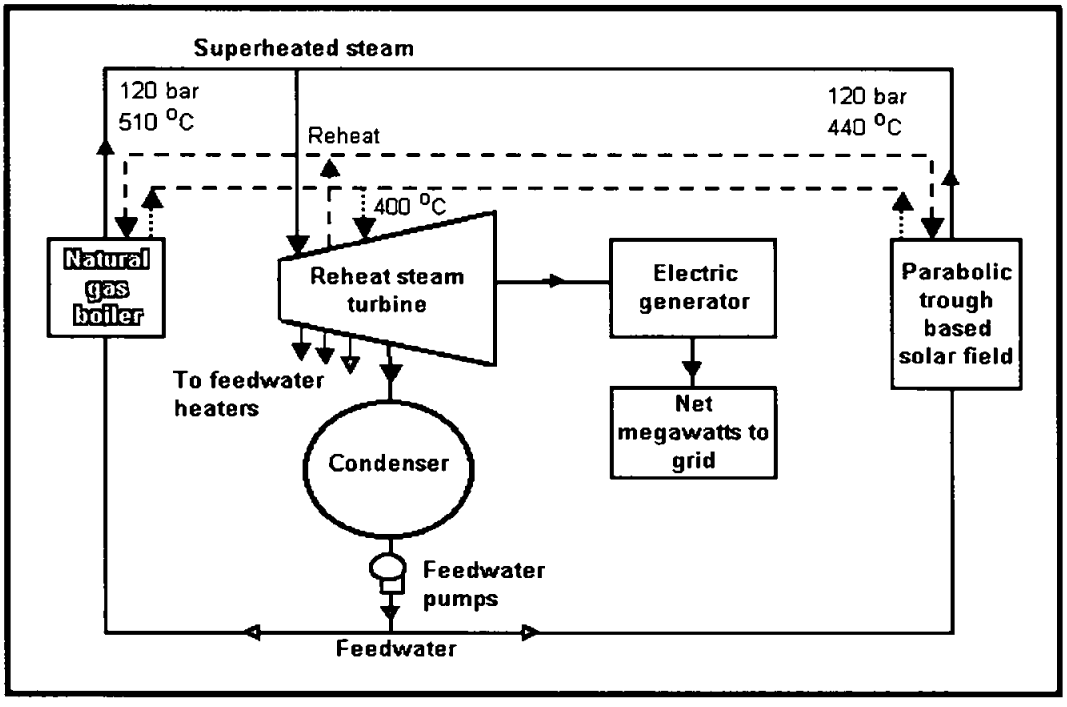

Figure 1.5 A typical schematic diagram of the processes at one of the Luz's SEGS hybrid power plant., which uses the direct steam generation concept.

A new configuration that shows potential to meet the continuous operation and peaking power requirements is the combination of SEGS parabolic trough technology with a gas turbine combined cycle power plant. This system will minimise the environment pollution, as compared to using only the conventional gas combine cycle. This relatively new configuration is known as Integrated Solar Combined Cycle System and will be discussed in the next section.

1.4 INTEGRATED SOLAR COMBINED CYCLE SYSTEM

Parabolic trough concentrating solar power system is reliable and should be considered seriously in the future electrical power plans. However, parabolic trough power plants rely on a secure and inexhaustible source of solar energy which can be integrated with fossil fuel technologies in hybrid power plants, which increases flexibility such as the Luz's SEGS projects as described in section 1.3.

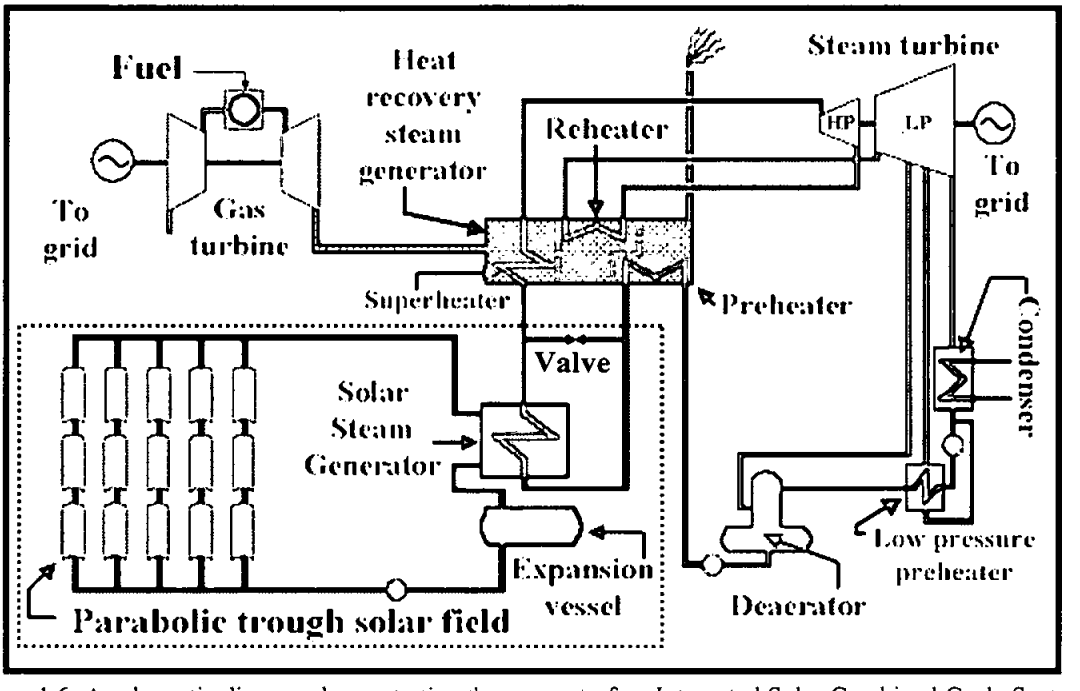

Figure 1.6 A schematic diagram demonstrating the concept of an Integrated Solar Combined Cycle Systems (Kelly *et al.*, 2001).

The integrated solar plant concept was initially proposed by Luz International Limited as a means of integrating a parabolic trough solar plant with modern combined cycle power plants (Laquil III *et al.*, 1993). The concept of Integrated Solar Combined Cycle System (ISCCS) is as shown in Figure 1.6, where the integrated plant consists of a conventional combined cycle plant, a parabolic trough solar collector field and a boiler, which acts as a solar steam generator. The parabolic trough solar field in the ISCCS concept uses an oil based heat transfer fluid. The method of utilizing the gas turbine exhaust gas for the Rankine cycle is not new, where it was first used in 1950 (Fujii, 1999) where a steam turbine was used to produce mechanical work, which was converted to electricity by a generator attached to it (Gretz *et al.*, 1984). The parabolic trough solar field is integrated into the conventional combine cycle plant, where the integration is as shown in Figure 1.6 by the boundaries defined by the dotted rectangular line rectangle.

The solar field contributes its power to the system when sunshine is available and the feed water that is withdrawn from the combined cycle plant heat recovery steam generator is hence converted to saturated steam in the solar steam generator. The saturated steam is then returned to the heat recovery steam generator where it is superheated. The heat recovery steam generator recovers the heat from the gas turbine's exhaust gas with its improved technology, which ensures that the steam that passes through it can achieve higher temperatures.

At night or when it is cloudy, the integrated plant operates as a conventional combined cycle plant and it is during this time that the valve opens. The overall advantage of the system is the shorter start-up period of 5 to 10 minutes from no load to full load, which makes it perfect for peaking or emergency backup services and due to this, the solar electric operating efficiency should be higher (Lammers, 1998). The heat exchanger system used in the solar steam generator can be eliminated, where direct steam generation

concept is used, thus reducing the capital costs. The parabolic trough based solar field is used for steam generation, while the entering gas-turbine exhaust gas is used to superheat the steam generated by the solar field. Solar hybrid combined cycle system can achieve net cycle efficiencies of 53 % to 55 %, which is around 6 % to 11 % higher than the conventional combined cycle efficiencies (Laquil III *et al.*, 1993). Although it has been 18 years since the technology was implemented in the United States, but continuous improvements are still being carried out on the parabolic trough concentrators. In the next section, a literature review is carried out on the parabolic trough concentrators that are currently available and research activities related to the process of improving their performance and cost-effectiveness. The limitations of parabolic trough concentrators will also be highlighted before the objectives of this research are identified.

CHAPTER 2

LITERATURE REVIEW

Solar thermal systems are used to convert sunlight into heat. The distinctive component of a solar thermal system is the solar collector. Among the popular solar collector is the flat-plate solar thermal collector. Energy delivered by the flat plate collector is at moderate temperatures and to obtain higher temperatures, concentrating solar thermal collectors are used. Concentrating solar thermal collectors achieve higher temperatures by using a concentrating reflector to direct sunlight from a large area to a smaller receiver and absorber area. A working fluid is passed through the absorber, where it is heated and then sent to a storage system or used directly for heating. As Figure 2.1 shows, the term concentrating collector defines the whole system, namely the receiver and the concentrator. Concentrator describes the optical reflecting subsystem, while receiver looks at the absorbing system (Twidell & Weir, 1998).

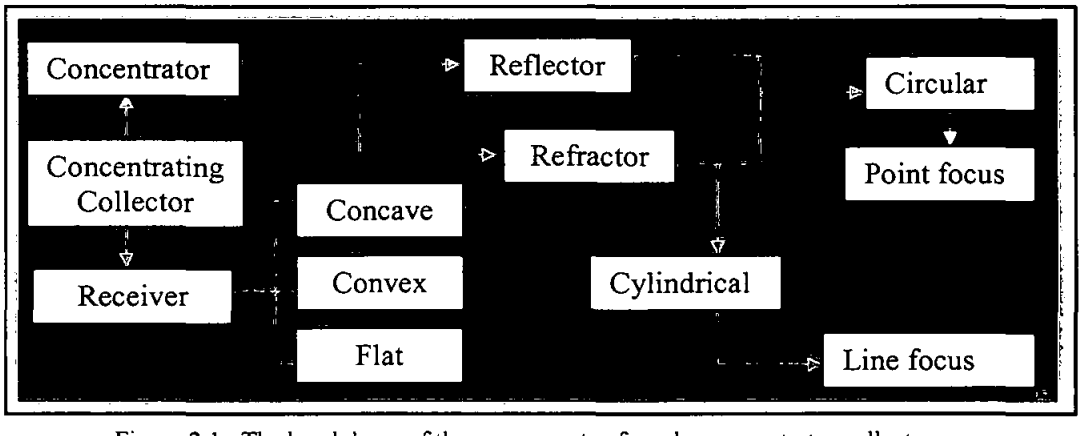

Figure 2.1 The breakdown of the components of a solar concentrator collector.

The concentrating collectors are usually compared by using the concentration ratio factor. Concentration ratio is a factor by which radiation flux on the receiver's energy-absorbing surface is increased. The increasing ratios mean increasing temperatures at which energy

can be delivered and also increasing its optical quality and correct positioning of optical systems. Concentration ratios can be theoretically very high for the imaging concentrators of precise optical elements and continuous tracking, which can be up to 40 000 (Rabl, 1980).

In this research, a solar parabolic trough type of concentrating collector is used. A typical parabolic trough concentrator consists of reflective glass mirrors that are curved to form a trough. The receiver's absorber tube is placed concentrically around the focal point of the concentrator. It is a common practice to coat the receiver's absorber tube with a high absorptance and low emittance selective surface coating especially black chrome and cermet (Cohen & Kearney, 1994). The receiver's absorber tube is encased in a glass envelope, acting as the cover. Parabolic troughs can achieve concentration ratios of between 10 and 100. Usually an oil based heat transfer fluid is pumped through the receiver's tube to remove the solar heat, which is transferred to water by using a heat exchanger. In general, a parabolic trough can collect up to 60% of the incident solar radiation (Industrial Solar Technology, 2003). The typical application related to the parabolic trough is to produce steam for electrical power generation. According to Kalogirou (2002 & 2003), parabolic trough collectors can also be used to supply solar industrial process heat.

2.1 APPLICATIONS OF SOLAR PARABOLIC TROUGH CONCENTRATOR

The commercial potential of solar thermal electricity on grid was realised in the 1980s (Cable *et al.*, 1997), although the basic technology for the production of mechanical energy, which is converted to electricity by using a conventional generator, had been under development for about 140 years (California Energy Commission, 2002). The efforts started with Auguste Mouchout designing the axicon type solar collector in 1878, attached

to a steam engine that generated 1.5 kW of electricity (Smith, 1995). In the same year, Abel Pifre used parabolic mirrors on Mouchout's axicon solar collector and successfully operated a steam engine to operate a printing press (Mills, 2003). Later in 1883, John Ericsson constructed a parabolic cylinder to focus the solar radiation on the absorbing tube mounted above the mirror and the parabolic trough concentrator was used together with the Ericsson-cycle hot-air engine (Meinel & Meinel, 1976).

The parabolic trough concentrator available at present time is almost similar to the operation of Ericsson's parabolic cylinder (Evans, 1977). Although the technology has been in existence for quite sometime now, extensive research activities are being carried out till today where the synthetic oil based systems are being replaced by systems that use direct steam generation concepts especially at utility-scale power plants (Zarza, *et al.*, 2001). The parabolic trough system can be considered as the most fully developed solar thermal technology whereby major installations for both process heat and electricity production have been commercialised (Laquil III, 1993).

In the year 1979, an electrical power test plant that used parabolic trough concentrators was used to generate 150 kW, for irrigation pumping facility in Coolidge, Arizona, U.S.A. (Hassani & Price, 2001). In Tehachapi, California, a parabolic trough concentrating collector system has reliably and efficiently provided high-temperature pressurised water for a state prison housing approximately 5,100 inmates. The system has been in operation since 1990 and demonstrated that parabolic trough based solar energy systems can be cost-competitive even with natural gas (Sheinkopf & May, 1997).

The commercialisation of solar thermal electric technology was initiated in the mid-1980's and early 1990's with the development of the SEGS plants in Mojave Desert, California. The SEGS plants used the parabolic trough technology integrated with steam Rankine

cycles, which generated a total of 354 MW grid electric power (Price *et al.*, 2002). The capacities of the SEGS plants range from 30 MW to 80 MW each and are operating till today. These plants have provided a wealth of operating experience and instilled confidence in a wide spectrum of observers on the viability of solar thermal technology as a future power source (Pilkington, 1996).

Besides the SEGS in the U.S.A, EuroTrough is another SEGS project with high commercial potential. EuroTrough consortium is made of companies from Spain and German and is fully supported by their governments. The European Commission financially supports the development and qualification testing of the EuroTrough. The high-performance EuroTrough parabolic trough collector models are ET100 and ET150. Both these models have been developed for the utility scale generation of solar steam for process heat applications and solar power generation. Their operating temperatures may reach over 500 °C and they can be integrated to generate up to 200 MW of solar thermal electrical power (Geyer *et al.*, 2002).

According to Garcia (2000), direct steam generation concept is being explored to improve performance, reduce costs and enhance safety at the SEGS plants. The direct steam generation collector field supplies the power generator with the required steam, where an auxiliary boiler is used to maintain steady steam generation during transient radiation conditions (Odeh *et al.*, 2003). Usually in the conventional SEGS plants, a heat exchanger is used, but in the case of the direct steam generation, the parabolic trough collector field is used directly to produce steam for the power generator (Zarza *et al.*, 2001). This offers a lower investment in terms of cost, as the heat exchanger and synthetic oil based heat transfer fluids are not required. Higher efficiency is expected when the direct steam generation process is combined with improved performance of the parabolic trough concentrators. A feasibility project that is being carried out is the European Direct Solar

Steam project (DISS) where the ability to generate steam directly at a pressure around 100 bars and 400 °C has been demonstrated (Eck *et al.*, 2003).

The parabolic trough concentrator is also used for industrial process heat applications, where the temperature requirements of solar industrial process heat applications range from 60 °C to 260 °C (Kalogirou, 2003). Although the most common application of the parabolic trough concentrator is for electrical power generation, but Norton (1999) presented the application of solar process heat obtained by using parabolic troughs for distillation, drying of agricultural products and industrial uses. A system suitable for community kitchens, bakeries and post harvest treatment by using solar process heat for decentralised applications were also presented (Spate *et al.* 1999). Benz *et al.* (1998) described the use of parabolic trough concentrators for producing process heat for a dairy farm in Germany. The solar process heat was used for the spray-dryers for milk and also during powder milk production. The thermal energy used for milk pasteurisation is within the temperature range of 60 °C to 85 °C and sterilisation is in the range of 130 °C to 150 °C. Overall, some of the important processes that use solar industrial process heat are sterilising, pasteurising, drying, hydrolysing, distillation and evaporation, washing and cleaning, and polymerisation (Kalogirou, 2003).

2.2 RESEARCH ACTIVITIES OF SOLAR PARABOLIC TROUGH CONCENTRATOR

Parabolic trough concentrator (PTC) is usually used for solar steam generation where temperatures above 300 °C can be obtained without any serious degradation in the collector efficiency. The steam generated by using PTC can be used for electricity generation and industrial applications and according to Murphy and May (1982), there are three ways of generating steam by using PTC. The first way is by using the steam-flash

concept, in which pressurised water is heated in the collector and then flashed to steam in a separate vessel. The second is the direct or in situ concept where two-phased flow is allowed in the PTC's receiver so that steam can be generated directly. The third involves the use of unfired-boiler concept, where a heat transfer fluid is circulated through the PTC and steam is generated via heat exchange in an unfired boiler.

Simulation and modelling methods are considered as an integral part of research work pertaining to the performance evaluation of PTC, where simulations can be repeated by using local weather conditions. Kalogirou *et al.* (1997) developed a modelling program called PTCDES, which was written in BASIC language to determine the quantity of steam produced by the steam generation system. In this program, the actual measured collector performance parameters and intercept factors are required. The same program was used to obtain system optimisation, where the simulation program used a constant radiation input of 500 Wm^{-2} and ambient temperature set at 30 °C. As reported the system performance tests indicate that the modelling program is accurate to within 1.2 % and their analysis showed that only 48.9 % of the available solar radiation is used for steam generation. The remainder of the solar radiation is lost either as thermal losses or collector losses. The collector losses are due to poor insulation of inlet and outlet fluid tubes that are connected between the PTC collector and the storage tank. The overall findings in terms of thermal losses and useful energy gained are given in Table 2.1. Bakos & Tsagas (2002) developed simulation software to evaluate the technical feasibility and economic viability of a small-scale grid connected PTC, based on the flowchart proposed by Kalogirou *et al.* (1997). They improved the program by incorporating the solar radiation data for the city of Xanthi, Greece.

Table 2.1 Percentage of system losses and percentage of useful energy for higher operating temperatures.

Collector operating temperature (°C)	Collector losses (%)	Thermal losses (%)	Sensible heat and thermal capacity losses (%)	Useful energy (%)
100	41.5	6.9	2.7	48.9
150	44.7	11.7	5.0	38.6
175	46.5	14.4	6.0	33.1
200	48.1	17.1	7.1	27.7

The concept of direct solar steam generation in a PTC system is widely investigated, as there is potential for improvement especially for solar thermal electricity generation. The direct steam generation PTC was proposed by Cohen & Kearney (1994) as a future development of the SEGS trough collector in order to eliminate the costly synthetic oil, intermediate heat transport piping loop and oil to steam heat exchanger. Dagan *et al.* (1992) and Lippke (1996) introduced three different concepts of direct steam generation. The three different concepts are the once-through concept that is used to generate steam in one pass, the re-circulation process to generate wet steam and injected water system is to control steam quality and flow instability along the absorber tube.

Odeh *et al.* (1998) did a modelling of parabolic trough direct steam generation solar collectors. He suggested that to improve the performance and reduce cost, direct steam generation concept should be adopted. The efficiency of the PTC is determined for operation with Syltherm, a synthetic oil and also water as the working fluid. A model was developed to evaluate the thermal performance of the PTC that used Syltherm based on measurements obtained from Sandia National Laboratory. A simulation software was developed to estimate the performance of direct steam generation collectors by varying the absorber tube sizes and by using predetermined solar radiation values that were not based on actual meteorological data. Due to this, the software was unable to determine the actual overall daily efficiency of the system. However, it was reported that the performance of the PTC increased with higher solar irradiation due to the increasing heat transfer coefficient

with flow rate. Hence, to maintain dry steam delivery at low radiation levels, a very low water flow rate is required.

The DISS project is a comprehensive research and development program aimed at developing a new generation of SEGS with direct steam generation in the absorber tubes of the PTCs. The financial support to start the project was provided by the European Commission JOULE Programme. The first phase of the project was between 1996 and 1998, where test facilities were implemented at the Plataforma Solar de Almeria to investigate the response of this new technology under real solar conditions. Zarza *et al.* (2001) reported that by replacing oil with direct steam generation system, results in lower investment and operating costs, as well as reduced environmental risk and fire hazards in case of leaks. Some of the expected improvements are the development and implementation of improved components for parabolic trough collectors, such as new economical absorber tubes with good optical and thermal properties, cheaper sun-tracking systems, better reflective mirror and films. Langkenkamp (1998) projected that the overall improvement shown in the DISS project can lower the electricity cost by 26 %.

Based on the outcomes from DISS, Eck *et al.* (2003) mentioned that the technical and commercial feasibility of direct steam generation process in a horizontal parabolic trough collector has been proven and the remaining technical tasks that have been identified for further development is the improvement to the parabolic trough collector design. Zarza *et al.* (2004) outlined the aim of technical task described by Eck *et al.* (2003) is to develop and test new components for parabolic trough concentrators. The new components that were tested are the glass reflector panels that are 5 mm thick and a new receiver configuration with a secondary stage concentrator placed directly opposite to the parabolic mirror. The thick glass reflectors are used so that there will be a reduced rate of mirror breakage.

Research work at smaller scales are also carried out at University levels. It is also reported by Almanza (1998) that small-scale electricity generation facilities are available at the Solar Power Plant of the Engineering Institute at National University of Mexico. It is possible to generate electricity by using direct steam generation and saturated steam at 165 °C and 6.89 bar, which can produce 2.24 kW of electrical power, by using a Stuart Swan's two pistons steam engine. Four modules of PTC, with an aperture of 2.5 m and 14.5 m long with an absorber diameter of 3.81 cm were used to produce 100 kg h^{-1} of steam. More steam can be produced, if the number of modules is increased and electricity generation by direct steam generation at lower power is technically possible.

2.3 DESIGNS OF NEW GENERATION PARABOLIC TROUGH

The practical parabolic trough design was implemented in the SEGS to produce grid-connected electricity. The operating companies have worked on improvement of operation and maintenance (Cohen *et al.*, 1998). The features of different PTC designs will be discussed in this section. However, the key elements of the existing technology are the parabolic concentrator and receiver. The research activities discussed in the previous section were in regard to the improvement of the materials that are used to make these components, without any change in the basic design. Usually PTCs are manufactured for large-scale utilisation and improvement projects are specific task based, especially for the application for electricity generation. Among the early noticeable effort to modularise the PTC to make it available domestically was done by the Beam Engineering company (Peterson, 1978). Beam Engineering made a small sheet aluminium parabolic trough with its own tracker. The collector was 1.83 m long, with an aperture of 0.51 m wide and the black copper absorber tube had a diameter of 5.08 cm. The collector had a clear Tedlar

front cover, placed on the concentrator to protect the reflective surface and the concentration ratio was around 3. Smaller PTCs can be coupled together to provide enough steam for electrical power generation at high thermal power as well as low thermal power to the order of 2.24 kW (Almanza *et al.*, 1997).

Richter (1996) reported that the linear focusing concentrator has an advantage of operating at temperatures high enough for many applications but not so high as to cause excessive radiation loss or serious material difficulties. He also proposed an alternative to the conventional parabolic trough, where he designed a two-trough collector. The two-trough collector used a stationary hemi-cylinder main reflector that tracks the sun by means of a second reflector that pivots around the axis of the hemi-cylinder. The main reflector with circular cross section is used as the radius is uniform and the secondary reflector corrects the spherical aberration of the main reflector and focuses the sunlight on the absorbing pipe. According to Richter (1996), under ideal conditions, the parabolic trough outperforms the two-trough collector, but in reality, the use of immobile, hemi-cylinder large reflector will enable his design to have a competitive edge.

Collares *et al.* (1991) and Collares & Mendes (1995) have proposed the use of asymmetric secondary concentrators with tubular receivers in parabolic trough concentrators. This effort was supported by Ajona *et al.* (1996) with aims directed at incorporating the latest know-how into a new generation of parabolic trough collectors. The new generation of parabolic trough collectors must be equipped with direct steam generation capabilities, secondary reflectors and innovative design to reduce heat losses. Spirkl *et al.* (1997) reported that the parabolic trough type solar power plants could reach higher efficiencies by using secondary reflectors, which increase the concentration of the solar irradiance onto the absorber tube. Modifications were then made to the secondary reflector to improve the

efficiency, where a compact secondary concentrator was proposed. It was found that the compact secondary concentrator significantly improved the concentration.

A point focusing double parabolic trough concentrator is a new concentrator design, which uses two one-dimensional mirrors in the shape of parabolic troughs to accomplish the performance of one two-dimensional concentrating mirror. This is a hybrid design that combines the design of a parabolic trough concentrator and paraboloidal dish (Murphree, 2001). The point focussing concentrator is made from two reflective primary and secondary parabolic troughs, where their longitudinal axes are in perpendicular directions. The two concentrators are separated by the difference of their focal lengths, where the focal lines merge into a point focus at the secondary focal point. However, the double parabolic trough suffers from reduced efficiency due to double reflection and imperfect mirrors increase the beam spread which lower the concentration. There is also a significant shading factor due to the incident flux block by the secondary concentrator.

Natan *et al.* (2003) designed a parabolic trough concentrator that has a receiver consisting of two parallel pipes with common inlet and outlet manifolds. It was reported that each receiver pipe received a different heating power due to focussing quality and they found that the water fed into the pipes absorbs less heat. This is an unfavourable conclusion from the practical operational point of view. The work with these pipes is continued, but further improvements are now carried out via simulations.

The hybrid design within the solar collector itself is not a new concept, where one such successful hybrid type is the photovoltaic/trough concentrator system (Blakers, 2001). The photovoltaic/trough concentrator system for the production of electricity in remote areas was developed in conjunction with Solahart, a solar company popular for producing domestic solar water heating systems. The PV/trough system is a solar concentrator system

suitable for the generation of both electricity and hot water. The system is based on sun tracking parabolic trough concentrator that reflects light onto a receiver lined with solar cells. The photovoltaic cells are illuminated with a concentration ratio of approximately 25 and convert about 20% of the sunlight into electricity. The remainder of the solar energy is collected by water flowing in a channel behind the solar cells. The resulting hot water that is collected can be used in the building on which the system is mounted. Suitable markets include light industrial enterprises such as hospitals, shopping centres and food processing plants, as well as residences may utilize this design system..

2.4 LIMITATIONS OF PARABOLIC TROUGH CONCENTRATOR

The benefits of parabolic trough concentrator have been highlighted in the previous sections of this chapter. The new parabolic trough designs indicate that there are research activities carried out to improve and enhance the performance of parabolic trough concentrators. Although improvement activities are intense, parabolic trough solar technology represents one of the successful renewable energy chronicles. Solar parabolic troughs are one of the lowest cost solar electric power options available today and have significant potential for further cost reduction (Price, 2003). The SEGS plants in California provide enough solar electricity to meet residential needs of 500,000 people (Cassady, 2003). Despite being the least cost solar power option, parabolic trough technology is still more expensive than the electrical power generated from conventional fossil fuelled power plants. Solar energy is usually complementary to fossil power sources, which include the parabolic trough based technologies (National Renewable Energy Lab, 2003).

Generally all types of solar collectors work best in climates that have high amount of solar radiation. They do not function as well on cloudy days, when available solar radiation is

mostly diffuse. Solar energy is normally considered as a diffuse energy source and to harness it can be costly. Reliable and cost-effective large-scale solar power generation requires the use of parabolic trough concentrators and these collectors work best with direct solar radiation (Price & Carpenter, 1999). Although the tropics have high solar radiation, the relatively high diffuse solar radiation make these regions less desirable but not totally impossible for large-scale solar electrical power generation.

There are reports stating that parabolic troughs are not used in Central Europe, because of its inability to utilise diffuse solar radiation (Solar Lexicon, 2004). Despite that, Krufer *et al.* (2000) carried out a study at the Test Centre of German Aerospace Research Institute in Koln-Porz to investigate the possibility of using parabolic troughs in Central Europe for solar process heat and solar district heat, with lower cost reflector materials. Herrmann *et al.* (2004) reported that thermal storage improves the overall performance and viability of parabolic trough power plants, allowing them to produce electricity on demand, independent of solar collection. Quaschning (2003) successfully used molten salt for high-temperature heat storage.

Almanza & Lentz (1998) compiled the research findings related to the current PTC electrical power systems where it was reported that the advantages of direct steam generation is the elimination of oil based heat transfer fluids and heat exchangers. But when Lippke (1996) made some theoretical studies related to direct steam production in a linear receiver under stratified conditions, he found out that thermal stress occurs in the pipe due to direct steam generation. Almanza *et al.* (1997) carried out experimental work and verified Lippke's findings. He found that the bend in the mild steel absorber pipe was over 6.5 cm when beam irradiance over the concentrator was around 980 W m^{-2} with a

flow of 1.0 liter min^{-1}. Such bends caused the glass envelopes to break and broken pieces from the glass envelope lead to severe and expensive damage to the mirrored reflectors. Almanza *et al.* (2000) reported that due to the bending of the receiver tube, the glass envelope tube was ruptured and the absorber tube was exposed to the atmosphere, ultimately creating an increase in heat loss. However, the impact of bending can be minimised by using a copper tube (Flores & Almanza, 2004).

The structure deformation of the concentrator made of mirrors due to winds can cause misalignment of the receiver's absorber tube and this deformation can also shatter the glass envelopes around the receiver tube (Eckhard *et al.*, 2001). The mirror strips used, as concentrators are fairly fragile and can easily break due to the structural deformation. Furthermore an enclosure is needed to protect the back of the mirrors from any stray flying objects especially during windy days. This will also add to the overall rigidity to protect the mirrors from cracking and will definitely increase the cost. The glass mirrors have an excellent reflective surface design, however mirror breakage would lead to an increase in maintenance costs. The method of attachment of the mirrors to the structure is not as reliable as required, leading to failures at the attachment interface (Cohen *et al.*, 1999). The reflector and protective structure must form an integral part of the concentrator to provide a highly reflective and accurately shaped parabolic trough (Kalogirou *et al.*, 1994a).

There is also a problem of getting the right curvature for the mirrors to be used. One such collector built for the test pilot plant of Mexico's Engineering Institute of Solar Thermal Power needed around 16 mirrors, each with a surface area of 0.18 m^2. The specular reflectance of the mirrors was around 86 % with around 90 % of the reflected beam solar irradiance arriving on a simulated receiver tube. These 16 mirrors had 3 different curvatures, in order to assemble a parabolic concentrator. Each mirror was fixed to the

parabolic trough support shell with silicone glue (Martinez *et al.*, 2000). Due to the need to prepare the mirrors with specific curvatures, mirrors are one of the major items contributing to the capital cost of parabolic trough concentrators. The maintenance cost is also high as these mirrors also face other problems such as surface abrasion, scratches and corrosion (Almanza *et al.*, 1995).

The price of parabolic trough's components are unlikely to fall dramatically with mass production, as the cost of the material already represents a significant fraction of the total cost. Significant price reductions are more likely to result from the development of innovative designs (Price & Carpenter, 1999) and these designs will be able to contribute an overall cost reduction for parabolic trough power plants of about 40 % within the next 10 years (Stephen, 1999). It can be summarised that the limitations faced by parabolic troughs are due to the application of current technology, which is inefficient, underdeveloped, and expensive (Price, 1999). But, the limitations can be solved and there are other considerations that should be made, where if solar parabolic trough thermal energy systems are well supported, their cost would be competitive even with today's low efficiencies (Price & Kearney, 2003). The fundamental justification for the application of parabolic trough concentrator is that energy from the sun is virtually free especially after the initial implementation cost has been recovered. Solar energy is clean, which is useful to preserve the environment while providing for a secure energy source for the future. By making use of solar energy, pollution can be reduced and this will ensure a better quality of life for our country.

2.5 RESEARCH OBJECTIVES

Malaysia is close to the equator and has abundant of sunshine. However, it is rare to have a full day with completely clear skies even in periods of severe drought. It is also equally

rare to have days without sunshine in a stretch, except during the northeast monsoon seasons. Clouds are the predominant atmospheric condition that determines the amount of solar radiation that reaches the earth. Therefore, the amount of solar energy that is available during the day depends on the local sky conditions. Zain-Ahmed *et al.* (2002) reported that solar energy is available anywhere in Malaysia on a reasonable scale with a predominantly intermediate sky.

If compared to Malaysia, Alaska's climate can be considered as an impractical location for the application of solar thermal energy. During midwinter in Alaska, the sun does not even come up, but in summer, it receives solar energy in an amount comparable to that received at the Equator. The annual solar energy available to the latitude region covered by Alaska is only about one-third of that available in Malaysia, but the amount is considered as substantial. It is projected that solar heating might take over completely in Alaska once there is an improvement in technology (Davis, 1979). Solar energy is viable even in harsh climates, where a suitable innovative design can be considered and simulations can be used together with the meteorological data of a particular location when designing a particular solar energy system (Quaschning *et al.*, 2001). Although parabolic trough based technologies might provide an intermittent energy supply at certain locations, solar power can be utilized through the integration of thermal energy storage (Herrmann *et al.*, 2004). Thermal energy storage allows thermal energy collected during clear sky hours to be later retrieved during unfavourable weather conditions.

The main objectives of this research are to develop theoretical formulations of a new design of a parabolic trough concentrator, to conduct experimental studies and compare with the theoretical results based on local meteorological data and to determine the effect of design parameters on the performance of the new parabolic trough system. In order to carry out the experimental studies, an experimental model is designed based on simulations

carried out on the parabolic trough's geometry. Simulation software is produced to carry out system simulation and the efficiency of parabolic trough collector can be determined by using local meteorological data. The meteorological data used is processed to separate beam and diffuse components. The simulation software will be used to carry out simulation studies at 5 different locations in Malaysia to show that it is viable to a certain extent to use parabolic trough concentrator.

This research work exploits the possibility of designing a hybrid parabolic trough concentrator that can procure the advantage of the flat plate collector and concentrating collector related technologies. A new design is proposed to utilise the unreflected and diffuse solar radiation. The new design uses a cost effective reflective film reflector over a rigid parabolic trough frame. The accuracy of the surface depends primarily upon the accuracy of the frame and this eliminates the need to use mirrors of different curvature to form the parabolic surface. The rigid frame will also minimise the deformation risk of the parabolic geometry. A description of the new design will be discussed in Chapter 6. The end products of this research work are a computer simulation program and an experimental prototype model. The simulation program is flexible, and can be used to predict the performance of this new design under a wide range of meteorological conditions and different design parameters. The simulation software was used to design the new prototype experimental model. The results obtained provided useful information pertaining to the performance of this new prototype model. The experimental results were also compared with the simulated data, and the simulation software gives good predictions, which are around 95 % accurate. The processing of the meteorological data will be discussed in the next chapter.

CHAPTER 3

PROCESSING OF METEOROLOGICAL DATA

There are different types of climate all over the world, where the warmer ones are closer to the equator and colder ones are nearer to the North and South Poles. The tropical climate zone is defined as the area of land and water between latitudes of 23.5° N and 23.5° S. The tropics occupy approximately 40% of the earth's land surface and provide home to almost half of the world 's population. There are variations in climate within the tropics, but 90% of the tropical zones represent hot and humid climatic regions and the remaining 10% is desert-like with hot and dry conditions (Baish, 1987). Malaysia is situated near the equator, between latitudes of 1.0° N and 6.0° N and has a tropical climate with high temperatures and rainfall all year round. The main differences of climate within the country are due to differences of altitude and the exposure of the coastal lowlands to the alternating northeast and southwest monsoon winds. Malaysia has abundant of sunshine but it is unusual to have a full day with completely clear skies. The relative humidity is in the range of 80 % to 90 %, and the temperature averages from 20° C to 30° C throughout the year.

3.1 SOLAR RADIATION

Solar radiation originates from the sun, which can be taken as a sphere of intensely hot gaseous matter. Solar radiation is the electromagnetic radiation emitted by the sun, where most of the radiation is in the broadband solar radiation wavelength region of 280 nm to 4000 nm. The region of the spectrum that is visible to all of us is in the wavelength range of about 380 nm to 720 nm (Serway & Beichner, 2000). Solar radiation which can be converted to useful energy lies between 0.3 μm and 3.0 μm (Garg & Prakash, 1997). The

sun's radius is estimated to be around 6.96×10^8 m, which is around 109 times the radius of the earth. The distance between the earth and the sun varies as the earth rotates around the sun in an elliptical orbit, where earth is approximately 1.47×10^{11} m away from the sun on 4th January and is approximately 1.53×10^{11} m away on the 4th July (Sukhatme, 1996). The variation in the distance between the earth and the sun does not have a significant effect on the amount of solar radiation that reaches earth. Although the outer surface effective temperature of the sun is approximately 6000 K, the innermost core temperature is estimated to be in the region of 8×10^6 to 40×10^6 K (Duffie & Beckman, 1980). The sun is a continuous fusion reactor where gravitational forces retain the constituent gases, mainly hydrogen followed by helium. All these gases are at very high pressures, suitable for nuclear reaction where four hydrogen atoms combine to form one lighter helium atom, in a process where energy is released (Knoepfel, 1986).

3.2 SOLAR CONSTANT

Solar constant refers to the rate at which solar radiation strikes the earth's upper atmosphere where it is the average amount of energy received in a unit of time on a unit of area perpendicular to the sun's direction at the mean distance of the earth from the sun (Thekaekara, 1973). The average intensity of solar radiation reaching the upper atmosphere is about 1353 W/m^2. The World Radiation Centre in Switzerland has adopted a different value for the solar constant, which is around 1367 W/m^2 (Frohlich & Brusa, 1981). The amount of this energy that actually reaches the earth's surface will vary according to atmospheric and meteorological conditions. The solar rays that move through the atmosphere can be absorbed, scattered and reflected by air molecules, water vapour, clouds, dust and pollutants. Global solar radiation refers to the sum of the beam and diffuse solar radiation. Figure 3.1 shows that atmospheric conditions can influence the amount of

solar radiation that is received at the earth's surface. The thick clouds that cover the sun for a period of approximately 6 minutes cause a sharp decline in the amount of solar radiation that reached the surface of the earth. This figure shows that the highest value of solar insolation that arrived at the surface of the earth at Bercham, Ipoh on the 25th January 2003 at 12.13 noon was 560 W/m^2, which is approximately 41 % of the solar constant of 1353 W/m^2. As the clouds move past the sun, the average fraction that arrived was around 15.2 %, which indicates that the impact of cloudiness is very significant.

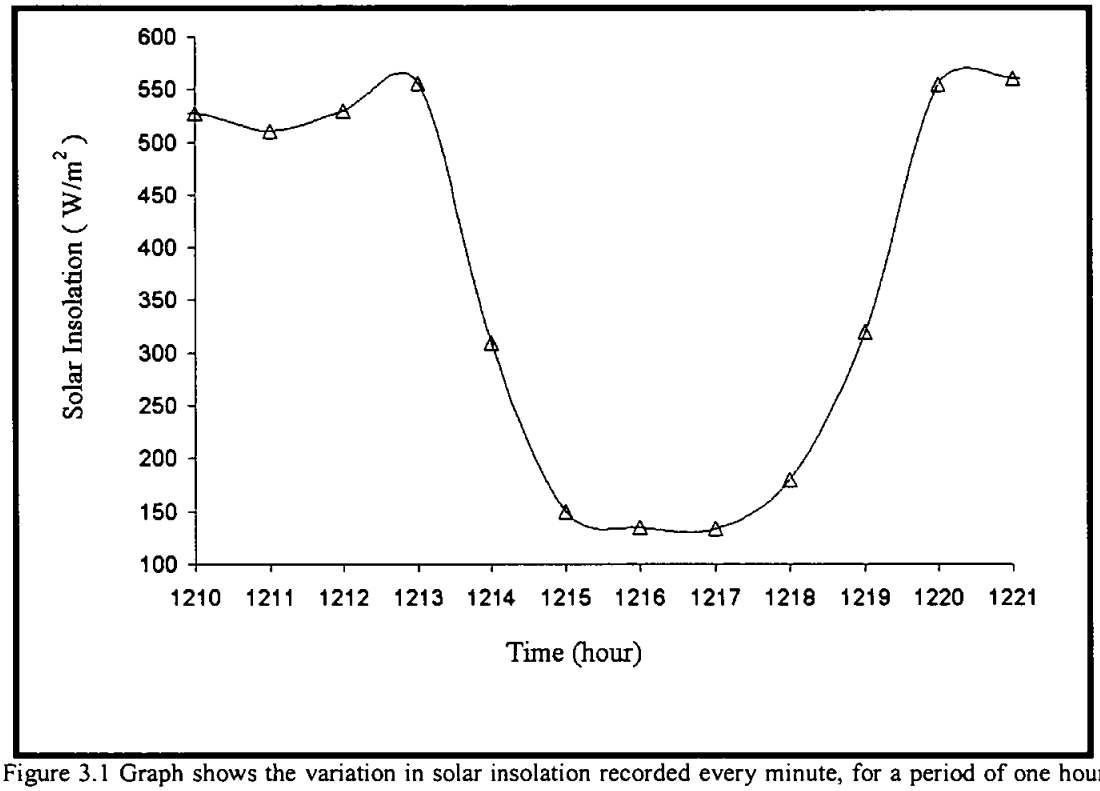

Figure 3.1 Graph shows the variation in solar insolation recorded every minute, for a period of one hour, from 12.00 noon to 1.00 pm, at a location in Bercham, Ipoh on the 25 January 2003.

3.3 EARTH'S ROTATION

Since the earth is rotating all the time, the daily rotations and seasonal movements on its axis have significant implications especially if the solar energy is to be harvested into useful energy. Due to the earth's daily rotation and yearly revolution around the sun, the amount of energy that reaches its surface varies on hourly basis and is even considered as seasonal and depends on the location. The earth rotates on its own axis of rotation and moves in an elliptical path as shown in Figure 3.2.

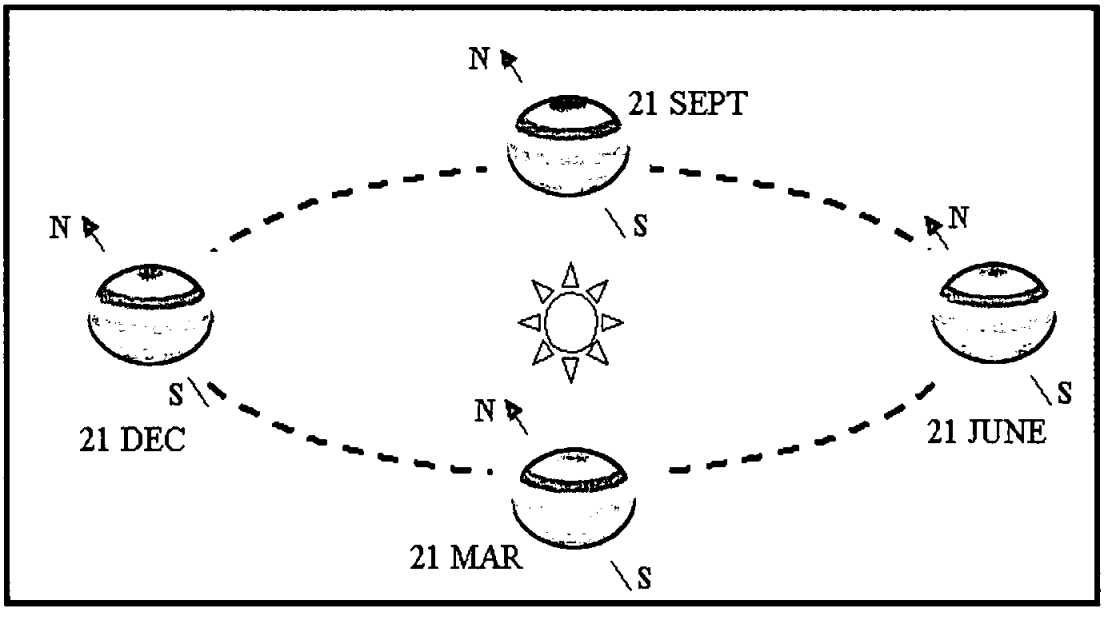

Figure 3.2 Positions of the earth, with the sun at the focus of the elliptical path of the earth's rotation around the sun.

The earth's axis of rotation is tilted at 23.5° with respect to its elliptical axis about the sun. The elliptical path is called the earth's orbit and earth keeps it axis orientated at the same tilted angle as it revolves around the sun. The following equation 3.1 relates the solar constant I_{SC} to extraterrestrial solar radiation I_{ET}, which varies with the time of the year where m is the day number counted from January 1st. The term extraterrestrial solar

radiation here refers to the radiation that would be received if there were no atmosphere (Anderson, 1983).

$$I_{ET} = I_{SC}\left(1 + 0.033\cos\frac{360m}{365}\right) \qquad (3.1)$$

The variation in the extraterrestrial solar flux is due to the variation in the earth-sun distance and this is caused by the revolution of the earth in its orbit as shown in Figure 3.2. The dates shown on Figure 3.2 are related to autumnal equinox on 21 September, vernal equinox on 21 March, winter solstice on 21 December and summer solstice on 21 June.

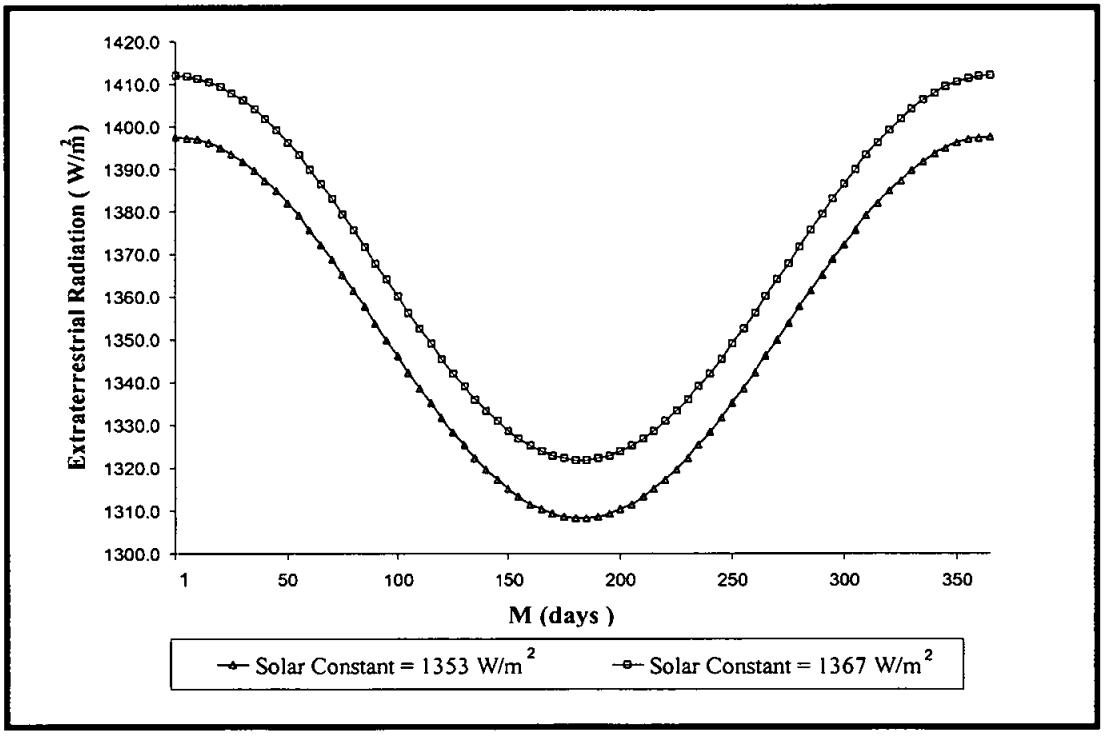

Figure 3.3 Graph showing the variation in the extraterrestrial solar radiation with the time of the year.

Malaysia is at the vicinity of the equator where the sun is most intense during the autumnal and vernal equinoxes as during this period the sun is directly overhead.

3.4 SOLAR RADIATION GEOMETRY

Based on the discussion in the previous section, it is clear that the sun's path in the sky on various days in a year is a fundamental pre-requisite for designing solar energy devices. Although the value of the solar constant indicates that the amount of solar radiation that reaches just outside the earth is high, about 30 % is reflected back into space, around 47 % of it is absorbed by the atmosphere, land surface and oceans and the remaining 23 % drives the evaporation, convection and precipitation phases (Halacy, 1980). The value of the solar constant that will be used in this thesis is 1353 W/m^2 and this equals to approximately 4.9 MJ/m^2 amount of energy per unit area, for a period of one hour. Since all these values sound promising, it would be worthwhile to investigate the solar geometry, for the optimal design of the whole system as tracking is necessary for parabolic trough concentrators.

3.4.1 DECLINATION ANGLE OF THE EARTH

The angular displacement of the sun from the plane of the earth's equator is referred to as the angle of declination δ. As the earth revolves around the sun, the angle of declination varies from +23.45° to –23.45°. The variation can be estimated based on the day of the year by using equation 3.2 (Cooper, 1969).

$$\delta = 23.45\sin\left[\frac{360(284+m)}{365}\right] \qquad (3.2)$$

The calculated δ can be assumed to be a constant for a particular selected day, where m is the day number counted from January 1st. Figure 3.4 shows the variation of δ with m day of the year.

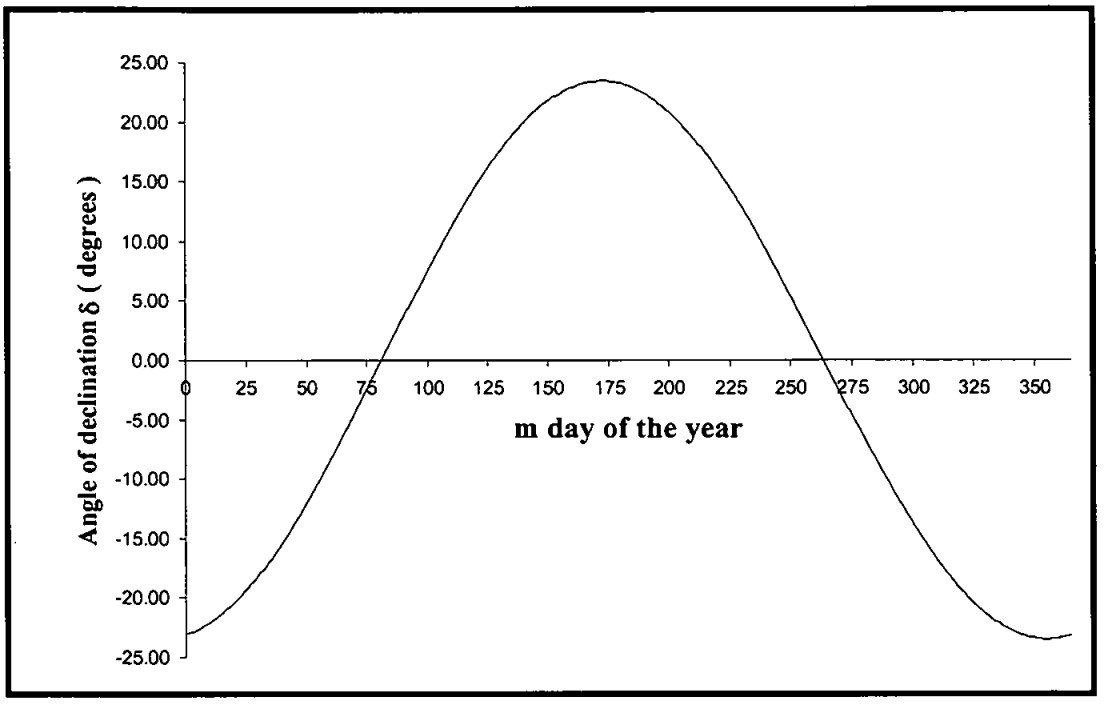

Figure 3.4 Graph showing variation in the angle of declination with m day of the year.

3.4.2 ANGLE OF INCIDENCE OF BEAM RADIATION

The angle of incidence θ is the angle between the beam radiation that strikes a surface and the normal of that particular surface. The evaluation of this angle is very important, as the tracking requirements are dependent on it. The value of θ can be obtained by using equation 3.3 (Magal, 1990).

$$\theta = \cos^{-1}[A - B + C + D + E] \qquad (3.3)$$

Equations 3.4 to 3.8 provide the values for the variables A, B, C, D and E used in Equation 3.3. The angles that are used in the equations are angle of declination δ, hour angle ω, surface azimuth angle γ, slope angle β and the latitude ϕ.

$$A = \sin\delta \sin\phi \cos\beta \qquad (3.4)$$

$$B = \sin\delta\cos\phi\sin\beta\cos\gamma \qquad (3.5)$$

$$C = \cos\delta\cos\phi\cos\beta\cos\omega \qquad (3.6)$$

$$D = \cos\delta\sin\phi\sin\beta\cos\gamma\cos\omega \qquad (3.7)$$

$$E = \cos\delta\sin\beta\sin\gamma\sin\omega \qquad (3.8)$$

The angles that are used to estimate the value of θ will be described in the next section, except for angle of declination δ, which was discussed earlier.

3.4.3 ANGLES USED IN ESTIMATING ANGLE OF INCIDENCE

The angles that were used to estimate the angle of incidence θ are the angle of declination δ, hour angle ω, surface azimuth angle γ, slope angle β and latitude ϕ. The hour angle is the angular displacement of the sun to the east or west of the local meridian and this is due to the earth's rotation on its axis at 15° per hour. The hour angle displacement in the morning is taken to be negative, while in the afternoon is positive. The exact value of the hour angle ω at any particular time t in hours can be obtained by using equation 3.9, which was developed specifically for simulation programming. The time that is expressed in hours must be separated to hour t_1 and minutes assigned to t_2. For example, if the time in hours is 10:45, then t_1 is 10 and t_2 becomes 45.

$$\omega = (0.25t_2 + 15t_1 - 180)^\circ \qquad (3.9)$$

Surface azimuth angle γ is the deviation of the projection on a horizontal plane of the normal to the surface from the local meridian. The angle is set at zero for direction towards the south meanwhile, the east and west directions are set to be negative and positive respectively. The range for this angle γ is from -180° to 180°. The slope angle β is usually referred to as the tilt angle as it is measured between the tilted surface and the horizontal. Lastly latitude angle ϕ is the angular location north or south of the equator. The northern latitude is set to have positive values and vice versa. The range of latitude is from –90° to 90°.

3.4.4 ANGLE OF INCIDENCE FOR TRACKING MECHANISM

In this section, based on equation 3.3, specialized equations to estimate the angle of incidence based on tracking specifications will be given. The description of different tracking modes will be done in the following chapter, however, derivations of the equations related to the modes are done in this chapter.

Tracking systems can be classified by the mode of their trailing motion. Tracking can be done in one dimension, which involves rotation about a single axis or tracking about two axes. If a plane is rotated about a horizontal east-west axis, with only a single daily adjustment, the angle of incidence is then given by equation 3.10 (Bush & Richards, 1980).

$$\cos\theta = \sin^2\delta + \cos^2\delta\cos\omega \qquad (3.10)$$

By using equation 3.10, the surface normal will coincide with the beam radiation at noon every day. If a plane tracks the sun continuously and is mounted on a horizontal east-west axis with the movement in the north-south direction, the minimum angle of incidence is given by equation 3.11 (Sukhatme, 1996).

$$\cos\theta = \sqrt{(1-\cos^2\delta\sin^2\omega)} \qquad (3.11)$$

Just like in the previous case, a continuously tracking plane now mounted on a horizontal north-south axis will have a minimum angle of incidence described by equation 3.12 (Duffie & Beckman, 1980).

$$\cos\theta = \sqrt{(\sin\phi\sin\delta+\cos\phi\cos\delta\cos\omega)^2+\cos^2\delta\sin^2\omega} \qquad (3.12)$$

Usually the last two tracking orientations are favourable, as they are used to maximize the solar energy interception. The angle of incidence for the plane rotated about a north-south axis, tilted at an angle equal to the local latitude, making it parallel to the earth's axis is given by equation 3.13 (Bush & Richards, 1980).

$$\cos\theta = \cos\delta \qquad (3.13)$$

The above way of mounting is sometimes referred to as polar mount and continuous adjustment is required. Finally for a two axis tracking plane, the angle of incidence is given perhaps by the simplest equation so far, for example equation 3.14 and in this tracking method, the plane faces the sun at all times (Duffie & Beckman, 1980).

$$\cos\theta = 1 \qquad (3.14)$$

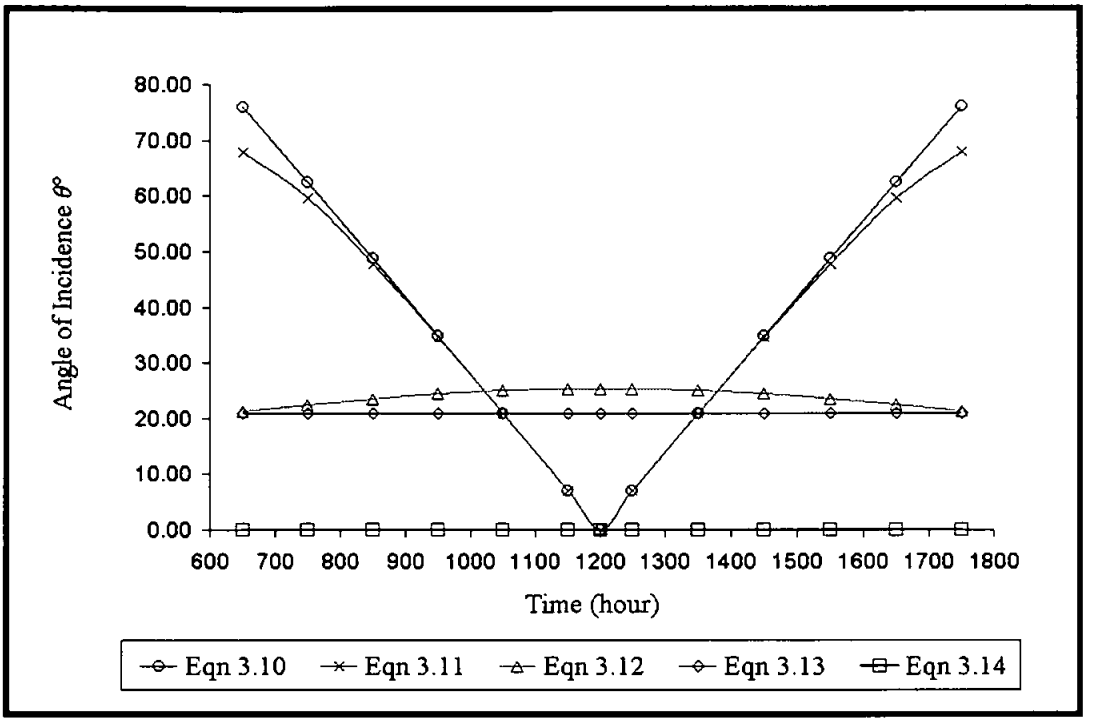

Figure 3.5 Graph showing the variation in the estimated value of angle of incidence with the local solar time, based on the five different equations discussed earlier. The calculations are for January, at a latitude of 4.57°, which is for Ipoh.

3.5 GLOBAL RADIATION SEPARATION METHOD

The solar radiation data obtained from the local meteorological department is the global or total solar radiation. The data is measured for horizontal surfaces and includes both direct and diffuse radiation. Direct or commonly referred to, as beam radiation is one of the components of global radiation, besides diffuse radiation. In the performance analysis of a parabolic trough concentrator, it is important to separate the beam radiation from diffuse radiation.

3.5.1 EXTRATERRESTRIAL SOLAR RADIATION ON HORIZONTAL SURFACE

Earlier, equation 3.1 gave the value of I_{ET}, the extraterrestrial solar radiation that would be received by a surface if there were no atmosphere. In the calculation of daily solar radiation, it is necessary to have the extraterrestrial solar radiation arriving on a horizontal surface to be integrated for daily solar insolation. The following equation 3.15 gives the daily horizontal extraterrestrial solar radiation obtained for the period from sunrise to sunset (Klein, 1977).

$$H_O = 27490.9 I_{ET}\left[\cos\phi\cos\delta\sin\omega_s + \left(\frac{11}{630}\omega_s\sin\phi\sin\delta\right)\right] \qquad (3.15)$$

Here the angle ω_s is the sunset hour angle and is obtained when the zenith angle θ_Z equals to 90°. Equation 3.16 gives the expression for zenith angle θ_Z, which will be used to derive equation 3.17 by using θ_Z equals to 90° (Goswami *et al.*, 2000).

$$\cos\theta_Z = \cos\delta\cos\phi\cos\omega + \sin\delta\sin\phi \qquad (3.16)$$

$$\cos\omega_s = -\tan\phi\tan\delta \qquad (3.17)$$

The monthly mean of the daily extraterrestrial solar radiation $\bar{H}_O$ is obtained by using m and δ for the mean day of a particular month. Once the value of $\bar{H}_O$ is obtained, together with the horizontally measured monthly mean of the daily global solar radiation $\bar{H}$, the monthly average clearness index can be determined by using equation 3.18 (Rabl, 1985).

$$\bar{K}_T = \frac{\bar{H}}{\bar{H}_O} \qquad (3.18)$$

3.5.2 MONTHLY MEAN OF THE DAILY DIFFUSE RADIATION

Still pursuing the jaunt of estimating the fractions of global horizontal solar radiation that are beam and diffuse, equation 3.19 is a general correlation developed by Page (1961). The correlation is used to estimate the monthly mean of the daily diffuse radiation, for latitudes between 40° N and 40°S. A similar correlation was also developed for Petaling Jaya by Azni-Zain *et al.*(1991) and seems to be agreeable to the one developed by Page (1961).

$$\overline{H}_d = (1.000 - 1.130\overline{K}_T)\overline{H} \qquad (3.19)$$

The estimated value of $\overline{H}_d$ is based on $\overline{H}$, which is the measured value for monthly mean of daily global horizontal radiation.

3.5.3 MONTHLY MEAN OF THE HOURLY DIFFUSE RADIATION

The last step in obtaining the desired hourly mean diffuse solar radiation is by using the correlation developed by Liu & Jordan (1960). The correlation is given as equation 3.20 and uses the hour angle ω as well as sunset hour angle ω_s (Liu & Jordan, 1960).

$$\bar{I}_d = \frac{11\overline{H}_d}{84}\left(\frac{\cos\omega - \cos\omega_s}{\sin\omega_s - \frac{11}{630}\omega_s\cos\omega_s}\right) \qquad (3.20)$$

Once the hourly mean diffuse solar radiation is determined, the hourly mean beam solar radiation I_b can be obtained by using a simple relationship as given by equation 3.21, where $\bar{I}_G$ is the measured hourly mean horizontal global radiation (Magal, 1990).

$$\bar{I}_b = \bar{I}_G - \bar{I}_d \qquad (3.21)$$

3.6 HOURLY SOLAR RADIATION ON TILTED SURFACES

Since the global solar radiation provided by the local meteorological department is measured horizontally, there is a need to calculate the hourly radiation on tilted surfaces. This is essential for the purpose of designing a solar thermal device and to carry out performance analysis of the whole system.

The geometric factor R_b that is the ratio of beam radiation on a tilted surface to the radiation on a horizontal surface will be useful to calculate the amount of solar radiation that is received by the tilted surface of solar collectors. The evaluation of R_b involves the angle of incidence θ and zenith angle θ_z. The relationship between these two angles is given in equation 3.22 (Liu & Jordan, 1961).

$$R_b = \frac{\cos\theta}{\cos\theta_z} \qquad (3.22)$$

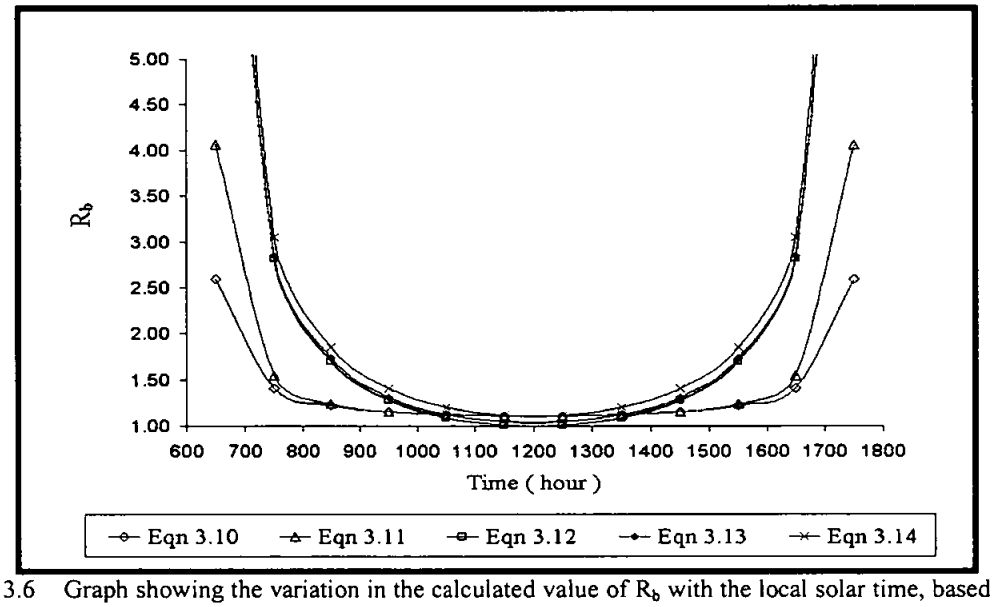

Figure 3.6 Graph showing the variation in the calculated value of R_b with the local solar time, based on the five different equations to calculate the value of θ, as discussed in section 3.3.4. These calculations are for January, at a latitude of 4.57°, which is for Ipoh.

The value R_b can be determined for the different tracking modes that have been discussed earlier. Figure 3.6 shows how R_b varies with the different tracking modes and analysing Figure 3.6 together with Figure 3.7 can explain the variation. Obviously as the sun moves to the highest position in the sky during solar noon, the zenith angle of the sun, normal to a horizontal plane reduces. This is shown in Figure 3.7 and by using equations 3.16 and the equations used to calculate angle of incidence; the amount of beam radiation received by moving surfaces can be determined.

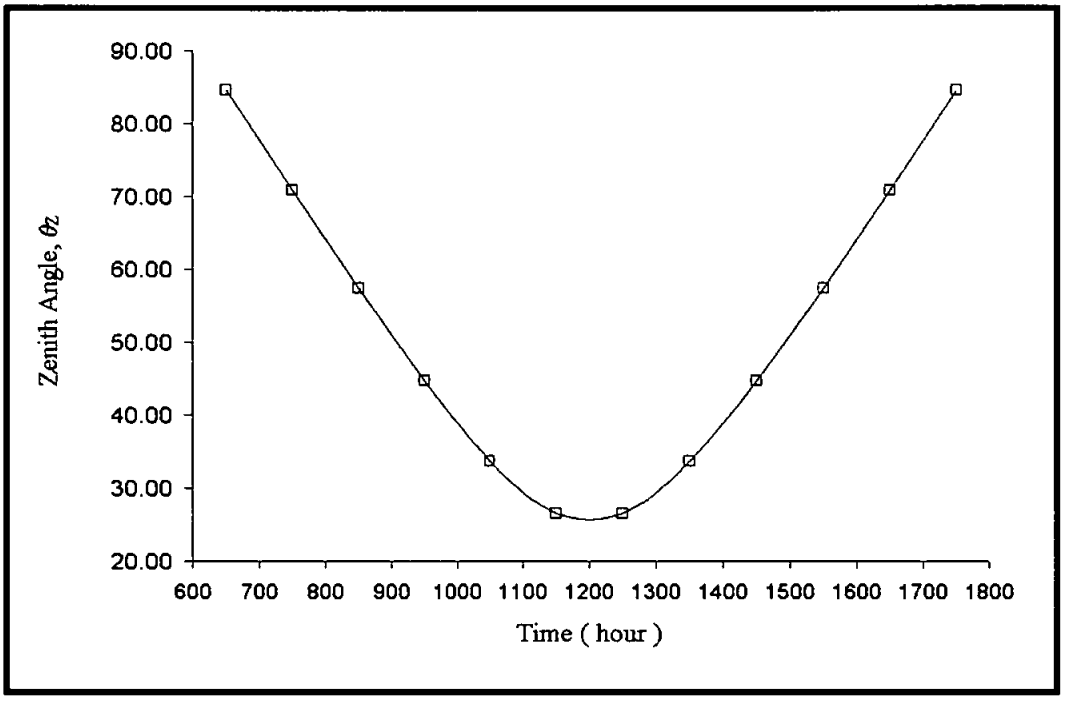

Figure 3.7 Graph showing the variation in the zenith angle with the local solar time, used to obtain the graph in Figure 3.6, where the angle of declination is calculated for a mean day in January at a latitude of 4.57°, which is for Ipoh.

The diffuse component of solar radiation also uses a factor R_d to calculate the diffuse radiation on tilted surfaces. The factor R_d is defined as the ratio of diffuse radiation on a tilted surface to diffuse radiation on a horizontal surface. The value of R_d can be obtained by using equation 3.23 (Liu & Jordan, 1961).

$$R_d = \frac{1+\cos\beta}{2} \qquad (3.23)$$

The global radiation on a tilted surface I_T can be calculated by using equation 3.24, however equation 3.25, which uses both the factors, is very useful as it summarises the whole process of estimating the amount of radiation that is received by tilted surfaces (Garg, 1982).

$$I_T = I_{bT} + I_{dT} \qquad (3.24)$$

$$I_T = I_b R_b + I_d R_d \qquad (3.25)$$

The symbols I_{bT} and I_{dT} represent the beam and diffuse radiations received on a tilted surface.

3.7 SOLAR INSOLATION DATA

The performance evaluation of parabolic trough concentrators requires simulation to be carried out where different design specifications can be simulated by using the same meteorological conditions. The locality is important as stable and high amount of solar insolation received can be identified. The solar radiation data for 5 different locations in Malaysia were obtained from the Meteorological Department. The solar radiation data was in text format and had to be re-arranged to fit into a spreadsheet, so that the data can be analysed. By using the spreadsheet, the data for a few locations can easily be compared, as shown in Figure 3.8. The data provided is daily hourly global solar radiation, in MJ/m^2. The data was used to get the average daily solar radiation for the month of May 2001 for Bayan Lepas, Ipoh and Cameron Highlands. On the monthly average, Bayan Lepas, Ipoh and Cameron Highland received 17.24 MJ/m^2, 17.96 MJ/m^2 and 16.31 MJ/m^2 respectively. The large amount of data shown in Figure 3.9 is only for a period of one month, for one particular location only. The task of storing all these values in programming software database is tedious.

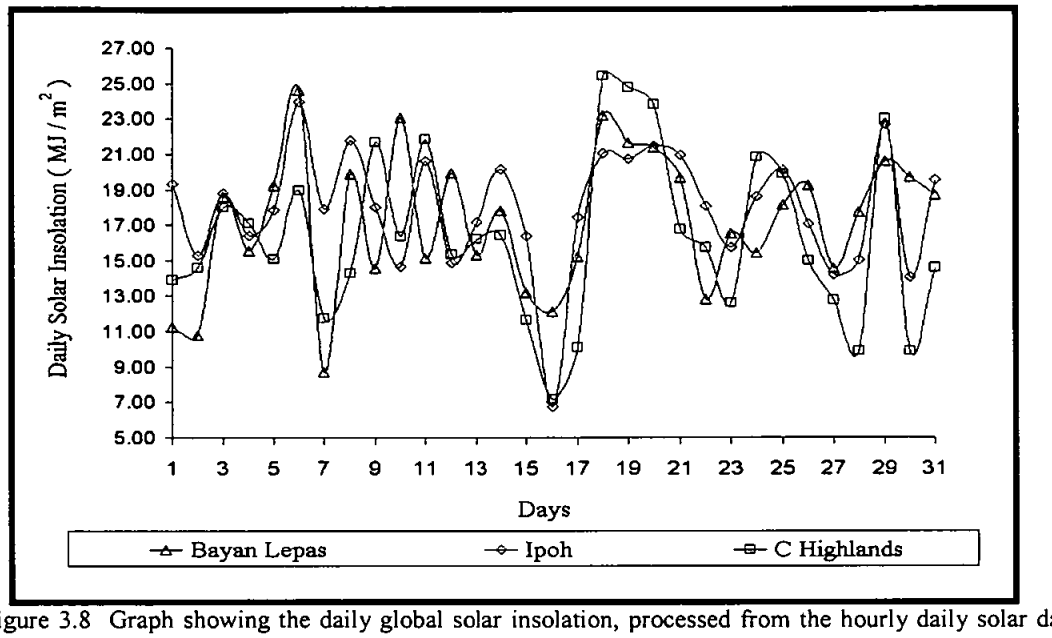

Figure 3.8 Graph showing the daily global solar insolation, processed from the hourly daily solar data obtained from the meteorological department.

Station : CAMERON HIGHLANDS
Lat : 04 ° 28 'N Long : 101 ° 22 'E
Ht. Above M.S.L. : 1545.0 m Unit : MJm^{-2}

Records of Hourly Global Radiation
Data for May 2001

day	Time in Hours														Daily Total MJm^{-2}
	6	7	8	9	10	11	12	13	14	15	16	17	18	19	
1	0.00	0.28	0.81	1.26	1.63	2.09	2.12	2.84	0.90	1.08	0.50	0.35	0.09	0.00	13.94
2	0.00	0.07	0.27	0.66	1.06	1.58	1.65	2.38	2.89	1.95	1.31	0.62	0.16	0.00	14.60
3	0.00	0.14	0.57	1.82	2.12	2.21	2.98	2.59	2.30	1.69	1.02	0.42	0.15	0.00	18.01
4	0.00	0.21	0.85	1.33	1.61	1.39	2.50	2.34	2.41	2.26	1.05	0.91	0.25	0.00	17.11
5	0.00	0.07	0.48	2.08	2.87	3.47	3.52	1.17	0.12	0.43	0.51	0.33	0.07	0.00	15.12
6	0.00	0.28	1.26	2.36	3.07	2.32	2.37	2.24	2.18	1.25	1.32	0.13	0.17	0.00	18.95
7	0.00	0.25	0.77	0.69	1.04	1.49	3.05	1.49	2.29	0.47	0.09	0.10	0.04	0.00	11.77
8	0.00	0.09	0.59	1.37	1.83	3.49	3.33	2.36	0.67	0.17	0.29	0.11	0.01	0.00	14.31
9	0.00	0.15	0.74	2.20	2.73	3.62	3.74	3.80	3.30	0.59	0.52	0.26	0.02	0.00	21.67
10	0.00	0.52	0.87	1.40	2.67	3.85	2.19	2.03	1.08	0.51	1.15	0.07	0.01	0.00	16.35
11	0.00	0.39	1.16	2.10	2.89	3.24	3.63	3.78	2.67	1.25	0.59	0.12	0.02	0.00	21.84
12	0.00	0.25	0.75	1.25	1.96	2.24	1.55	1.56	2.21	2.23	0.71	0.53	0.14	0.00	15.38
13	0.00	0.21	0.89	1.56	1.53	1.92	2.86	2.52	0.97	1.53	1.63	0.37	0.21	0.00	16.20
14	0.00	0.19	1.01	1.98	2.15	2.04	2.98	2.20	1.98	0.71	0.64	0.52	0.02	0.00	16.42
15	0.00	0.18	0.74	1.13	1.57	1.46	1.15	2.04	1.11	0.59	0.94	0.50	0.21	0.00	11.62
16	0.00	0.12	0.28	0.49	0.27	0.17	0.95	1.17	1.54	0.70	0.77	0.57	0.17	0.00	7.20
17	0.00	0.13	0.48	1.32	1.07	1.55	1.03	0.87	1.16	0.48	0.77	0.99	0.25	0.00	10.10
18	0.00	0.17	0.87	1.81	2.76	3.40	3.81	3.93	3.13	3.05	1.69	0.65	0.11	0.00	25.38
19	0.00	0.25	1.04	2.04	2.90	3.40	3.95	3.98	2.94	2.11	1.35	0.59	0.23	0.00	24.78
20	0.00	0.35	1.23	2.04	2.83	3.51	3.76	3.12	2.76	2.84	1.11	0.14	0.12	0.00	23.81
21	0.00	0.27	1.02	1.63	2.04	2.19	2.01	1.45	2.60	2.13	0.93	0.37	0.10	0.00	16.74
22	0.00	0.10	0.37	0.81	1.44	1.89	2.90	2.86	2.19	0.81	0.99	1.14	0.23	0.00	15.73
23	0.00	0.07	0.62	2.06	2.09	1.46	1.82	1.84	1.56	0.36	0.29	0.30	0.12	0.00	12.59
24	0.00	0.13	1.01	2.00	2.89	3.49	3.35	2.99	2.43	1.75	0.53	0.24	0.02	0.00	20.83
25	0.00	0.33	0.59	0.44	1.86	3.27	3.65	3.41	3.27	2.12	0.52	0.27	0.17	0.00	19.90
26	0.00	0.19	0.63	1.20	1.47	1.98	2.05	2.31	1.13	1.17	1.46	1.26	0.13	0.00	14.98
27	0.00	0.28	0.92	1.83	2.31	2.91	2.83	0.49	0.47	0.27	0.26	0.16	0.05	0.00	12.78
28	0.00	0.23	1.07	1.29	1.95	1.52	0.99	0.38	0.63	0.95	0.41	0.37	0.11	0.00	9.90
29	0.00	0.30	0.92	2.13	2.70	3.13	2.88	3.24	3.01	2.64	1.26	0.62	0.18	0.00	23.01
30	0.00	0.26	1.13	1.39	1.74	1.34	1.21	0.87	0.17	0.15	0.92	0.66	0.03	0.00	9.87
31	0.00	0.39	1.23	2.05	2.75	3.07	1.15	0.87	1.08	0.15	1.28	0.53	0.09	0.00	14.64
Monthly Total	0.00	6.86	25.17	47.72	63.80	74.68	77.96	69.12	57.15	38.39	26.81	14.20	3.68	0.00	506.53
Monthly Mean	0.00	0.22	0.81	1.54	2.06	2.41	2.51	2.23	1.84	1.24	0.86	0.46	0.12	0.00	16.31

Figure 3.9 The hourly solar radiation data re-compiled from the data provided by the meteorological data, which was in a text format. By using the data arranged in a spreadsheet, some instant statistical analysis can be carried out.

In Figure 3.10, the monthly daily hourly mean solar insolation data is plotted for the month of May 2001 for Ipoh and a sinusoidal fit is applied to the curve. Using the same plot for the month of May 2001, a polynomial fit is also applied and is shown in Figure 3.11 for comparison purpose.

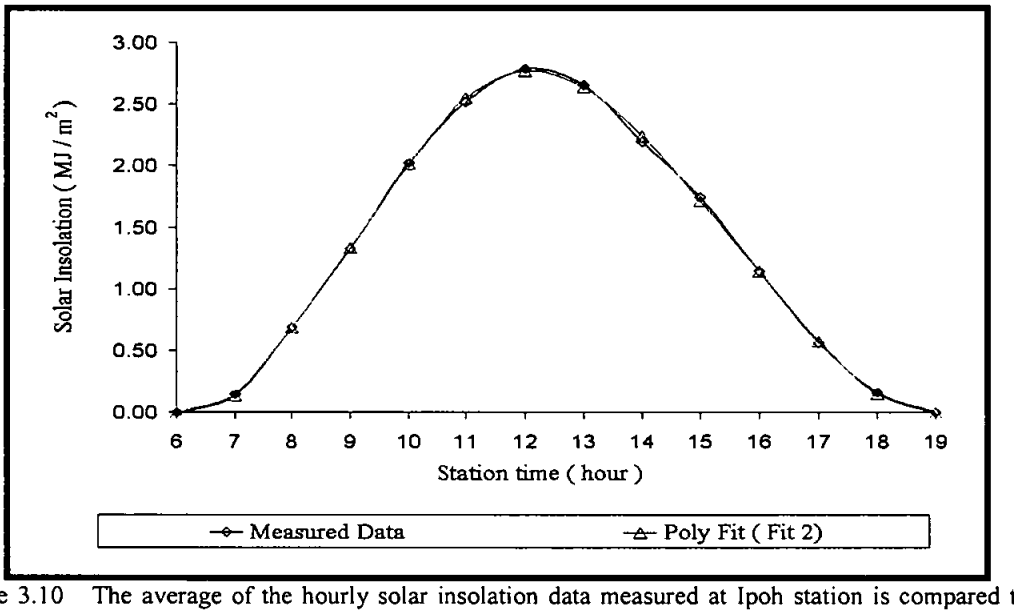

Figure 3.10 The average of the hourly solar insolation data measured at Ipoh station is compared to a polynomial curve fit.

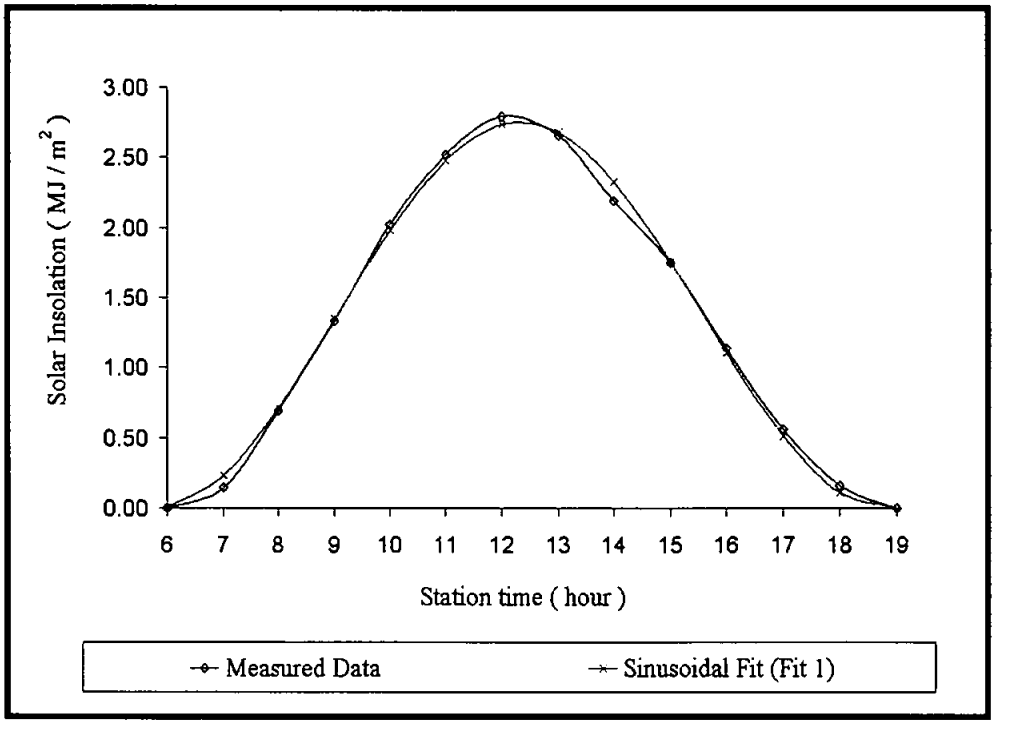

Figure 3.11 The average of the hourly solar insolation data measured at Ipoh station is compared to a polynomial fit.

The correlation coefficient for the sinusoidal fit and measured data is 99.85 % and the equation defining this curve fit for the month of May 2001 for Ipoh is given as equation 3.26.

$$I_G = 1.3720 + [1.3764\cos(0.4796t + 0.3748)] \qquad 6 \le t \le 19 \qquad (3.26)$$

However the correlation coefficient of the polynomial fit and measured data is 99.98 % and is to the order of nine. The equation defining this curve fit for the month of May 2001 for Ipoh is given as equation 3.27.

$$I_G = 1225.24 - 1011t + 363.51t^2 - 74.737t^3 + 9.67517t^4 - 0.8173t^5 + 0.04506t^6 - 0.00156t^7 + (3.11\times10^{-5})t^8 - (2.7\times10^{-7})t^9 \qquad 6 \le t \le 19 \qquad (3.27)$$

As both the fits have very high percentage of accuracy, any one of them may be selected, depending entirely on the type of programming software. The same process was also repeated for the other months, where sinusoidal and polynomial fits showed high degrees of accuracy, exceeding 96 %. If the sinusoidal or polynomial fits are used, it is noticed that the processing time is reduced, when compared to using the solar radiation data that have to be downloaded from a large database file. Equations 3.26 and 3.27 can be easily incorporated into the simulation software, without the need to create and call-back large amount of data from the solar radiation database.

The snapshot of the program shown in Figure 3.12 is part of bigger software, designed and developed for this study to do a full system simulation. Therefore part of the simulation software is capable of analysing the solar radiation, by using equations or by direct input of solar insolation data that will be placed in a database created by the software. The use of the polynomial and sinusoidal curve fitting methods are preferred, but the choice is left

entirely to the users. In future, if smaller programs are needed to be developed, then the choice is obviously the curve fit equations.

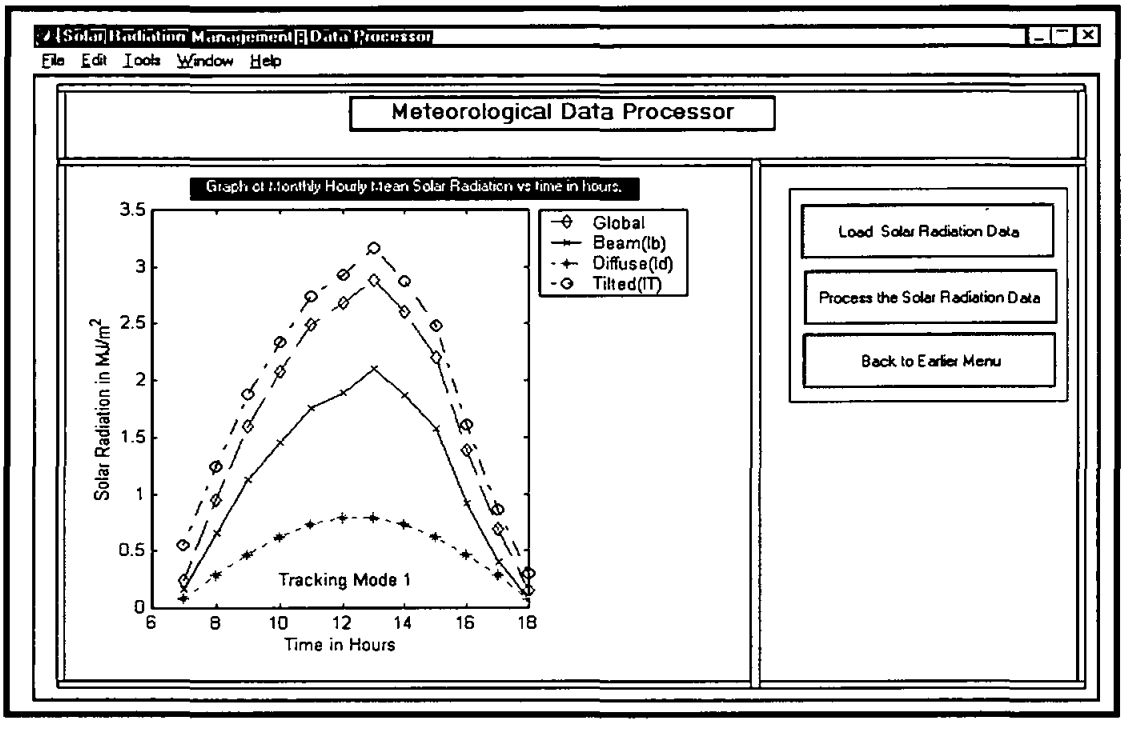

Figure 3.12 A snapshot of the solar data processing menu, designed based on the polynomial fit and global radiation separation method that was discussed.

3.8 DIFFUSE RADIATION IN MALAYSIA

Simulation studies were carried out based on meteorological data for Bayan Lepas, Ipoh, Cameron Highlands, Kuantan and Senai. It can be seen from Figure 3.13 that there is enough solar insolation received at these locations throughout the year, where the yearly averaged clearness index is around 44.41 %. The effect of latitude on the yearly averaged clearness index obtained by analysing the results presented in Figure 3.13 is given in Figure 3.14.

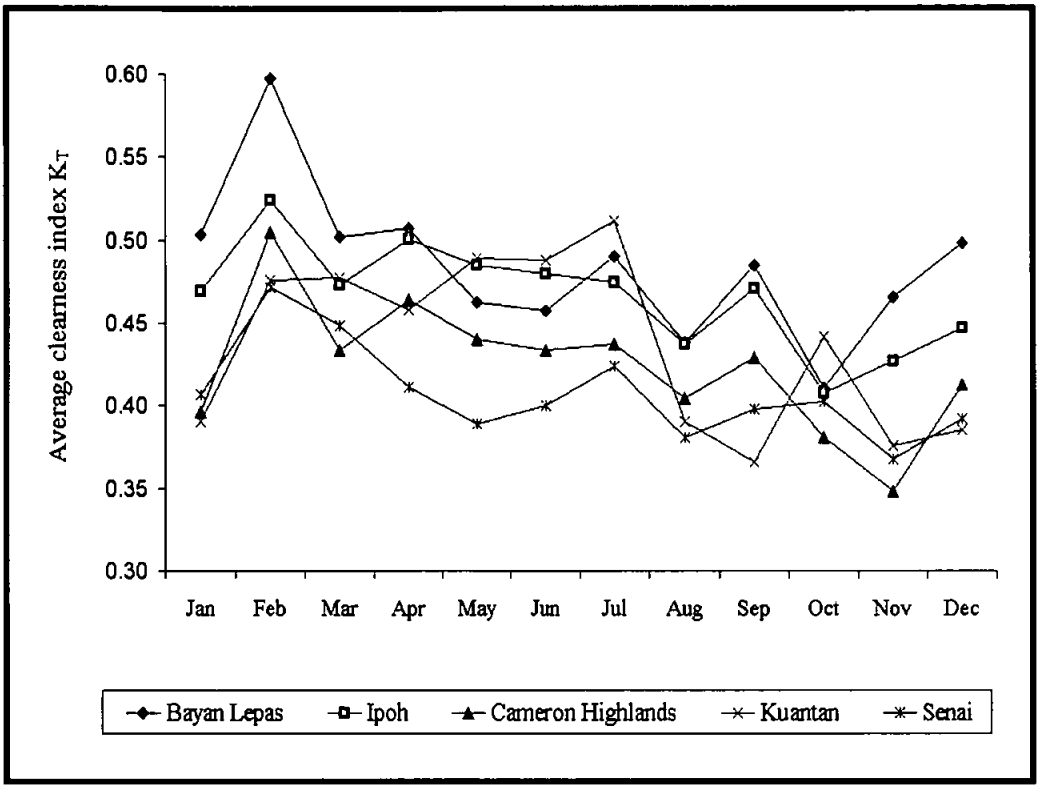

Figure 3.13 Graph of yearly monthly average clearness index K_T versus months in the year 2001, for Bayan Lepas, Ipoh, Cameron Highlands, Kuantan and Senai.

It can be seen from Figure 3.14 that the locations in Malaysia have an average clearness index exceeding 0.40. The following equation 3.28 derived in this research work can be used to estimate the average clearness index at a particular location.

$$\overline{K}_T = 0.601 - (0.199\exp(-0.0061\phi^{-2.694})) \qquad 0 \le \phi \le 8.0 \qquad (3.28)$$

The ratio of diffuse radiation received by a horizontal surface, H_d, to monthly average global radiation received by horizontal surface, H, for the months in year 2001 for Bayan Lepas and Ipoh is shown in Figure 3.15. Based on these ratios, the monthly average diffuse radiation received by horizontal surfaces in Bayan Lepas and Ipoh are 7.71 MJ/m^2 and 7.81 MJ/m^2 respectively. This is consistent with Azni-Zain (2002) reporting that on the

average, the amount of solar diffuse radiation received at any particular location in Malaysia is around 30 % to 40 % of the global solar radiation.

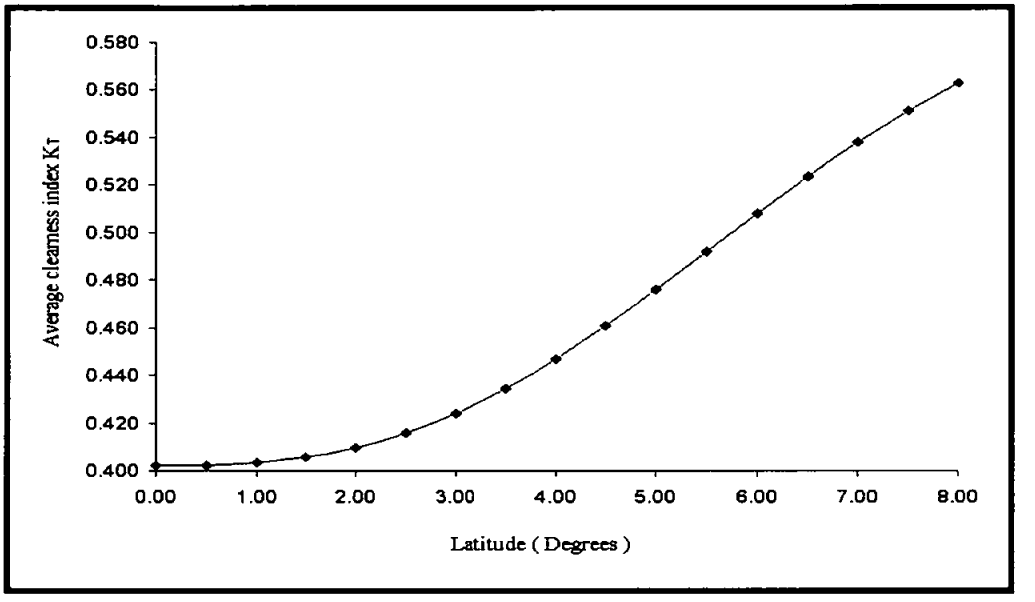

Figure 3.14 Graph of average clearness index K_T versus latitude.

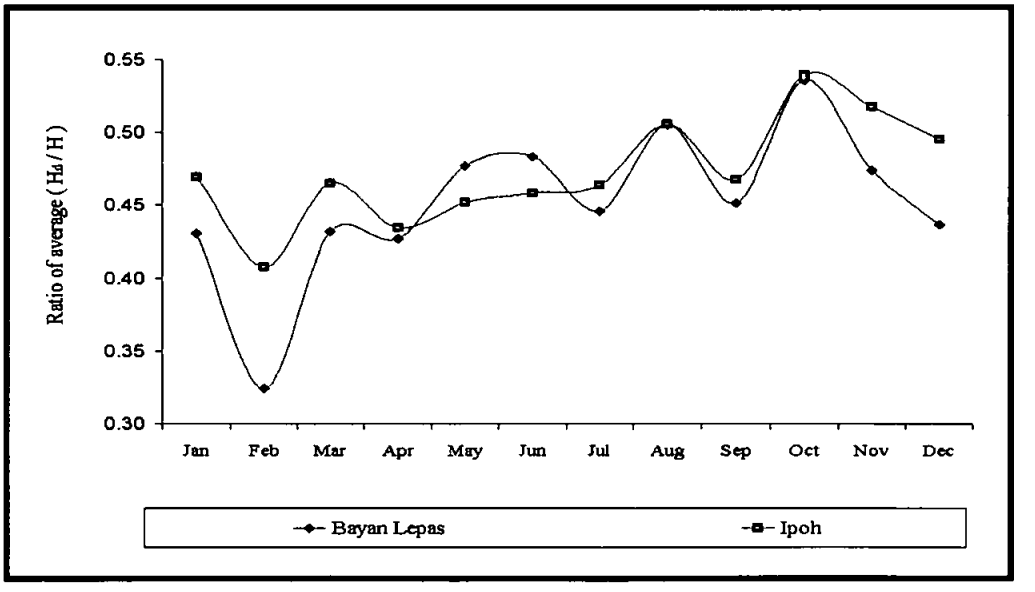

Figure 3.15 Graph of average (H_d / H) versus months in the year 2001, for Bayan Lepas and Ipoh.

The decision to use the considerably sufficient amount of diffuse radiation by introducing the new concentrator's design is justified by these meteorological statistics. The theory of this new design will be discussed in the next chapter.

CHAPTER 4

PARABOLIC-TROUGH CONCENTRATING SYSTEM

The basic operation of any type of solar thermal device works on the principle of heat gained, removed and lost. There must be an energy balance between these parameters and to remove a large fraction of the absorbed solar energy as useful heat, the losses must be kept at a minimum value. The main function of concentrating thermal devices is to focus solar radiation onto a small absorbing area, usually referred to as receivers. The solar radiation that arrives at a significantly large concentrating area is reflected to the focus point or focus line, depending on the geometry of the collector. Concentrating collectors are designed to operate at higher temperatures than flat plate collectors and have the ability to provide significant amount of thermal energy (Winston, 1974).

As discussed in Chapter 2, parabolic-trough concentrating system (PTCS) is a proven renewable energy technology, which converts the abundant amount of solar radiation, that enters the earth's atmosphere to useful thermal energy (Zarza *et al.*, 2001). The sunlight is concentrated before it actually strikes the receiver's absorber, where the incoming solar radiation is reflected to a focus line by the reflecting surface of the concentrator. A circular shaped cylindrical receiver, that acts as an absorber is placed concentrically, at the focal line. Usually, a PTCS uses the direct beam radiation and in order to maximize its collection a tracking system is used. In this research, a new parabolic trough model is proposed where the design is made so that the diffuse radiation is also collected and converted to useful heat energy. In the next few sections, discussions will be focussed to develop the theoretical model of the new parabolic trough concentrator (PTC) design.

4.1 COMPONENTS OF THE NEW PTC DESIGN

The main operating parts of the new PTC design are the concentrator, receiver and the conduit tubes welded to the back of the concentrator. The concentrator has a reflecting surface and absorbing back surface, and the receiver is the main heat absorber of the system. The heat is transferred from the collector by using suitable heat transfer fluids. The conduit tubes, which are actually an important part of the concentrator, besides the cover system, is placed concentrically, with the focal line as its axis (Stine & Harrigan, 1985). The orientation of the concentrator and receiver is very important and the position must be accurately calculated. Another component that is equally essential is the tracking mechanism, which is used to track the sun to ensure that the principal axis of the concentrator is parallel to the solar rays.

4.1.1 CONCENTRATOR

The concentrator is the main component of a PTC, where the ability to focus the maximum incoming solar radiation to concentrate at a single point or a line is considered as its main function (Rabl, 1980). In this study, another function was explored and added to the concentrator, where a new PTC theoretical model is developed as will be discussed in section 4.4. Here the focal point is extended to a focal line. The curved reflecting geometry is selected to be parabolic, as it can reflect most of the incoming rays that pass through the aperture area of the PTC. The rays that are quite a distance away from the principal axis can also be reflected to the focus line, unlike the spherical concentrator. With a ray-tracing program that was developed in this study, Figure 4.1 shows a graphical display of ray tracing of the solar radiation.

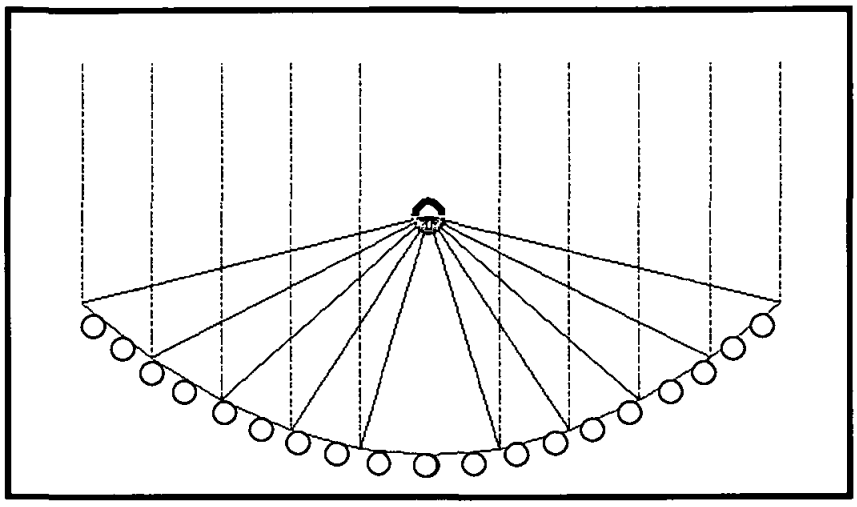

Figure 4.1 Graphical display showing how the incidence solar radiation is reflected towards the focal point and intercepted by a receiver of a certain diameter.

Since the reflecting surface is a parabolic trough, its construction requires a high level of precision, as off-normal incidence rays might not be directed towards the focus. The geometrical design parameters must be carefully derived based on the design specifications, such as the width, depth and length. The rays that are parallel to the principal axis will be concentrated, so it is mandatory for the concentrator to track the sun. Some commonly used reflecting surfaces of the concentrator are curved back-silvered glass, thin electro polished anodised aluminium sheets, silver coated acrylic films and aluminised reflective films (Goswami *et al.*, 2000).

4.1.2 RECEIVER

A receiver is the part of the PTC, which absorbs solar energy and transports it via heat transfer fluid, as useful heat. Usually the receiver of a PTC is referred to as omnidirectional receiver. Omnidirectional receivers can accept optical input from any direction (Stine & Harrigan, 1985). The difficulty that exists at the receiver is to maintain a balance between the thermal and optical losses. This is explained by the taking into consideration that if the area of the receiver's absorber is increased, than the chances of intercepting

more rays are higher, but this leads to higher thermal losses. If the area is decreased, then the optical losses increase as the chances of striking the receiver's absorber is less, unless the whole PTC's design is highly precise, such as the trueness of the parabolic geometry. Therefore the evaluation of the receiver's performance must take into consideration the thermal and optical analysis (Duffie & Beckman, 1980). Usually the absorber tube is made of mild steel or copper with a diameter of 2.5 to 5.0 cm and generally surrounded by a concentric glass cover with an annular gap of 1.0 to 2.0 cm. In the case of high performance collectors, the absorber tube is coated with selective surface like black chrome and the space between the tube and glass cover is evacuated. In some of the collectors, a plastic or a glass sheet covering the whole aperture area of the collector replaces the concentric cover (Garg & Prakash, 1997).

4.1.3 HEAT TRANSFER FLUIDS

Heat transfer fluid plays an important part in transporting the collected heat, from any types of solar collector. It is perhaps the blood of the solar collector system and the selection of the type of fluid depends on factors such as the operating temperature, collector's application and also the geographical location. Geographical location is an important factor to consider, as the working fluid might freeze during cold weather. In Malaysia, such a problem will not arise, as the weather does not record very low temperatures. Due to the high temperature capability of PTC, a comparison of heat transfer properties is important. The commonly used heat transfer fluids are water, saturated water, caloria, dowtherm, therminol and syltherm (Stine & Harrigan, 1985).

It can be seen from Figure 4.2 that there is a sharp increase in the value of the specific heat capacity after 175 °C for saturated water. Generally, the heat transfer fluids should have

high specific heat capacities, high operating temperatures, stability at high temperatures, low material maintenance, non-corrosive and low vapour pressure (Garg & Prakash, 1997).

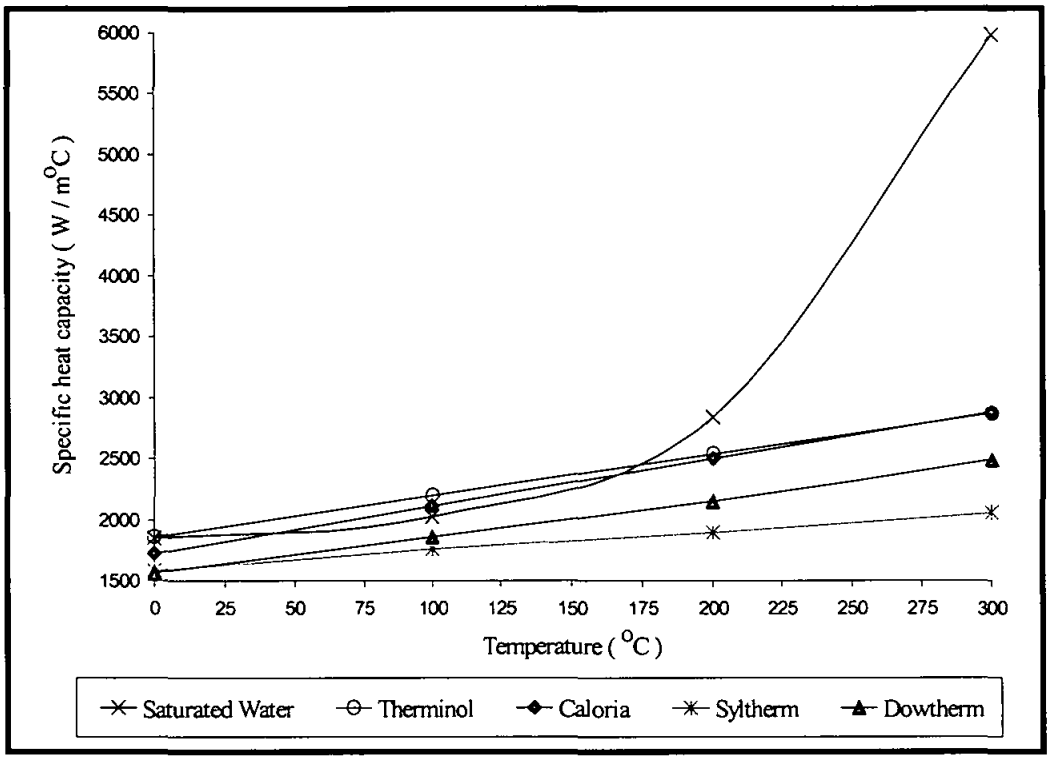

Figure 4.2 Graph of specific heat capacity versus temperature for five different types of heat transfer fluids.

4.1.4 PTC FRAME STRUCTURE

Proper design of the frame holding the PTC components is important as it influences the orientation of the reflecting surface. The components of the PTC structure assembly are the endplates, steel frames, receiver's absorber tube supports and cantilever arms components. The issues concerning the built of the structure are related to the weight and deformations. Deformations are caused by the weight of the structure itself and also by wind loading. There is currently a new design that reduces torsion and bending of the structure during operation and results in an increased optical performance and wind resistance. The design is known as torque-box, and is used in the Euro Trough project (Geyer *et al.*, 2002). However the Euro Trough design, utilizes mirror supports that make use of the glass facets

as static structural elements which has a risk of glass sheet breakage, especially during maintenance and at high wind speeds.

4.1.5 TRACKING MECHANISM

As mentioned earlier, tracking is an important part of the system, for tracking the movement of the sun, so that solar rays are always parallel to the principal axis of the parabolic concentrator. There are altogether five different types of tracking modes that are used for simulation purposes and all the equations describing these modes have been elaborated in section 3.3.4.

A PTC should be orientated by taking the focal axis as the reference. The focal axis can be pointing in the east-west or north-south direction. If the east-west orientation is selected, then the focal axis must be horizontal, meanwhile if the orientation is north-south, then the focal axis can be horizontal or inclined. Tracking mode I, requires the focal-axis to be in the east-west orientation and must be horizontal. The PTC is rotated about an east-west axis and adjusted once a day, in order for the solar beam to be normal to the aperture plane at solar noon. Tracking mode II is orientated in the similar manner as in tracking mode I, except that it is adjusted continuously so that the solar beam radiation makes the minimum angle of incidence with the aperture plane at all times. Tracking mode III is used when the north-south orientation is applied to the focal axis. The PTC is rotated about a horizontal north-south axis and adjusted continuously so that the solar beam radiation always makes the minimum angle of incidence with the aperture plane.

Tracking mode IV is used when the focal axis is in the north-south orientation and inclined at a fixed angle equal to the latitude, making it parallel to the earth's axis. The PTC is rotated about an axis parallel to earth's axis, at an angular velocity that is equal and

opposite to earth's rate of rotation of 15° per hour. The PTC must be adjusted in such a way that the aperture plane is inclined facing due south or north, at solar noon. Tracking mode V is the most effective and preferred choice of tracking for PTC, as the solar beam is always ensured to be normal to the aperture plane. The focal axis is in the north-south orientation and inclined. PTC is rotated continuously about an axis parallel to the focal axis and about a horizontal axis perpendicular to it.

The tracking unit follows the path of the sun during operation by using a hydraulic drive system, which consists of two hydraulic cylinders mounted on the central drive pylon (Geyer *et al.*, 2002). The other integral parts of the tracker are the signal and power lines that lead to the hydraulic unit, rotational encoder, limit switches and temperature sensors. The system uses software to do tracking, instead of the traditional sun-tracking unit with sensors that detect the position of the sun. The tracking is based on the calculation of the sun's position using a mathematical algorithm, with a 13-bit optical angular encoder mechanically coupled to the rotation axis of the collector (Blanco-Muriel *et al.*, 2001). An electronic device compares the collector axes and suns positions, after which a signal is sent to the drive system to position the aperture normally to the solar beam radiation. Any designed software to calculate the solar coordinates can be checked against the Multiyear Interactive Computer Almanac (MICA), a software product of the United States Naval Observatory (2002).

4.2 THE OPTICS OF PARABOLIC CONCENTRATOR

The concentration of solar radiation can occur by reflection or by refraction. In the case of the PTC's concentrator, reflecting surface is used and concentration can be measured in terms of optical concentration ratio. Optical concentration ratio is defined as the ratio of solar flux intercepted by the receiver to the flux that reached the concentrator's aperture.

The other index used to analyse the optical effectiveness is the optical efficiency. There are several optical performances that must be considered collectively, to evaluate the optical efficiency. The optical efficiency depends on the surface reflectance of the concentrator, transmittance of the receiver's cover, surface slope errors, solar image spread, tracking error and off normal incidence effects (Stine & Harrigan, 1985).

4.2.1 PARABOLIC GEOMETRY

As mentioned earlier, the parabolic geometries dominate the design of the solar concentrators. The analytical description of parabolic geometry is important. The concentrator optics are closely related to the parabolic geometry and physical law of reflection. The parabolic curve would focus all the rays to a focal point, and a trough normally extends the shape in three dimensions to turn the focal point into a focal line. Equation 4.1 shows the parabolic equation with the important relationship between the width, W and depth, d and equation 4.2 is used to calculate the focal point, F (Fauziah & Balbir, 2003b).

$$Y = \frac{d}{(0.5W)^2} X^2 \qquad (4.1)$$

$$F = \frac{W^2}{16d} \qquad (4.2)$$

The following Figure 4.3 shows the design based on equations 4.1 and 4.2, where the receiver is placed concentrically along the focal line. The design was determined by using computer-modelling software produced in this research work where the snapshots of the software menu, together with the design parameters are shown in Figure 5.15.

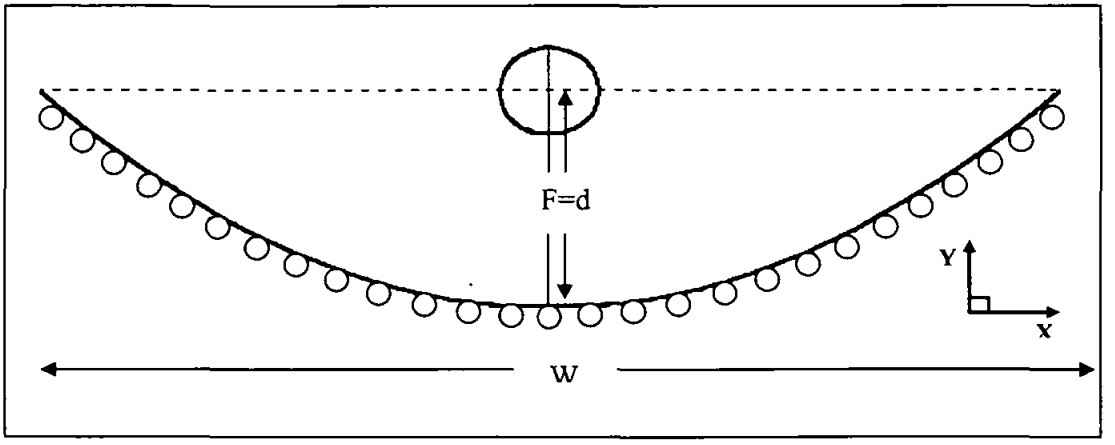

Figure 4.3 A computer model of the parabolic concentrator, where the focal point is set to be equal to the depth and receiver is placed concentrically about the focal point.

Equation 4.3 is used to calculate the rim angle, based on the focal point F, width W and depth d (Fauziah & Balbir, 2003b).

$$\cos\phi_R = \frac{2F}{\sqrt{(0.5W)^2 + (d-F)^2}} - 1 \qquad (4.3)$$

A rim angle of 90° is preferred as it gives an optimum intercept factor and allows the depth to be the focal point. The focal point, where the rim angle is set at 90° can be calculated by using the width value alone, as shown by equation 4.4.

$$F = \frac{W}{4} \qquad (4.4)$$

The parabolic equation that is determined by using equation 4.1 is useful to calculate the XY-coordinates, which can be used to obtain the horizontal and vertical displacements that will enable the concentrator to be bent into a parabolic shape precisely. The amount of material needed to bend it to the shape of a parabola can only be determined by considering the arc length. The evaluation of arc length can be done by integrating the infinitesimal arc length of very small segments, over the entire width. The other simpler way to calculate the arc length S_{arc} will be by using equation 4.5 (Stine & Harrigan, 1985).

The comparison between the arc length calculated by using equation 4.5 and by using the integrating method resulted to 99.9 % accuracy. Therefore equation 4.5 can be used directly in the programming.

$$S_{arc} = 0.5W\sqrt{\frac{16d^2 + W^2}{W^2}} + 2F\ln\left[\left(\frac{4d}{W}\right) + \sqrt{\frac{16d^2 + W^2}{W^2}}\right] \qquad (4.5)$$

The cross-sectional area of the parabola A_{CS}, with a line across its aperture is given by equation 4.6 and the volume V_T, with the length of trough taken to be L is given as equation 4.7 (Stine & Harrigan, 1985).

$$A_{cs} = \frac{2}{3}Wd \qquad (4.6)$$

$$V_T = \frac{2}{3}WdL \qquad (4.7)$$

4.2.2 CONCENTRATION RATIO

Although the level of concentration is restricted by the design parameters, the choice of concentration ratio depends on the compromise between optical and thermal performance. The geometrical concentration ratio, C_G, is the ratio of the effective aperture area to the receiver tube area and is shown in equation 4.8, where W is the width of the concentrator and D_R is the diameter of the receiver. So both the concentrator and receiver collectively influence the geometrical concentration ratio (Sukhatme, 1996).

$$C_G = \frac{W - D_R}{\pi D_R} \qquad (4.8)$$

4.2.3 SPECULAR REFLECTANCE

The basic principle of reflection states that the angle of incidence is equal to the angle of reflection. The reflection is considered as specular, if the incoming solar radiation is reflected at angles that can be determined and is considered as non-specular, if the angles cannot be determined by the general surface contour of the reflector. Normally, both specular and non-specular reflections can exist at the same time. The ability of a surface to reflect light is evaluated based on the reflectance value. Specular reflectance is the fraction of light that is reflected such that the reflected angle with respect to the normal of the reflecting surface is equal to the incidence angle with respect to the normal of the reflecting surface. The values for specular reflector materials are given in Table 4.1 notably the new electroplated silver surface is capable of providing a clear undistorted image (Duffie & Beckman, 1980).

Table 4.1 Normal specular solar reflectances of reflecting surfaces.

Surface	ρ_s
Electroplated silver	0.96
High-purity aluminium	0.91
Sputtered aluminium	0.89
Brytal processed aluminium	0.89
Back-silvered water white plate glass	0.88
Al, SiO coating	0.87
Aluminium foil, 99.5 % pure	0.86
Aluminized Type C Mylar	0.76

4.2.4 ACCEPTANCE HALF ANGLE

The ideal concentration ratio gives the highest possible theoretical concentration and equation 4.9 relates the concentration ratio of a trough, C_{trough} to acceptance half-angle, θ_c.

The maximum value of C_{trough}, based on the sun's subtend acceptance half angle of 0.27° is 212. This value is taken to be as the thermodynamics limit of a parabolic trough concentration ratio (Hottel & Sarofim, 1967).

$$C_{trough} = \frac{1}{\sin\theta_C} = \frac{1}{\sin(0.27°)} = 212 \tag{4.9}$$

If the maximum concentration value of 212 is to be achieved by using a PTC with a width of 1.0 m, by using equation 4.8, the receiver's diameter is calculated to be 9.4 mm. This is a very small sized receiver, and there are other implications, especially if nonparallel solar rays are taken into consideration. All the parameters derived in section 4.2.1 are based on solar rays that are taken to be ideally parallel to the principal axis of the parabolic surface. Due to the finite angular size of the sun's disc, the rays reaching the concentrator are not parallel. The reflected rays tend to form an image of finite size centred about the focus.

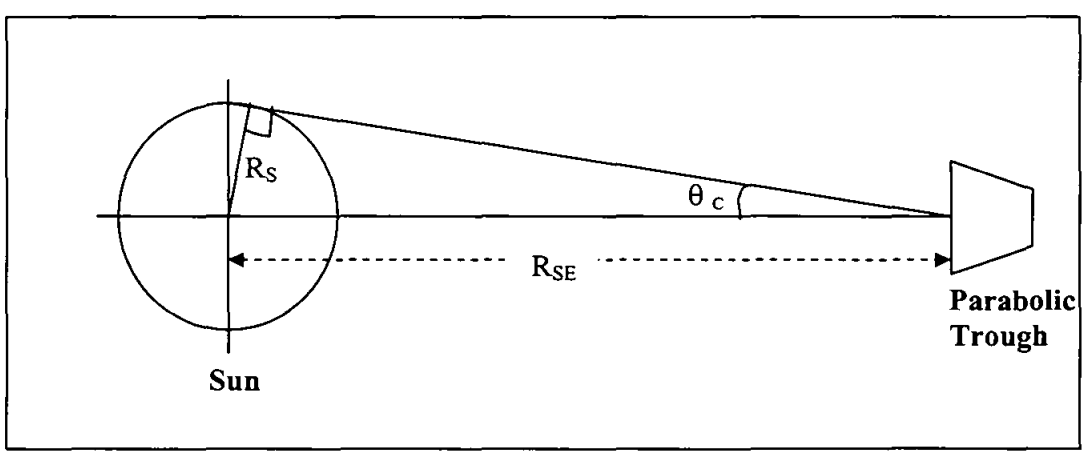

Figure 4.4 Diagram shows the schematic sun, at a distance R_{SE} from a parabolic trough concentrator.

Based on Figure 4.4, the sun's subtend angle is evaluated by using equation 4.10. The value of θ_C is the acceptance half-angle and this angle is used in equation 4.9 to calculate the maximum concentration ratio.

$$\tan\theta_C = \frac{R_S}{R_{SE}} \qquad (4.10)$$

The reflected solar rays that reache the receiver with the largest deviation, just barely touching the receiver, dictate the receiver's acceptance half-angle and can be used to calculate the concentration ratio. The effect of acceptance half angle in determining the receiver's size will be discussed in the next section.

4.3 THE OPTICS OF CIRCULAR CYLINDRICAL RECEIVER

The optical analysis of the receiver relies highly on the reflected solar rays directed towards the focal point. These rays are intercepted by the receiver, at certain points before the focal point, depending on the geometry of the receiver. This will cause the reflected solar rays to be distributed, as the distance from the reflection points to the receiver varies. It can be seen from Figure 4.5 that as the parallel incidence rays move closer to the principal axis, they will be blocked by the receiver and the effect is called shading. Due to this reason, the effective aperture area A_{eff} is calculated based on equation 4.11.

$$A_{eff} = (W - D_R) \times L \qquad (4.11)$$

This limits the size of the receiver, which is used to select the appropriate diameter of the absorbing tube. In Figure 4.5, the area shaded in blue is the region where there are no

incoming rays that are parallel to the principal axis, reaching the reflecting surface, except for the rays that are reflected close to the boundary lines that are shown by using the red vertical lines.

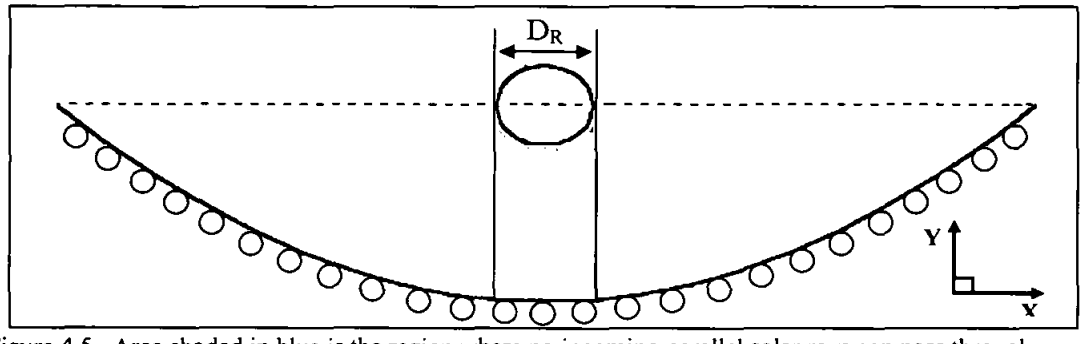

Figure 4.5 Area shaded in blue is the region where no incoming parallel solar rays can pass through.

Equation 4.12 is used to calculate the optical concentration ratio C_o based on a compromise between optical and thermal performance. It shows that the receiver's absorber is supposed to be as small as possible, in order to reduce heat losses, but yet large enough to intercept almost all of the solar rays that are parallel and almost parallel with the principal axis of the reflecting surface. The optical concentration ratio C_o is considered to be more precise than the geometrical concentration ratio C_G, as it takes the rim angle of the concentrator and acceptance half-angle of the receiver into consideration (Rabl, 1980).

$$C_o = \frac{\sin \phi_R}{\pi \sin \theta_C} \qquad (4.12)$$

The relationship between rim angle ϕ_R, acceptance half-angle θ_C, rim radius R_r and receiver's radius r_a is as shown in Figure 4.6 and can be represented by equation 4.13.

$$r_a = R_r \tan\theta_c \qquad (4.13)$$

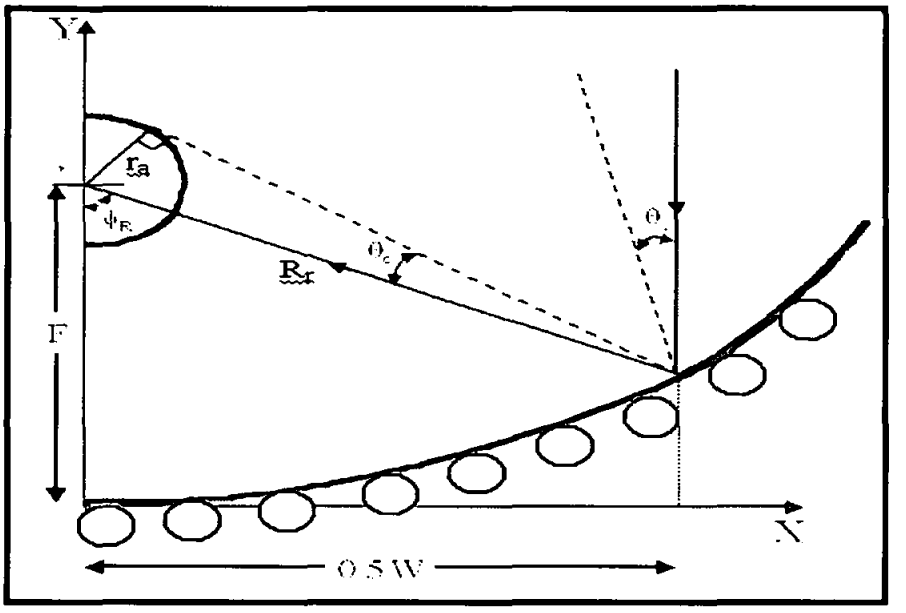

Figure 4.6 Diagram showing the acceptance half-angle θ_C, rim angle ϕ_R, rim radius R_r and receiver's radius r_a .

Equation 4.13 can be used to determine the size of the receiver, where the parameter R_r can be obtained by using equation 4.3 and equation 4.14.

$$R_r = \frac{2F}{1+\cos\phi_R} \qquad (4.14)$$

Equation 4.12 is used to simulate the effect of the rim angle on the concentration ratio, at four different acceptance angles. The results are shown in Figure 4.7 and it can be seen that the maximum concentration ratio occurs at rim angle of 90°. A good choice for designing, is to set the rim angle at 90° as it will also simplify the calculation of the focus F. Equation 4.15 incorporates the width of the concentrator, to determine the right size for the receiver at rim angle of 90°.

$$r_a = \frac{1}{2} W \tan\theta_c \qquad (4.15)$$

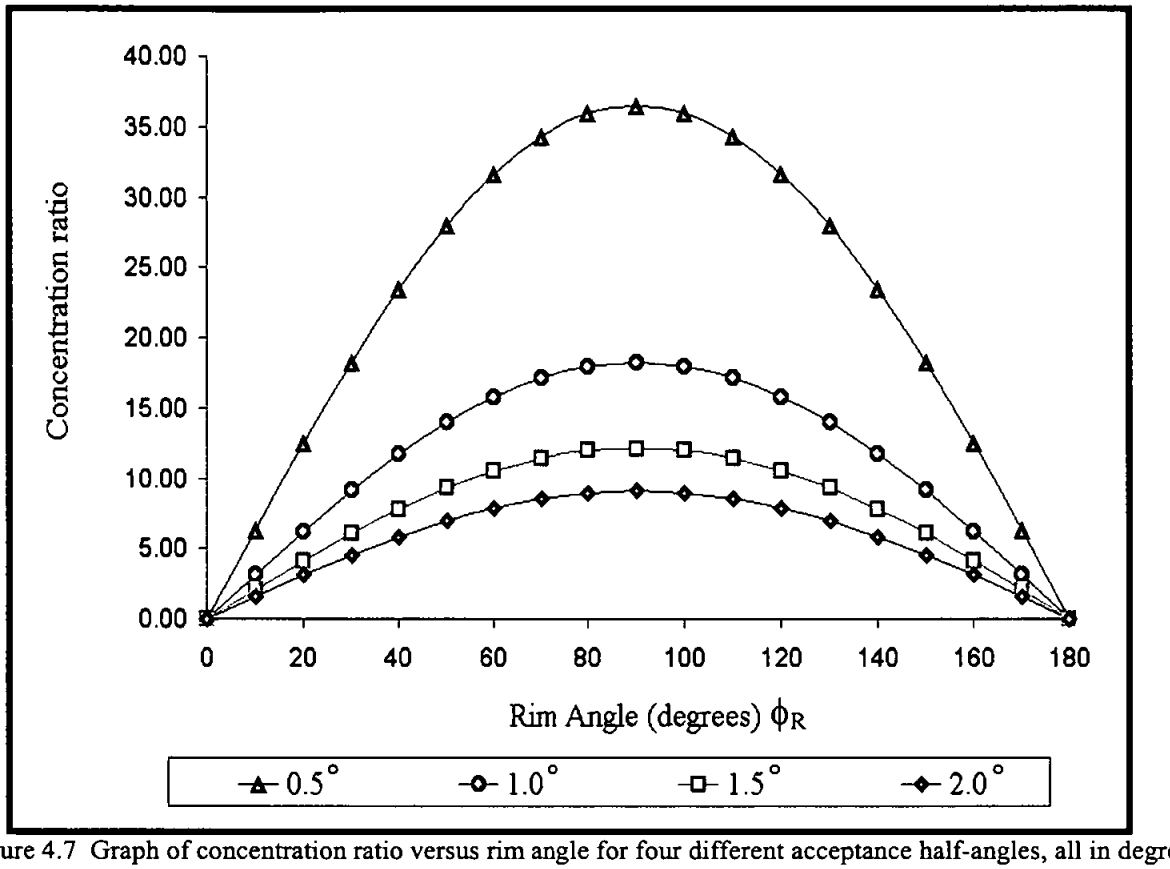

Figure 4.7 Graph of concentration ratio versus rim angle for four different acceptance half-angles, all in degrees.

The width of the beam spread that arrives at the receiver depends on the spread of the nonparallel rays and errors contributed by the slope of the reflecting surface, tracking mechanism and the finite size of the sun's disc. The effect of these errors will be discussed in the next section.

4.3.1 CONTRIBUTION OF ERRORS

Until now, the sizing of the receiver has been based on the width of half of the beam spread due to the finite angular size of the sun's disc. There are other factors that must be addressed, before a precise optical analysis result can be incorporated to determine the size of the receiver. These factors will be referred to as errors and besides the sun's disc error, other errors include, the conformity of the mirror to a true parabolic shape, nonspecular reflection of

the incident beam, inefficient tracking and imperfect receiver alignment. All these errors will cause the reflected beam to spread further and their contributions will cause the value of the acceptance half-angle to increase. Figure 4.8 shows the effect on the concentration ratio due to increasing acceptance half-angle at five different rim angles. A significant improvement in the concentration ratio can be achieved if the value of the acceptance half-angle is below 1.50°.

The errors mentioned earlier are all assumed to be random, so that they can be analysed statistically. Although the solar intensity is not normally distributed across its disc, the error is approximated as a standard distribution and will be treated similarly with the other errors.

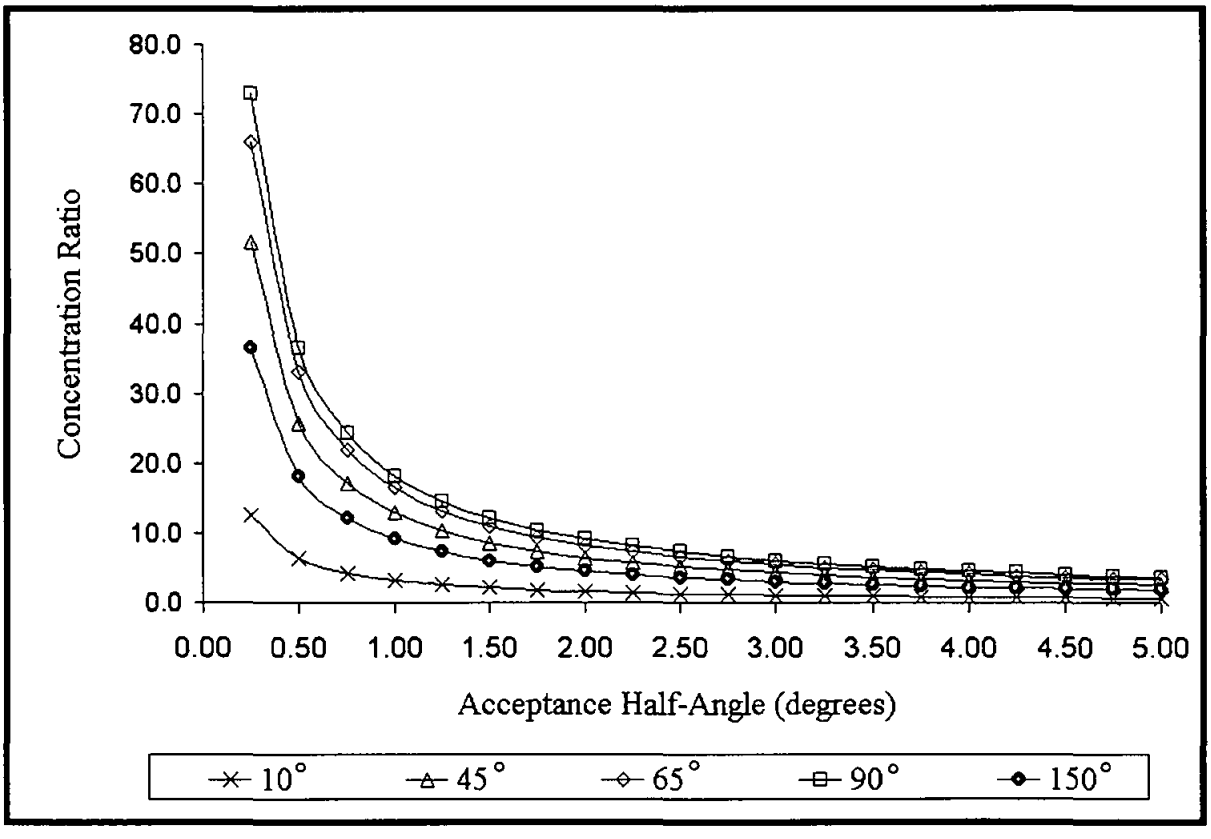

Figure 4.8 Results obtained by simulation, where the curves are obtained for different rim angles, expressed in degrees.

The standard deviations are then combined to form the resultant standard deviation, σ_R. After the resultant standard deviation is calculated, the next step would be to find an appropriate size for the receiver, so that the new acceptance half-angle can be accommodated.

$$\sigma_R = \sqrt{\sigma_1^2 + \sigma_2^2} \qquad (4.16)$$

σ_1 includes the structural, tracking and receiver alignment errors while the reflector's specular reflectance and the sun's finite disc width errors are grouped together as σ_2 (Goswami *et al.*, 2000). The error σ_1 is contributed by the tracking mechanism's sensor σ_{sensor} and motor σ_{drive}, reflective surface's slope error σ_{slope} and receiver's position error σ_{rec}. It can be seen from equation 4.17 that the slope error is multiplied by 2 to account for Snell's law. Here the reflecting surface's direction is changed, while the receiver's position is not.

$$\sigma_1 = \sqrt{(2\sigma_{slope})^2 + (\sigma_{sensor})^2 + (\sigma_{drive})^2 + (\sigma_{rec})^2} \qquad (4.17)$$

The error σ_2 as in equation 4.18 is contributed by the angular width error of the sun σ_{sun}, non-specular reflectance error σ_{refl} and the angle of incidence θ depending on the type of tracking mode used.

$$\sigma_2 = \frac{\sqrt{(\sigma_{sun})^2 + (\sigma_{refl})^2}}{\cos\theta} \qquad (4.18)$$

Equation 4.13 is now expressed in terms of the number of resultant standard deviations n and resultant standard deviation, σ_R (Stine and Harrigan, 1985).

$$r_a = R_r \tan(n\frac{\sigma_R}{2}) \qquad (4.19)$$

A receiver sized based on equation 4.19 will be able to intercept all reflected radiation within the error limits defined by n, provided the individual assessment of the errors is done as accurately as possible (Goswami *et al.*, 2000).

4.3.2 INTERCEPT FACTOR

In the earlier section, it was noted that the effects of all the various errors caused the reflected beam to spread. The spread out beam can be captured, if the receiver size is increased. When the receiver size is increased, the area of the receiver too increases and this will cause the thermal losses to increase. However, as the area is decreased to reduce thermal losses, optical losses increase which lead to an optimization solution. The intercept factor accounts for the optical losses in this problem and is defined as the fraction of the specularly reflected radiation, which is intercepted by the receiver. The factors affecting the intercept factor should be outlined, before the analytical part is developed. Intercept factor is considered, as an optical analysis and their errors contributed are similar to the errors discussed in the earlier section.

To simplify, the list includes irregularities on the reflector's surface, rim angle of the reflector and shape of the receiver.

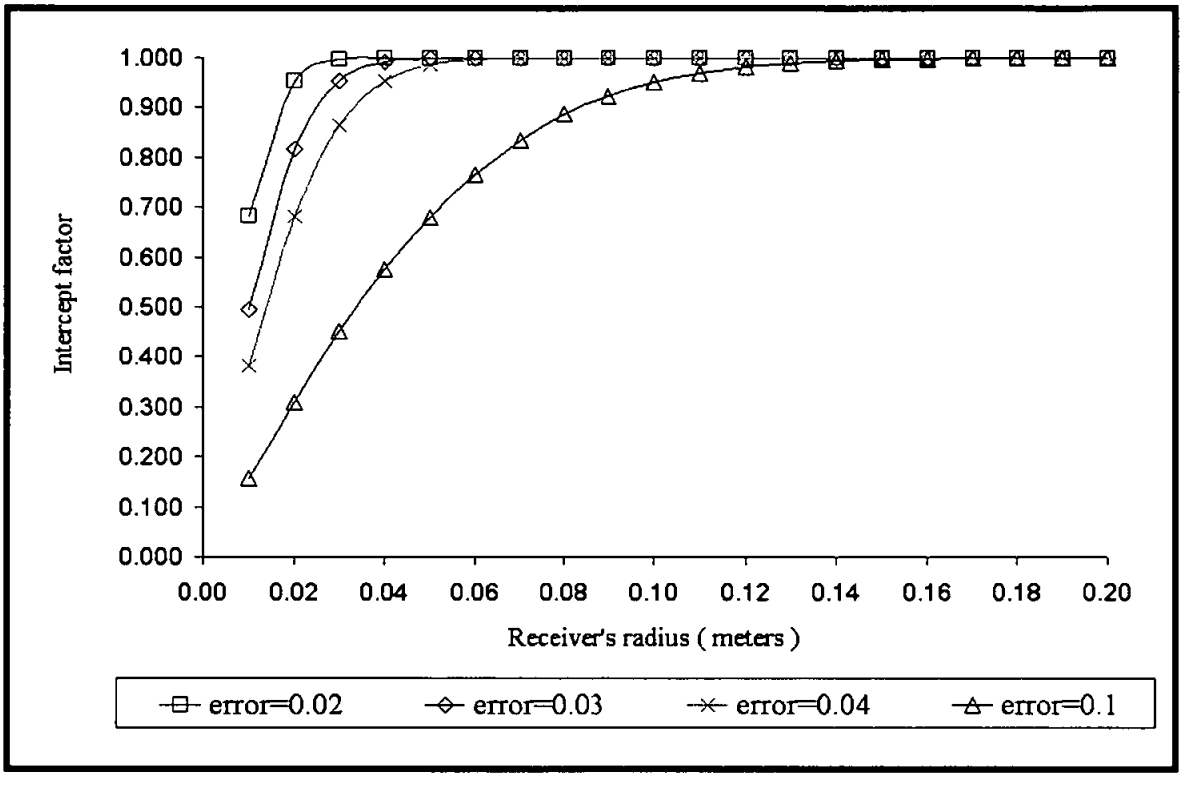

Figure 4.9 Results obtained from simulation, where the curves are obtained for different error levels, in radians.

It can be seen from Figure 4.9 that the intercept factor increases with the diameter of the receiver. The analysis to obtain the intercept factor is solely done by statistical analysis, where the normal distribution approximation is applied to the beam spread that is intercepted by the receiver. The contribution from this analysis is very important, as it influences the size of the receiver.

The intercept factor γ_s of the reflected solar radiation considered to be an important design factor that is distributed normally can be obtained by using the following polynomial approximation equation 4.20.

$$\gamma_s = -3.835998\times10^{-3} + \sum_{i=1}^{9} P_i n^i \qquad 1.0 \le n \le 8.2 \qquad (4.20)$$

Table 4.2 Values of the polynomial coefficients P_i to be used with equation 4.20.

Polynomial Coefficient P_i	Value
P_1	4.127312×10^{-1}
P_2	-2.121346×10^{-2}
P_3	1.735772×10^{-3}
P_4	-9.861089×10^{-3}
P_5	4.029031×10^{-3}
P_6	-7.453351×10^{-4}
P_7	7.476230×10^{-5}
P_8	-3.979757×10^{-6}
P_9	8.869948×10^{-8}

The value of the intercept factor reaches a maximum value of one if n is equal to or more than 8.2. Equation 4.21 is important for sizing the receiver and contributes to the overall optical performance of the concentrator (Stine & Harrigan, 1985).

$$n = 2(\sigma_R{}^{-1})\left[\tan^{-1}\left(\frac{r_a}{R_r}\right)\right] \qquad (4.21)$$

4.4 DEVELOPMENT OF THEORETICAL MODEL

The concentrator of the new PTC design is to collect direct radiation, the diffuse radiation and the unreflected radiation. In this section, a theoretical heat balance model will be derived. The new design of the concentrator has copper conduit tubes running underneath the concentrator's surface. The thermal analysis is divided to two parts, where the first part deals with the concentrator's thermal analysis and the other is related to the receiver. Usually in a parabolic trough concentrator, the thermal analysis is always done on the receiver only. The concentrator in this new design is also an absorber to a certain extent. The contribution of the concentrator as an absorber is to increase the temperature of the inlet fluid to the receiver.

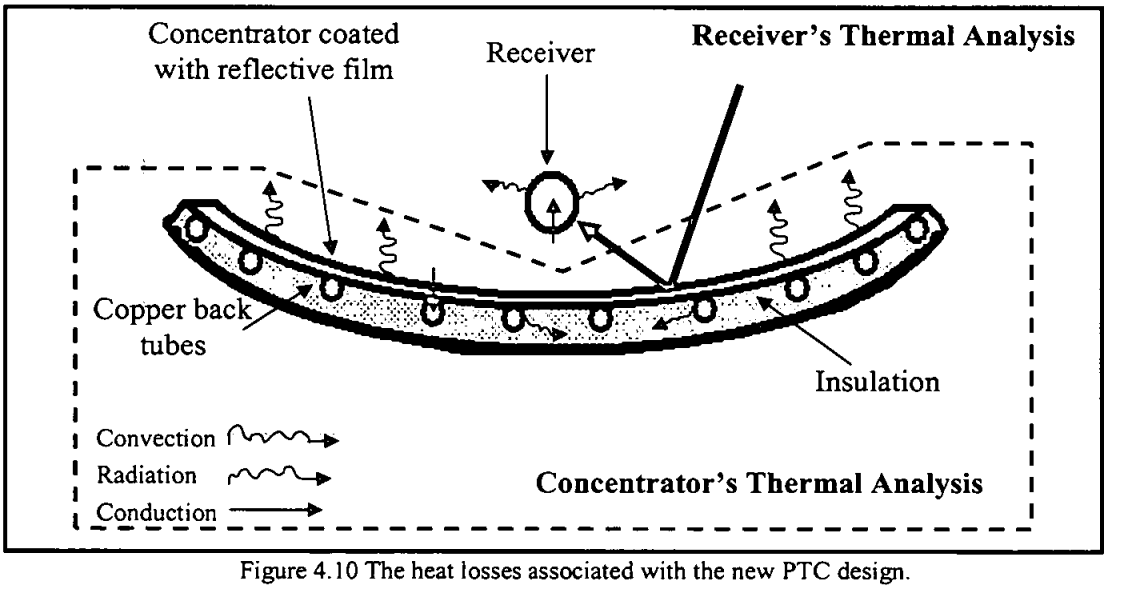

Figure 4.10 The heat losses associated with the new PTC design.

Generally, the thermal analysis is carried out with the isolation of the surface that absorbs the incoming radiation and an energy balance is achieved between inflow and outflow of heat to and from it. In this research work, there are two absorbing surfaces. The main absorbing surface is the receiver's conduit tubes, while the concentrator is also an absorber plate. The copper tubes welded at the back of the concentrator collect the heat absorbed by the concentrator plate. The general heat balance equation that is used is given below in

equation 4.22, where Q_g is the rate of useful energy gained, S_A is the rate of absorbed solar radiation and Q_{loss} is the rate of thermal energy loss from the absorber.

$$Q_g = S_A - Q_{loss} \qquad (4.22)$$

The useful energy collected is transported by a suitable working fluid and due to this, equation 4.22 is multiplied by the heat removal factor F_i and the energy balance is evaluated based on the fluid inlet temperature, rather than the mean plate temperature. By considering the heat removal factor Q_i, the rate of useful energy leaving the absorber is as shown in equation 4.23 with A_i as the total surface area and S_i is the absorbed solar radiation.

$$Q_i = A_i F_i S_i - A_i F_i Q_{loss} \qquad (4.23)$$

4.4.1 THERMAL ANALYSIS OF THE CONCENTRATOR

The thermal analysis of the concentrator can be described by the general heat balance equation 4.23. The rate of total heat loss Q_{LC} from the concentrator is the sum of the rate of heat loss to the back Q_{BC}, the edge Q_{EC} and the top Q_{TC}.

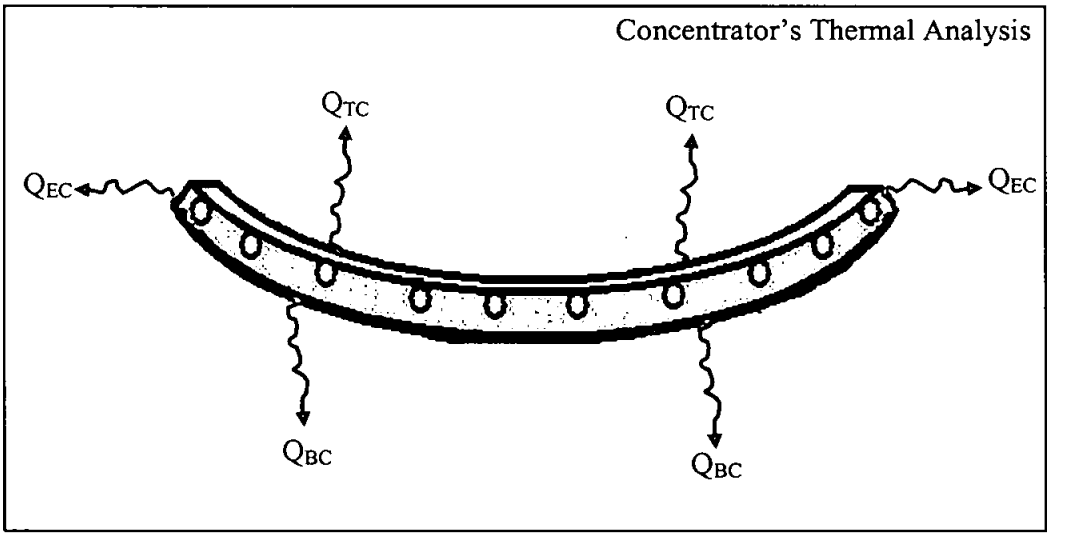

Figure 4.11 The rate of heat losses from the concentrator of the new PTC design.

The individual rates of heat losses can be evaluated based on equations 4.24, 4.25 and 4.26 and are expressed in terms of top loss coefficient U_{TC}, edge loss coefficient U_{EC} and back loss coefficient U_{BC}.

$$Q_{TC} = U_{TC}A_C(T_{pm} - T_a) \tag{4.24}$$

$$Q_{EC} = U_{EC}A_C(T_{pm} - T_a) \tag{4.25}$$

$$Q_{BC} = U_{BC}A_C(T_{pm} - T_a) \tag{4.26}$$

The following equation 4.27 shows the rate of total heat loss Q_{LC} that is expressed in terms of the overall heat loss coefficient, U_{LC}.

$$\begin{aligned} Q_{LC} &= Q_{TC} + Q_{EC} + Q_{BC} \\ &= (U_{TC} + U_{EC} + U_{BC})A_C(T_{pm} - T_a) \\ &= U_{LC}A_C(T_{pm} - T_a) \end{aligned} \tag{4.27}$$

It can be seen from equation 4.27 that the overall heat loss coefficient U_{LC} is the sum of U_{TC}, U_{EC} and U_{BC} and based on this, the following equation 4.28 is derived to estimate U_{LC}.

$$U_{LC} = \left(\frac{k_i}{L_e}\right)\left(\frac{A_e}{A_C}\right) + \frac{k_i}{L_b} + \varepsilon_s\sigma(T_{pm}^2 + T_a^2)(T_{pm} + T_a) + h_{wc} \tag{4.28}$$

The material used for insulation is important where k_i is the value of its thermal conductivity and L_e is the edge insulation thickness. Equation 4.29 can be used together with equation 4.5 to calculate A_C, where L is the length of the concentrator and equation 4.30 is used to calculate the edge area A_e of the concentrator based on inner arc length of collector S_{arc} and concentrator thickness L_{ct}.

$$A_C = S_{arc}L \tag{4.29}$$

$$A_e = 2(S_{arc} + L)L_{ct} \tag{4.30}$$

4.4.2 THERMAL ANALYSIS OF THE RECEIVER

The receiver consists of a circular cylindrical conduit tube made of copper, which is enclosed in a cover. The evaluation of heat losses from the receiver is as important as the evaluation of optical losses, as an optimum receiver size would allow higher energy gain where both the losses are minimized. The energy balance given as equation 4.23 described the thermal analysis of the receiver as well, with the concentration ratio included. The rate of total heat loss Q_{LR} from the receiver is the sum of the rate of heat losses as shown in Figure 4.12. The general relationship between the heat losses due to radiation and convection is shown in equation 4.31.

$$Q_{LR} = Q_{conv,cover} + Q_{conv,tube} + Q_{rad,cover} + Q_{rad,tube} \qquad (4.31)$$

$$Q_{LR} = \frac{U_{LR}}{C_G} A_{eff} (T_{rm} - T_a) \qquad (4.32)$$

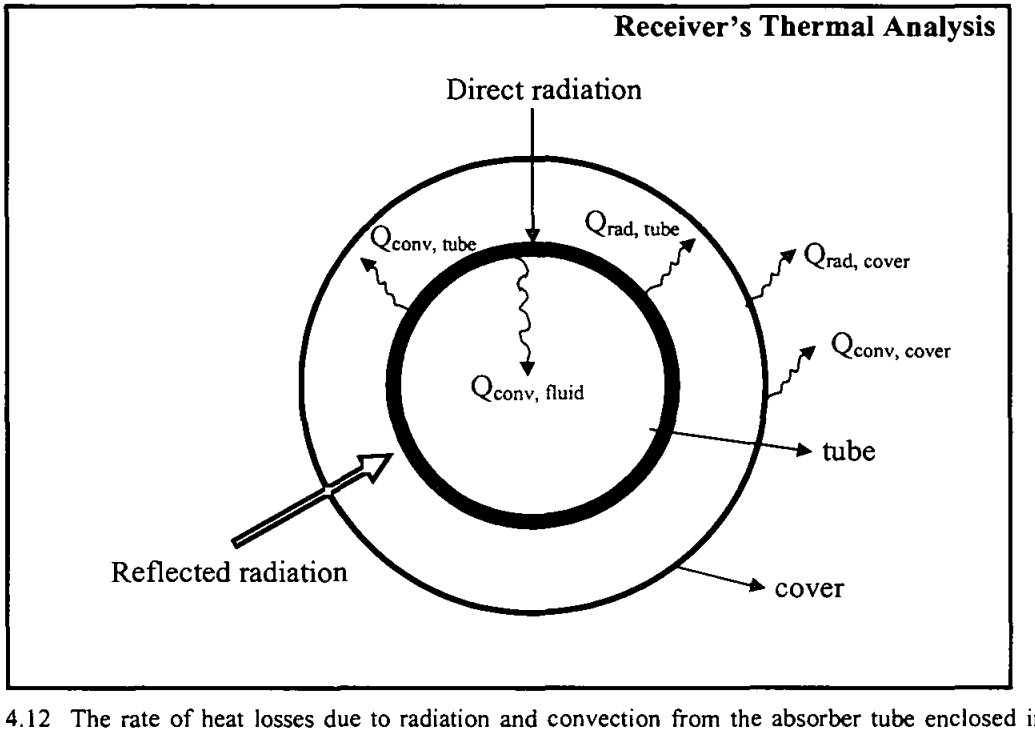

Figure 4.12 The rate of heat losses due to radiation and convection from the absorber tube enclosed in a cover.

The evaluation of the overall heat loss coefficient U_{LR} for the receiver can be estimated by using the semi-empirical equation developed by Mullick & Nanda (1989). Equation 4.33 is used to calculate the overall heat loss coefficient directly by taking into consideration the heat losses due to radiation and convection from the absorber tube enclosed in a cover, as shown in Figure 4.12.

$$U_{LR} = \left(\frac{1}{C_1 (\delta T_1)^{0.25} + \left[\frac{\sigma (\delta T_2)(\delta T_3)}{C_2} \right]} + \left[\left(\frac{D_O}{D_{co}} \right) \left(\frac{1}{C_3} \right) \right] \right)^{-1} \qquad (4.33)$$

The constants C_1, C_2 and C_3 are obtained from the correlation of Raithby & Hollands (1975) and are given in equations 4.34, 4.35 and 4.36.

$$C_1 = \frac{17.74}{(\delta T_2)^{0.4} D_O \left(D_O^{-0.75} + D_{ci}^{-0.75} \right)} \qquad (4.34)$$

$$C_2 = \frac{1}{\varepsilon_p} + \frac{D_O}{D_{ci}} \left(\frac{1}{\varepsilon_C} - 1 \right) \qquad (4.35)$$

$$C_3 = h_W + \left(\sigma \varepsilon_C (\delta T_4)(\delta T_5) \right) \qquad (4.36)$$

The temperature coefficients can be evaluated based on equations 4.37 to 4.41. The temperatures that are required to evaluate the coefficients are ambient temperature T_a, cover temperature T_c and receiver's mean temperature T_{rm}.

$$\delta T_1 = T_{rm} - T_C \qquad (4.37)$$

$$\delta T_2 = T_{rm} + T_C \qquad (4.38)$$

$$\delta T_3 = T_{rm}^2 + T_C^2 \qquad (4.39)$$

$$\delta T_4 = T_C + T_a \qquad (4.40)$$

$$\delta T_s = T_C^2 + T_a^2 \qquad (4.41)$$

All the temperature values are expressed in Kelvin and the following equation 4.42 and 4.43 are used to evaluate the cover temperature T_C. Equation 4.42 is to be used if the T_{rm} is in the range of 333 K< T_{rm} <513 K and equation 4.43 if the range is 513 K< T_{rm} <623 K (Sukhatme, 1996).

$$T_C = T_a + \left[\left(0.04075\left(\frac{D_O}{D_{ci}}\right)^{0.4} h_w^{-0.67}\left(2 - 3\varepsilon_p + \frac{(6+9\varepsilon_p)T_{rm}}{100}\right)\right)(T_{rm} - T_a)\right] \qquad (4.42)$$

$$T_C = T_a + \left[\left(0.163\left(\frac{D_O}{D_{ci}}\right)^{0.4} h_w^{-0.67}\left(2 - 3\varepsilon_p + \frac{(1+3\varepsilon_p)T_{rm}}{100}\right)\right)(T_{rm} - T_a)\right] \qquad (4.43)$$

The design specifications that are needed include the outer diameter of the receiver tube D_O, the inner and outer diameter of the receiver's cover D_{ci} and D_{co}. The manufacturing specifications are the emitance of the receiver tube ε_p and emitance of the cover ε_c. The evaluation of h_w is discussed in section 4.4.6.

4.4.3 HEAT REMOVAL FACTORS

The heat removal factor is an important design parameter that measures the thermal resistance encountered by the absorbed solar radiation in the working fluid. There are two heat removal factors that are evaluated. The heat removal factor F_C is the concentrator's heat removal factor and F_R is the receiver's heat removal factor. The concentrator's heat removal factor F_C takes into account the flowrate and configuration of the back tubes, while the receiver heat removal factor F_R includes the flowrate in the receiver's conduit tube. Generally, the heat removal factor can be viewed as the ratio of the actual useful

energy gain by the heat-absorbing surface to the useful energy gain if the entire absorber surface was at the fluid inlet temperature. The heat removal factors F_C and F_R can be evaluated by using equations 4.44 and 4.45 (Goswami *et al.*, 2000).

$$F_C = G_C F_{CE}(1 - e^{-\frac{1}{G_C}}) \qquad (4.44)$$

$$F_R = G_R F_{RE}(1 - e^{-\frac{1}{G_R}}) \qquad (4.45)$$

The factors G_C and G_R are the dimensionless collector capacitance rate for the concentrator and receiver respectively (Sukhatme, 1996) and is shown in equation 4.46 and 4.47 below:

$$G_C = \frac{J_C C_p}{A_C U_{LC} F_{CE}} \qquad (4.46)$$

$$G_R = \frac{J_R C_p}{A_R U_{LR} F_{RE}} \qquad (4.47)$$

4.4.4 PTC EFFICIENCY FACTORS

The analysis of PTC efficiency factors is based on the concentrator and receiver's efficiency factors. The contributions from different configurations of back tubes are included in the concentrator's heat removal factor. In order to ensure that heat transferred from the absorber to the working fluid is higher than the heat losses, a suitable back tube configuration is necessarily selected. The back tube configuration is described by the concentrator's efficiency factor F_{CE}. The concentrator's efficiency factors of the parallel flow and serpentine flow (Duffie & Beckman, 1980) back tubes are given as equations 4.48 and 4.49 respectively.

$$F_{CE} = \left[W_s U_{LC} R + \frac{W_s}{D_{CTi} + (W_s - D_{CTi}) F_U} \right]^{-1} \quad (4.48)$$

$$F_{CE} = \left(\frac{P_K}{U_{LC} W_s} \right) \left[\frac{P_K R(1+\nu)^2 - 1 - \nu - P_K R}{(P_K R(1+\nu) - 1)^2 - (P_K R)^2} \right] \quad (4.49)$$

The parameter F_U depends on the inner diameter D_{CTi} and spacing of the back tubes W_s, thickness L_{ct} and thermal conductivity k_c of the concentrator, and overall heat loss coefficient (Sukhatme, 1996).

$$F_U = [\tanh(0.5 E_D (W_s - D_{CTi}))][0.5 E_D (W_s - D_{CTi})]^{-1} \quad (4.50)$$

$$P_K = \frac{\sqrt{U_{LC}}}{E_D^2} [\sinh((W_s - D_{CTi}) E_D)]^{-1} \quad (4.51)$$

$$\nu = -2\cosh((W_s - D_{CTi}) E_D) - \frac{D_{CTi} U_{LC}}{P_K} \quad (4.52)$$

$$R = \frac{\pi D_{CTi} h_{ce} + C_B}{\pi D_{CTi} h_{ce} C_B} \quad (4.53)$$

$$E_D = \sqrt{\frac{U_{LC}}{k_c L_{ct}}} \quad (4.54)$$

The serpentine configuration is easier to construct, less prone to leaks, less expensive and to a certain extent is more efficient than the parallel flow geometry. Although the flow rate is uniform, there is a flow rate restriction problem, which leads to higher pumping requirements. Usually by connecting two or more serpentine tubes in parallel can reduce

the flow restriction problem. As for the parallel flow geometry, the flow rate drops towards the centre of the tubes where most of the heat is concentrated.

The receiver's efficiency factor F_{RE} is evaluated based on equation 4.55, where U_{LR} is the overall heat loss coefficient, h_{CR} is the convective heat transfer coefficient inside the tube of the receiver and k is the thermal conductivity of the receiver tube (Duffie & Beckman, 1980). Here the receiver's inner diameter D_i and outer diameter D_O are also required.

$$F_{RE} = \frac{U_{LR}^{-1}}{\frac{1}{U_{LR}} + \frac{D_O}{h_{CR} D_i} + (D_O \ln(\frac{D_O}{D_i})(2k)^{-1})} \qquad (4.55)$$

4.4.5 ENERGY BALANCE EQUATION

The energy balance equation is the useful heat gain rate of the new parabolic trough concentrator design. The concentrator's energy balance is given as equation 4.56.

$$Q_C = A_C F_C [S_C - U_{LC}(T_{ci} - T_a)] \qquad (4.56)$$

In this equation, A_C refers to the total area of the concentrator, F_C is the heat removal factor, S_C is the amount of solar radiation absorbed by the concentrator, U_{LC} is the concentrator's overall heat loss coefficient, and T_{ci} and T_a are fluid inlet and ambient temperature respectively. After the concentrator's energy balance equation is obtained, the outlet fluid temperature T_{co} from the back tubes can be estimated by using equation 4.57.

$$T_{co} = T_{ci} + \frac{Q_C}{J_C C_p} \qquad (4.57)$$

The receiver's energy balance equation Q_R is given as equation 4.58 where C_G is the concentration ratio and T_{co} and T_a are the fluid outlet and ambient temperatures respectively. The term A_{eff} refers to the area that is not shaded of the aperture, S_R is the absorbed solar radiation energy and T_{co} is the fluid temperature that exits from the concentrator's back tubes (Sukhatme, 1996).

$$Q_R = F_R A_{eff}\left[S_R - \frac{U_{LR}}{C_G}(T_{co} - T_a)\right] \qquad (4.58)$$

The efficiency η_T of the new PTC design is estimated based on equation 4.59, where $Q_{(C+R)}$ is the total heat gained calculated by adding Q_C and Q_R.

$$\eta_T = \frac{Q_{(C+R)}}{WL(I_T)} \qquad (4.59)$$

4.4.6 EVALUATION OF HEAT LOSS COEFFICIENTS

Reynolds, Nusselt and Prandlt numbers are used to evaluate the heat transfer coefficient of fluid flows h_i. The properties of the parameters defining these numbers are dependent on temperature. The general relationship between h_i and Nusselt number is given in equation 4.60, while the Reynolds number is evaluated based on equation 4.61, depending on the mean flow velocity V, diameter D and the kinematic viscosity ν (Incropera, 1996).

$$h_i = \frac{Nu \times k}{D} \qquad (4.60)$$

$$Re = \frac{VD}{\nu} \qquad (4.61)$$

Prandlt number is given in equation 4.62, where μ is the dynamic viscosity, C_p and k is the specific heat capacity and thermal conductivity of the fluid flowing in the tube respectively (Holman, 2002).

$$Pr = \frac{\mu C_p}{k} \qquad (4.62)$$

The nature of fluid flow is determined by using the Reynolds number. The information provided in Table 4.3 is used to identify the nature of flow during simulation. It is also useful to know the nature of the flow, especially in evaluating the Nusselt number.

Table 4.3 Indicators to classify the nature of fluid flowing in smooth tubes.

$Re < 2300$	Laminar flow
$2300 \leq Re \leq 4000$	Transition from laminar to turbulence flow
$Re > 4000$	Turbulence flow

The computational analysis of heat transfer coefficients can be tedious, especially if it is carried out in an environment where there is a change in temperature. The properties of the parameters involved in evaluating heat transfer coefficients can be obtained from handbooks but to a certain limit as the supplied data is recorded at certain temperature intervals. The resolution of the data depends on these temperature intervals. This limitation can slow down the computer simulation process, whereby a large database system must be created, to cater for the change in values for certain temperature dependent parameters. If the fluid gains heat, there will be an increase in temperature and this can cause variation in the values of the temperature dependant parameters such as density ρ, dynamic viscosity μ, specific heat capacity C_p and thermal conductivity k. The exact evaluation of these parameters at certain temperatures is usually not possible, unless temperature dependent factors used in the research work are developed. The temperature dependent factors will be

described when the relevant heat transfer coefficients are derived. The convective heat transfer coefficients h_{wc} and h_w are due to wind blowing across the concentrator and receiver respectively. Reynolds number is used to determine the nature of the fluid's motion. The parameters defining the Reynolds number depend on temperature, where a temperature dependent factor R_{AIR} is introduced.

$$\mathrm{Re} = V_W L \; R_{AIR} \tag{4.63}$$

$$R_{AIR} = \sum_{i=0}^{n} R_i T^i \tag{4.64}$$

In this study, the Nusselt number equation used in the evaluation of h_w is based on a correlation derived by Churchill and Bernstein (1977). The correlation is given as equation 4.65 and involves the Reynolds and Prandlt numbers as well. The Reynolds number is evaluated by using equation 4.63 and Prandlt number is calculated by using equation 4.62.

$$Nu = 0.3 + \frac{0.62\,\mathrm{Re}^{1/2}\,\mathrm{Pr}^{1/3}}{[1+(0.4/\mathrm{Pr})^{2/3}]^{1/4}}\left[1+\left(\frac{\mathrm{Re}}{28200}\right)^{5/8}\right]^{4/5} \tag{4.65}$$

$$h_W = \frac{Nu_W K_{AIR}}{D_R} \tag{4.66}$$

$$K_{AIR} = \sum_{i=0}^{n} K_i T^i \tag{4.67}$$

The concentrator's h_{wc} is evaluated after the nature of flow is determined by using equation 4.64. The h_{wc} can be approximated by using equations 4.68 and 4.69, for laminar and turbulent conditions, where T_{pm} is the mean concentrator plate temperature, T_a is the ambient temperature, and ε_s is the emissivity of the reflective surface

$$h_{wc} = \frac{453 Re^{0.5} Pr^{1/3} K_{AIR}}{500L} \qquad \text{(Laminar)} \qquad (4.68)$$

$$h_{wc} = \frac{77 Re^{0.8} Pr^{1/3} K_{AIR}}{(2\times10^{3})L} \qquad \text{(Turbulent)} \qquad (4.69)$$

The method to evaluate the convective heat transfer coefficients h_{cc} and h_{cr} for fluid flowing in the back tubes and the receiver's conduit tube respectively, are evaluated by using comprehensive fluid flow mechanics. The evaluation of these coefficients makes use of H_{FACTOR} (Balbir & Fauziah, 2001), R_{FACTOR} (Fauziah & Balbir, 2002) and K_{FACTOR}. These factors depend on the type of heat transfer fluid used and its mean temperature. There are a few types of fluid where the H_{FACTOR}, R_{FACTOR} and K_{FACTOR} are already determined. These working fluids are saturated water, water vapour and synthetic oil such as dowtherm. These factors are used in order to reduce the burden of providing large physical properties database. Besides, once the simulation is being run, it cannot be stopped to provide the right values of the temperature dependent parameters. Before the convective heat transfer coefficient h_{cc} for the working fluid flowing in the back tubes is determined, the nature of flow is first determined by using equation 4.70 for flows in circular tubes (Fauziah & Balbir, 2002).

$$Re = \frac{14J}{11D_i}\left(\frac{1}{R_{FACTOR}}\right) \qquad (4.70)$$

The method used to find the R_{FACTOR} is by using the linear curve fitting method. R_{FACTOR} is an equation that varies with temperature and is obtained by doing a curve fitting on the plot of dynamic viscosities of the heat transfer fluid for a certain range of temperature. After the nature of flow is determined by comparing the calculated Reynolds value with the range shown in Table 4.3, for a laminar flow where Re<2300 (Cho *et al.*, 1998), the Nusselt

number is equal to 3.66 (Suryanarayana, 2000). In order to determine h_{CC}, equation 4.71 is used, where k_f is the working fluid's thermal conductivity and D_{CTi} is the concentrator's back tubes inner diameter.

$$h_{CC} = 3.66\frac{k_f}{D_{CTi}} \qquad (4.71)$$

$$h_{CC} = 3.66\frac{K_{FACTOR}}{D_{CTi}} \qquad (4.72)$$

The K_{FACTOR} used in equation 4.72 is based on the thermal conductivities of the heat transfer fluids which varies with temperature and is obtained by doing a curve fitting on the plot of thermal conductivities of the heat transfer fluid for a certain range of temperatures.

For a turbulent flow where Re>2300, the Nusselt number is given in equation 4.73, which is known as Dittus-Boelter equation (Cengel, 1998) and the value of h_{CC} is then obtained.

$$Nu = 0.023\,Re^{0.8}\,Pr^{0.4} \qquad (4.73)$$

$$h_{CC} = \frac{(0.023\,Re^{0.8}\,Pr^{0.4}) \times k_f}{D_{CTi}} \qquad (4.74)$$

In this research work, the tubes welded to the concentrator are circular cylindrical tubes and equation 4.75 (Balbir & Fauziah, 2003) is derived to evaluate the h_{CC}.

$$h_{CC} = 0.028\frac{J_C^{0.8}}{D_{CTi}^{1.8}}H_{FACTOR} \qquad (4.75)$$

$$H_{FACTOR} = \frac{C_p^{0.4} k^{0.6}}{\mu^{0.4}} \qquad (4.76)$$

The evaluation of h_{cr} is similar to the method of calculating h_{CC}. The main parameters that are changed to evaluate h_{cr} are the tube diameter and the mass flowrate.

$$h_{cr} = 3.66 \frac{K_{FACTOR}}{D_R} \qquad (4.77)$$

$$h_{cr} = 0.028 \frac{J_R^{0.8}}{D_R^{1.8}} H_{FACTOR} \qquad (4.78)$$

Some of the parameters that have been determined to be used in the optimisation process, as outlined in Figure 7.7, are the optimum values of the rim angle and acceptance half-angles. The optimum rim angle to be used is 90° and the acceptance half-angle below 1.77° will provide more flexibility in designing, especially when dealing with the errors described in section 4.3.1. It can be seen from Figure 4.2 that saturated water is used as the heat transfer fluid in this research work because the increase in the specific heat capacity of saturated water, as the temperature increases. In the next chapter, the discussion will be on the principles of simulation and modelling, where useful flowcharts will be given for the main simulation components.

CHAPTER 5

SIMULATION AND MODELLING

The struggling days with low level programming languages of the last century, have been replaced with high-level programming and authoring tools such as MATLAB that made computer simulation an important aspect in almost any scientific research. The initial simulation work is done by using Microsoft Excel 2000, in dealing with the solar insolation data. The simulation concepts are time dependent, and in line with the changing technology where they must be revised and refined continuously. The fundamentals of simulation work will be discussed in this chapter.

5.1 PRINCIPLES OF SIMULATION AND MODELLING

In line with the current technology development, the escalating complexity of energy and environmental systems are dealt with computer modelling and simulation. These tools are emerging as a viable approach to design and performance evaluation. There is a need to understand the theoretical and operational principles underlying this technology, as the solar thermal processes are dynamic in nature. The traditional way of designing is by developing a prototype using some basic calculations where data is collected for a certain period of time. If the performance is not as expected, then continuous refinements are carried out and the whole process of testing is repeated. Usually, after a few refinements, if the prototype fails, it is discarded.

Computer simulation is one of the most powerful tools currently used for analysing and designing complex systems. According to Aburdene (1988), simulation is the process of developing a simplified model of a complex system that is used to analyse and predict the behaviour of a real system. Simulation is carried out because real-life systems are often difficult to be analysed due to their complexity. It is generally possible to develop a model that can be used to predict the behaviour of the real system to an accuracy of 95 % and above, as demonstrated by using TRNSYS computer program (Kalogirou & Papamarcou, 2000).

5.1.1 SIMULATION AND MODELING DEFINITIONS

The definitions of modeling and simulation are necessary in order to begin describing the simulation methodology, where a model is described as a simplified representation of a system, process or theory that is intended to enhance our ability to understand, predict, and possibly control the behaviour of the system (Neelamkavil, 1987). Simulation is described as a procedure in which one system is substituted for another system that it resembles in certain important aspects (Carroll, 1987). In order to set the frame of reference, it is necessary to explain where simulation and modelling fits into the entire design process, prototyping and testing. In the design process there are sub-categories, which include problem definition, conceptual design, embodiment design, and detailed design. Modelling and simulation are part of the embodiment design where product structure and the association between product elements are established (Pickett & Boyse, 1984).

5.1.2 CLASSIFICATION OF MODELS

There are many ways, in which a model can be classified, but in this study there are two categories that will be highlighted. The two ways of categorising a model is by

determining the class and type of model to be used. There are three basic classes of models, which are the iconic, analogue and symbolic models. The iconic models are the scaled depiction of the real physical system. The models resemble the actual system, except that they are scaled down or up, depending on the nature of investigation. The simulation that is carried out is also a real dynamic process. The analogue models are also actual physical models, but represented by a different physical system as compared to the original model. Usually the mechanical models are easily understood when electrical models represent them. Some heat transfer problems use electrical resistance analogy to provide good solutions (Raven, 1995).

The class of model that is used in this research work is known, as a symbolic model. It is a mathematical model that uses variable relationships to model and simulate the real physical system. There are three types of symbolic model that come under this category. They are the deterministic, stochastic and discrete models (Osborne & Watts, 1977). A model is classified as discrete when the dependent variables change by discrete amounts at specified points and the stochastic model deals completely with random variables or variables based on a certain probability distribution. A deterministic model works on input variables that are not uncertain and represent certain physical quantities. Therefore the simulation model in this research work is a symbolic deterministic model and the prototype will be an iconic model.

5.1.3 PLANNING AND ORGANISATION

One of the critical aspects of simulation and modelling in this research work is the planning and organisation of mathematical equations that will be useful to build a reasonably true symbolic deterministic model, and management of input and output data. This will influence the output of the simulation to a certain extent, where the desired

outcome must be able to resemble the behaviour of the real system to a certain level of reliability and acceptability. Often the last part of the simulation process is unplanned and the results obtained by the simulation process are not readily transferable to useful presentation format. The ability to translate the results of simulation to clear, concise and quantitative information will accelerate the decision making process, so that a prototype can be produced to validate the simulation. The results must also indicate how successful the simulation is where its acceptability is very important. The acceptability for a valid simulation is based on its model and it should be an accurate representation of the actual system (Law & Kelton, 2000).

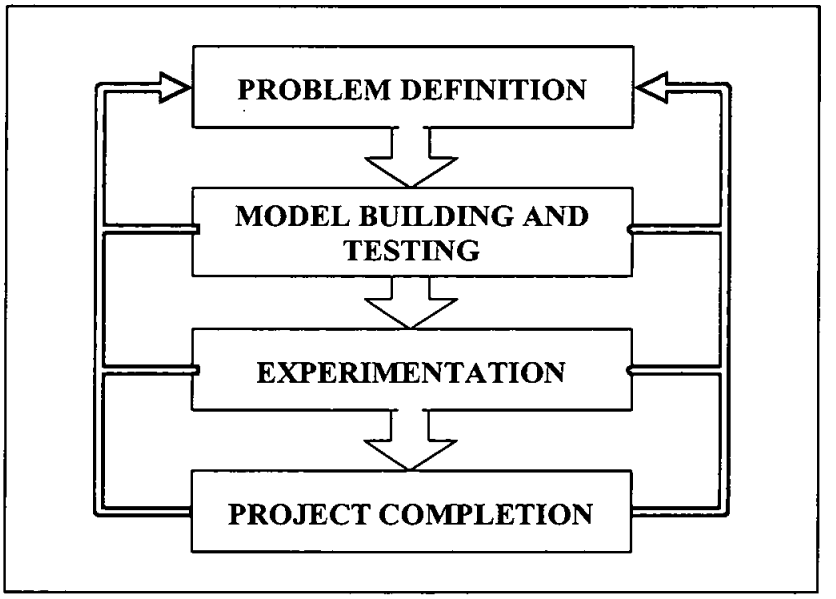

Figure 5.1 An overview of the simulation project.

The overall simulation process should be mapped accordingly and as for the planning and organisational aspects, a four-phase approach was adopted based on Robison's (1994) suggestions. The four-phase approach turns the simulation process into a project-based simulation as shown in Figure 5.1. The additional blue lines show that the process is iterative in nature and the movement is not necessarily downward. This flexibility allows the model to be revised at any stage of the four phases. The components of the four-phase

approach are simplified and presented as Table 5.1. The components are useful in the planning and organization of the simulation work that is carried out in this research work.

Table 5.1 Components of the four-phase approach.

Phase One **Problem Definition**	Identify the problem and set the objectives
	Define the experimental factors and reports
	Determine the scope and level of the model
	Collect and analyse the data
	Provide a project specification
Phase Two **Model Building and Testing**	Structure the model
	Build the model : coding, documenting, verifying
	Validate the model
Phase Three **Experimentation**	Performing experiments
	Analyse the results and draw conclusions
Phase Four **Project Completion**	Communicate the results
	Complete the documentation
	Review the project
	Perform further simulation work

5.1.4 SIMULATION PROCESS FLOW DIAGRAM

The process flow diagram is important to adopt and apply the four phases described earlier. A process flow diagram ought to be determined, but the movements in the flowchart must be flexible enough to incorporate changes along the way.

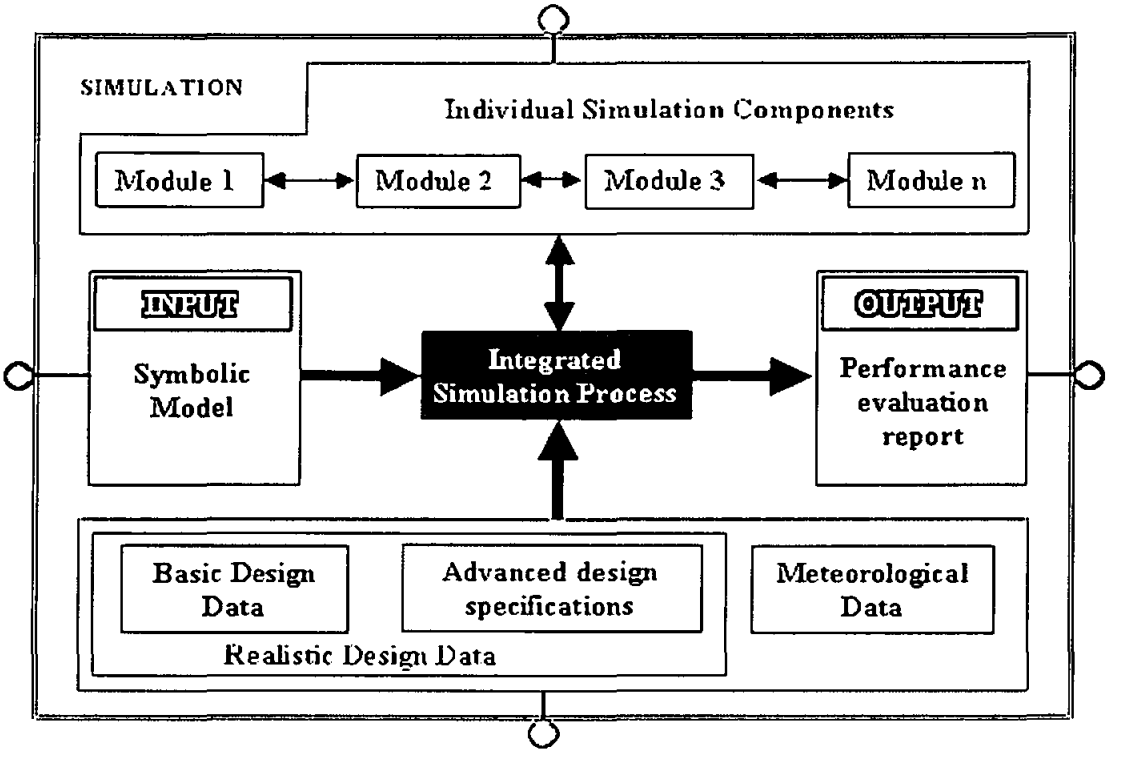

Figure 5.2 Simulation process flow diagram developed for this research work.

The integrated simulation process is flexible and the model can be refined, even if there is no change of the data. The integrated simulation procedures are modular and have the flexibility of incorporating changes at any stage, unlike the traditional simulation methods whereby the whole simulation program has to be rewritten. In fact the meteorological data processor can be made to function on its own and simulation can also be carried out to separate the global solar radiation into beam and diffuse components. By using the integrated simulation process, the modules can be made to interact with each other, if there is a need. The bubble connectors show how the components within the simulation block diagram are connected to the external environment. The iterative processes within the simulation block are self-sustaining for optimisation purposes, but that does not mean that there is a need to operate in isolation.

5.2 SOFTWARE USED FOR SIMULATION

The design tools used to develop the model must have an adequate accuracy and therefore it is important to select the right programming tools before the simulation program is written. MATLAB is a high-performance language for technical computing and integrates computation, visualization, and programming in an easy-to-use environment where problems and solutions are expressed in familiar mathematical notation. Among its capabilities are user-friendly algorithm development environment, data acquisition and analysis, modelling, simulation, prototyping and engineering graphics. In this research work, MATLAB is used for its simulation needs.

5.3 SIMULATION OF THE NEW PARABOLIC TROUGH CONCENTRATOR

The simulation design of a parabolic trough concentrator for this research is based on the integrated simulation process. The integrated simulation process basically deals with the design requirements, design analysis and system performance assessment. This methodology is based on a mathematical structure that captures all the required and necessary equations in a modular form. Since the main part of this research work is related to the simulation process, the prototype design process relies on the output from the computer simulation. The approach used is an integrated simulation approach, where two different models are used and the simulated output of one model is used as part of the input for the other model. Due to this, the receiver modules and concentrator modules are assessed separately, and they are the important components of a parabolic trough concentrator. The concentrator modules formed the first model and receiver modules are part of the second model. The use of the integrated simulation approach allows the final outcome to be combined, with the overall efficiency of the parabolic concentrator easily computed. The first step of the simulation process is to define the purpose and this has

been discussed in Chapter 2. The main objective is to carry out a solar energy conversion system assessment by using a parabolic trough concentrator for possible electrical power generation.

5.3.1 INDIVIDUAL SIMULATION COMPONENTS

The data collected by simulation has to be captured systematically and proper analysis is vital to ensure the success of any simulation process. Preliminary simulations might be necessary and is allowed in an integrated simulation approach. These simulations are necessary to determine the engineering options and alternatives that are useful. The initial design module will attempt to include all initial design parameters that will define a reference system that has to be modelled, especially in terms of its boundaries. The type of model used here is the symbolic deterministic model.

The individual simulation components, as shown in Figure 5.2, have bubble connectors that can allow the modules within its boundary to interact with the external environment. Further enhancement to the simulation process is achieved, as the modules can be inter-connected. In the same figure no names are specified for the modules, as the simulation process flow diagram is designed in such a way that it can be used to simulate any solar energy related systems. The modules in this simulation design work are the initial design module, meteorological data processing module, concentrator's thermal module, concentrator's optics module, receiver's thermal module and receiver's optics module.

5.3.2 INITIAL DESIGN MODULE

The process of defining a parabolic trough concentrator model for simulation is not easy as the surface geometry has to be detailed out carefully. The operation of a line focus

parabolic trough solely depends on the accuracy of the surface geometry. So it is important to define this module first, before any other related simulation activities can be performed.

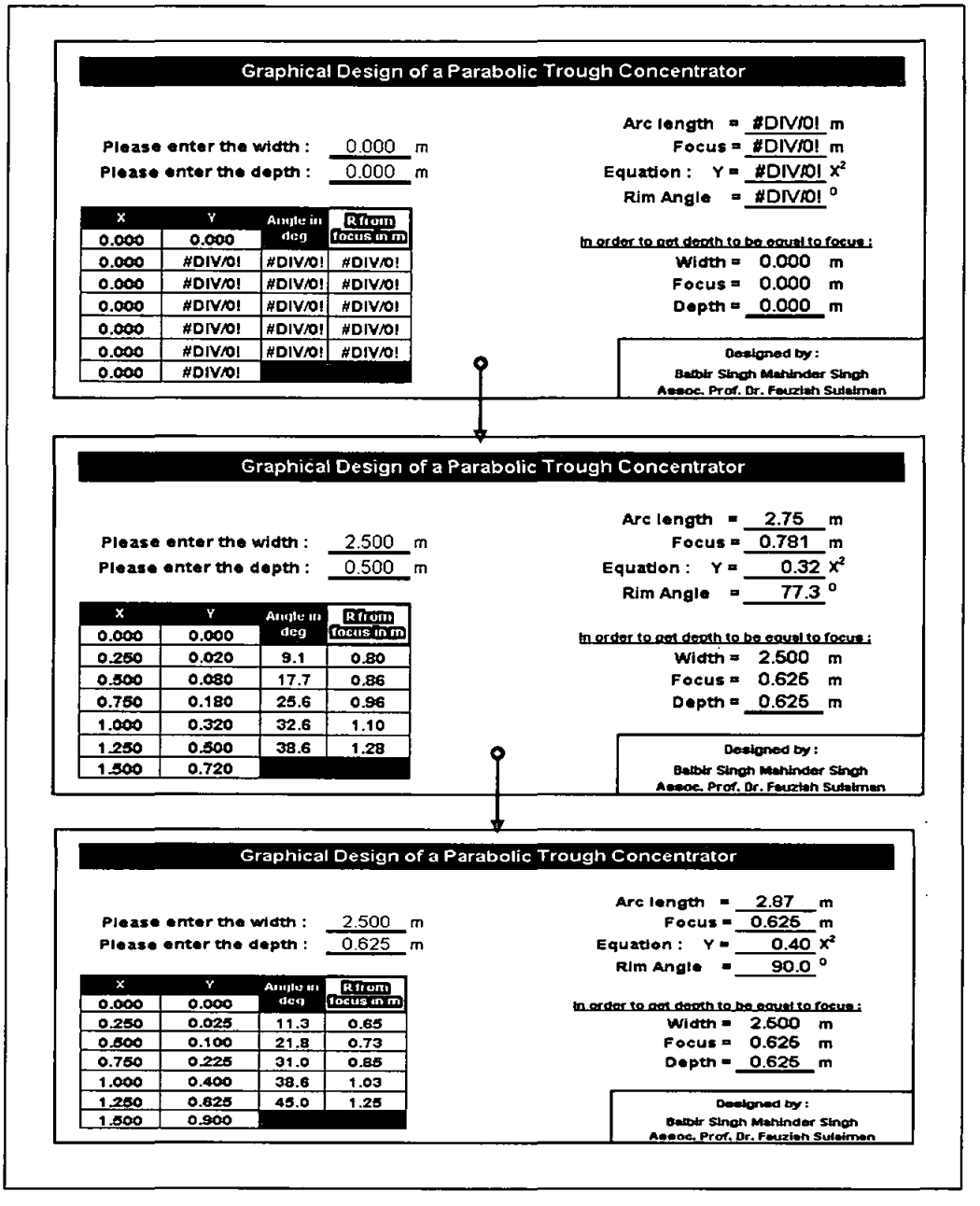

Figure 5.3 Snapshots of Microsoft Excel 2000 initial design menu.

Initial design inputs are the aperture width and depth of the trough. The ray tracing procedures, based on the reflection law will be used to identify the focal point. The snapshot of the interactive menu is given in Figure 5.3, where design coordinates are given. The parabolic equation is calculated to allow smaller segments to be defined, for

better surface accuracy. In this figure, the first snapshot shows that there is no initial design data supplied yet and the cells where the calculated values will be shown have error messages. Once the input data is assigned, then the calculated values are returned to all these cells.

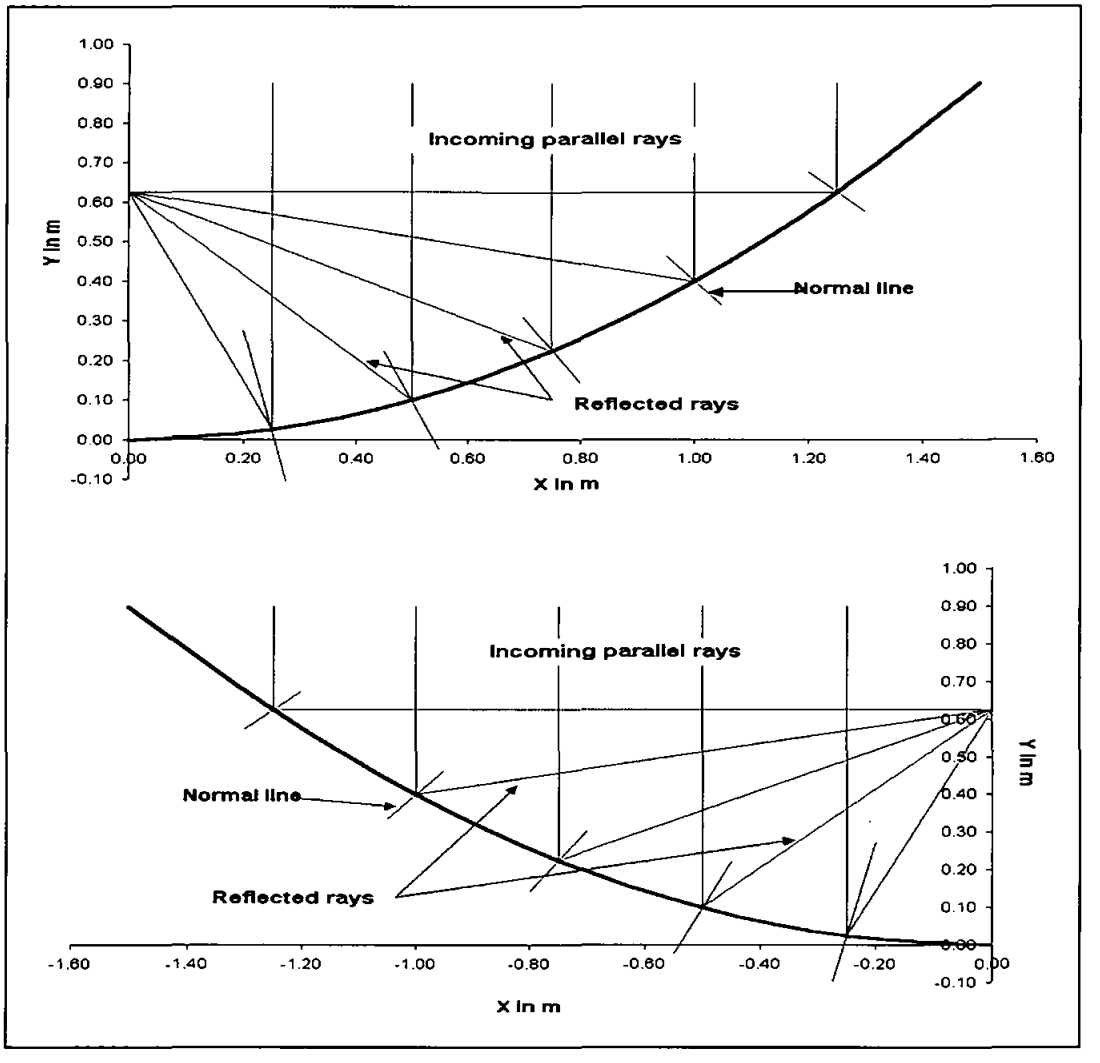

Figure 5.4 The above snapshots show the right and left side parabolic geometry and are simulated by using the same spreadsheet as shown Figure 5.3.

The data shown in Figure 5.3 is the actual design details of direct steam generators that are found at the solar power plant of the Engineering Institute at the National University of Mexico (Almanza & Lentz, 1998). The aperture of each module is 2.5 m, while the focus of the parabola is at 0.625 m, where the rim angle is 90°. Based on this figure, it can be

seen that if the focus is set to be at 0.625 m, then the rim angle must be 90° and it is a good initial verification to the simple simulation program, which is later translated to the MATLAB software. The same worksheet shown in Figure 5.3 is used to display the graphical representation of the parabolic shape in 2-D graphics as shown in Figure 5.4. The graphical displays are useful visual aids that can be used to provide some fundamental design information for actual fabrication process.

5.3.3 METEOROLOGICAL DATA PROCESSING MODULE

The Meteorological Services Department collects weather related data at its 317 stations distributed throughout Malaysia. Although there are 317 stations altogether, but only limited stations collect data related to solar radiation. The solar radiation data provided by the meteorological department is in text format. Figure 5.5 shows the format of the data obtained from the meteorological department, which requires the Microsoft WordPad software for viewing purposes only. The solar radiation data should be in the form, where it can be incorporated into simulation programs without much hassle. The beam and diffuse components too need to be separated, before they can be used to analyse the performance of a solar collector. The global solar radiation data is re-compiled to fit into a Microsoft Excel spreadsheet. The data can be transferred as text that will be placed in columns, as shown in Figure 5.6. The format of the characters can be changed to numerical values. There are repetitive data, such as the station number and hours where there is no sunlight. The main template is designed to accommodate the necessary data only and part of it is shown in Figure 3.9. The template should be made to look like the example given in Figure 3.9, as some instant statistical analysis such as the daily averages and monthly averages can be computed within the Excel spreadsheet itself. Preliminary investigations and presentation of data is important, as a thorough analysis of the concentrating systems is

necessary. The performance test is considered complete if they are exposed to the local weather conditions via the solar radiation data.

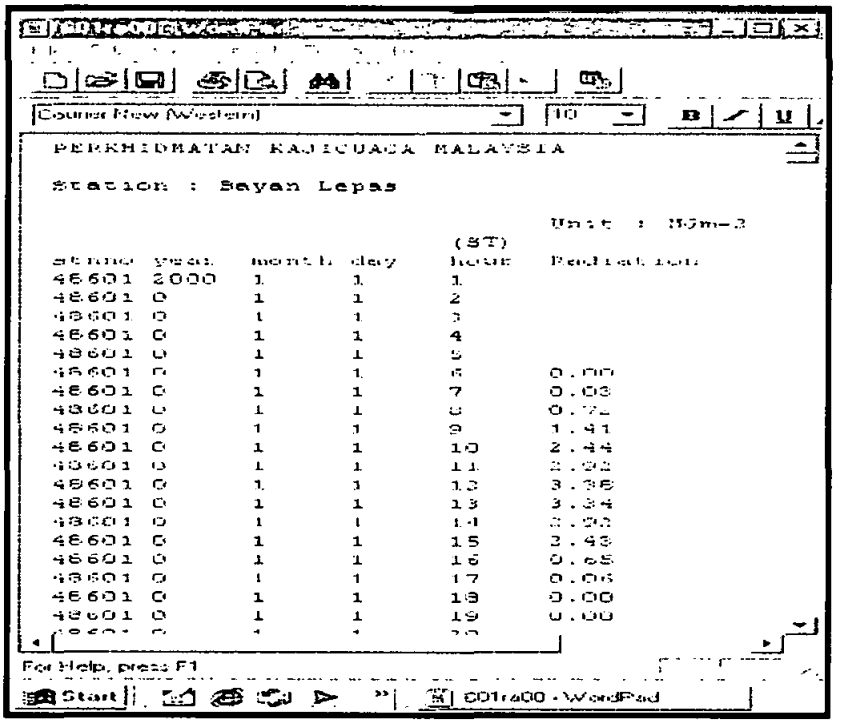

Figure 5.5 Snapshot of the format in which the global solar radiation data was supplied by the Malaysian Meteorological Department.

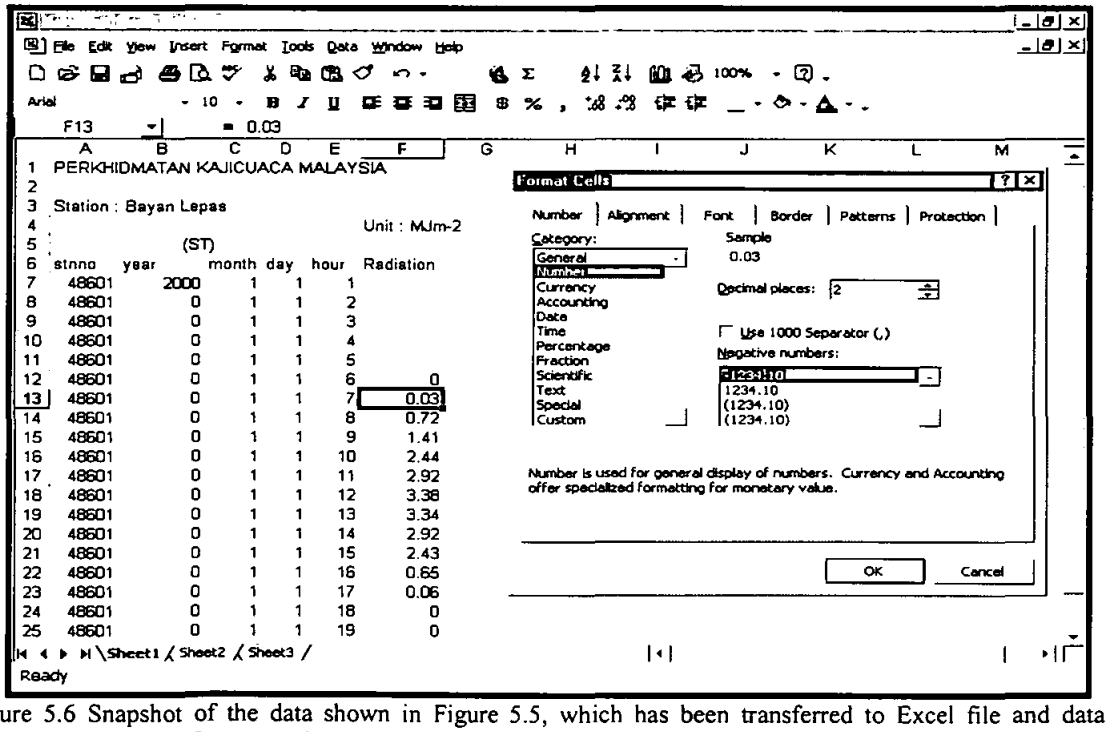

Figure 5.6 Snapshot of the data shown in Figure 5.5, which has been transferred to Excel file and data converted from text characters to numbers with the right decimal places.

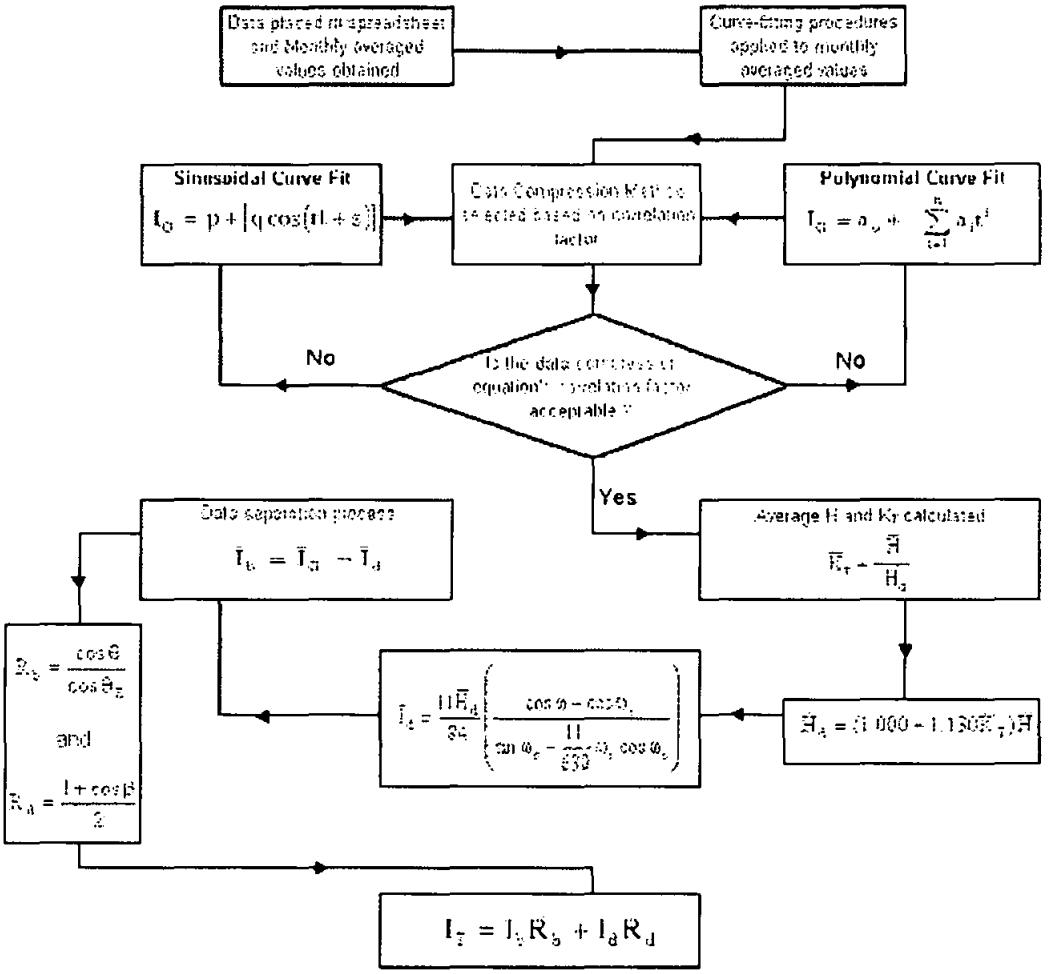

Figure 5.7 A meteorological data processing module flowchart to process the meteorological data for simulation.

Proper simulation procedures together with reliable solar radiation data are important for the writing of a computer program to evaluate the parabolic trough concentrating system. A whole system analysis of a parabolic trough concentrator requires simulation to be carried out, where design specifications are changed and simulated under the same weather conditions. This provides a good basis for comparison. The locality is also important as the place where there is a stable and high amount of solar insolation received can be marked as an important site where a solar thermal plant may be installed.

After the data has been compiled, using the format as shown in Figure 3.9, the next step is to process the data to obtain equations to compress the data and separate them to beam and

diffuse radiation components. Once the components are obtained, then the data is adjusted to obtain the solar insolation received by tilted surfaces. The flowchart shown in Figure 5.7 is used to write the programs in MATLAB and the Meteorological Data menu is shown in Figure 5.8. A user-friendly menu as shown in Figure 5.9 is used to input the global solar radiation data, or the data compression pushbutton can be pressed to key-in the coefficients of the curve-fitted equations, as described in section 3.6.

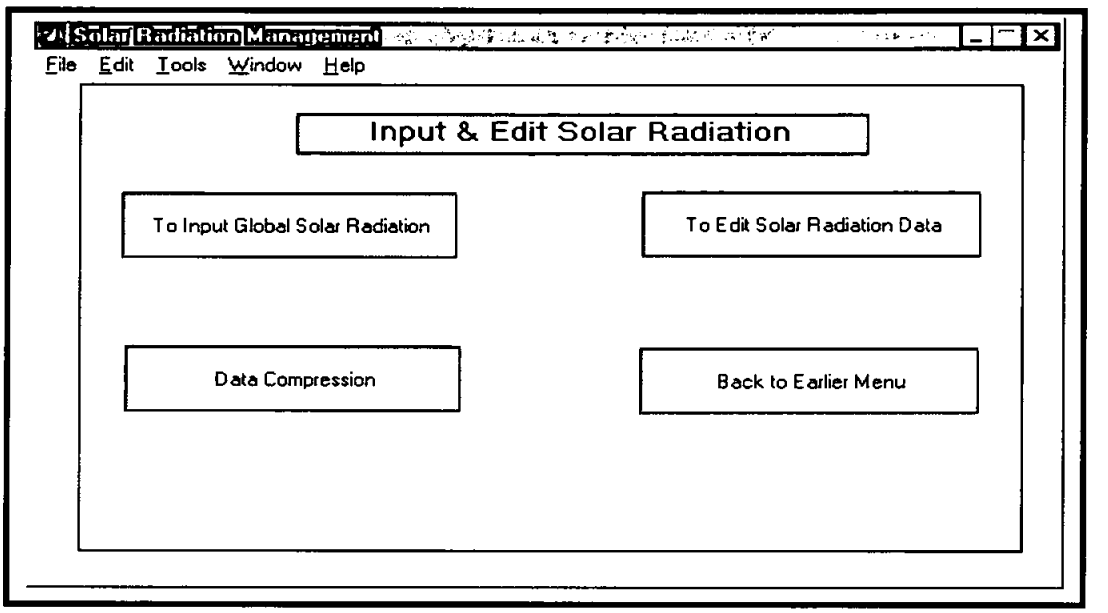

Figure 5.8 A user-friendly menu created to handle the solar radiation data.

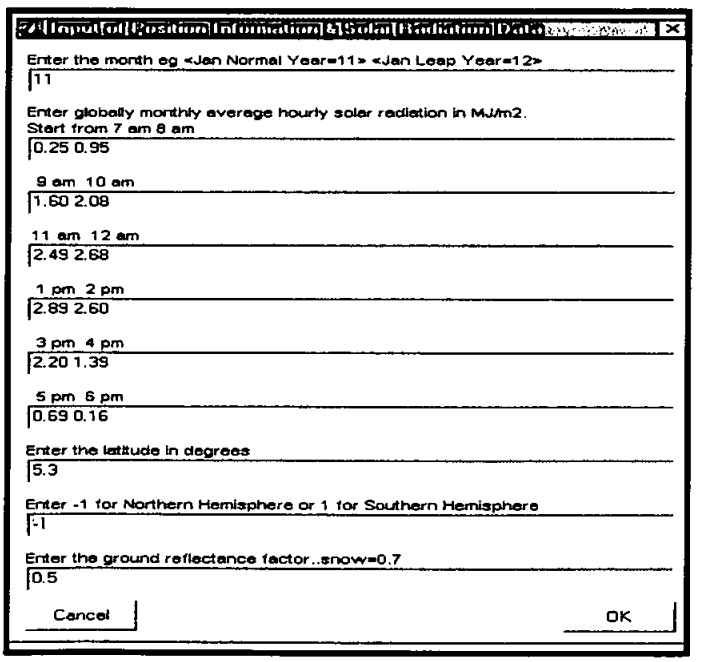

Figure 5.9 A user-friendly input menu that can be used to key-in the solar radiation data.

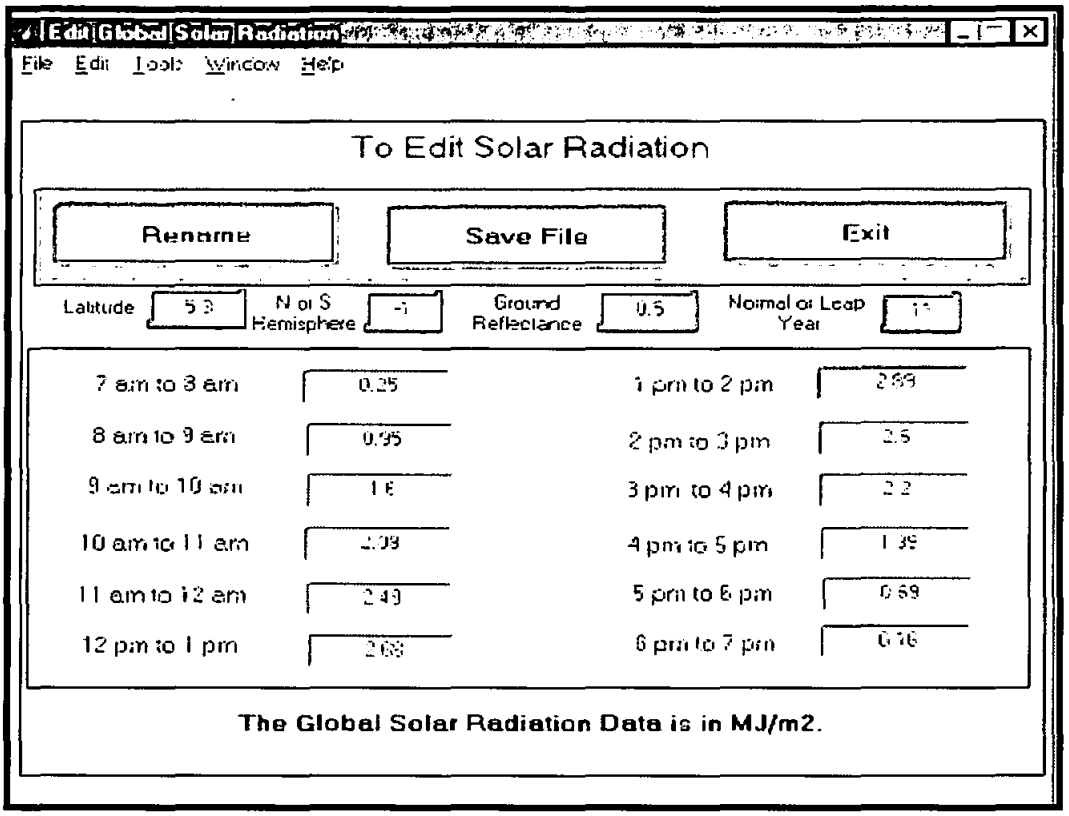

Figure 5.10 A user-friendly menu that can be used to edit the saved solar radiation data.

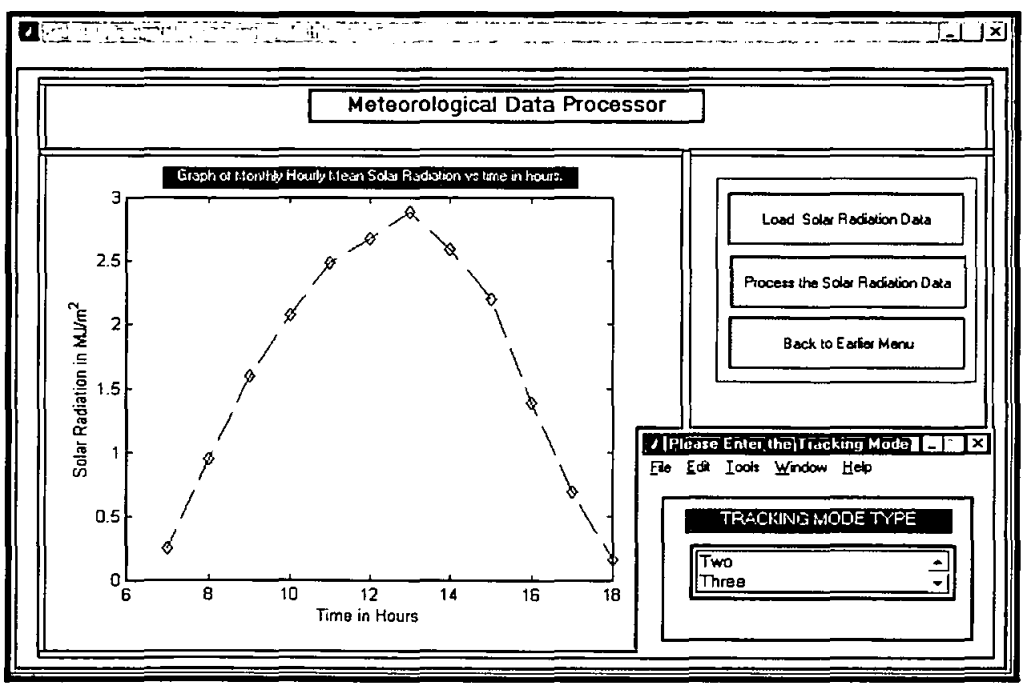

Figure 5.11 A Meteorological data processor menu.

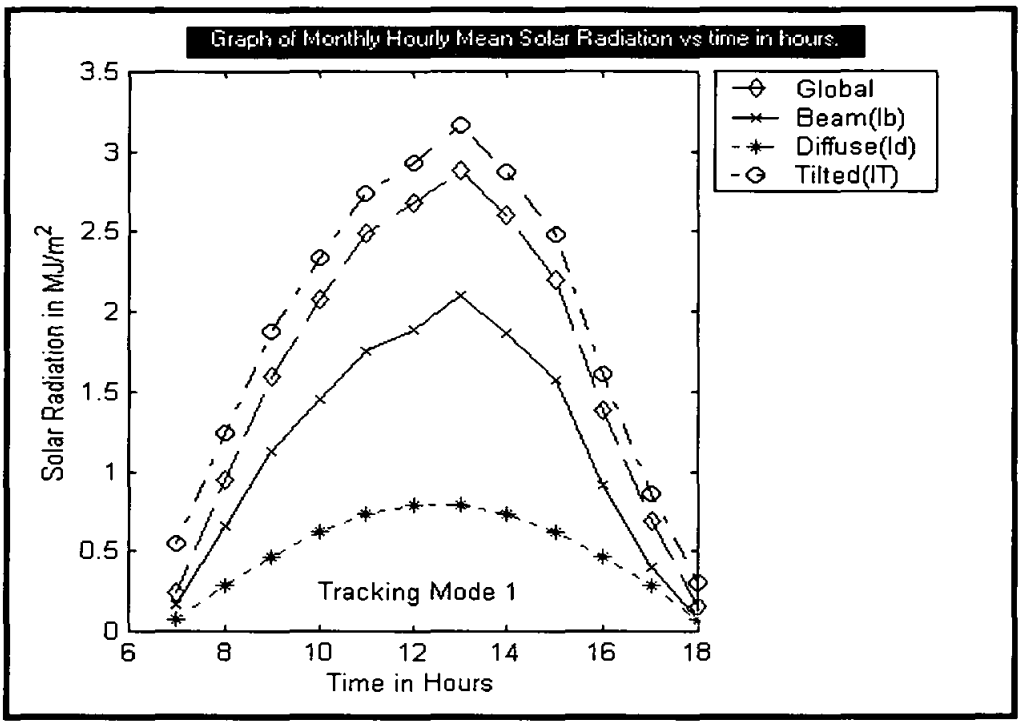

Figure 5.12 Graphs of processed solar radiation displayed in the same menu as that shown in Figure 5.11.

Figure 5.10 can be called if the edit solar radiation pushbutton is pressed and before this menu pops up, there is another menu, which is used to select the filename. This menu can be used to confirm the data that has been keyed-in or for purely editing purposes. MATLAB also has a special function called Excel Link, which will create a menu in the Excel program and can be used to interchange data. Figure 5.11 shows the menu that is used to load the solar radiation data that was captured earlier and displayed in graphical form. There is a tracking mode menu that can be used to specify the type of tracking that will be used, so that a proper analysis can be carried out by using the processor pushbutton.

The separation of the global solar radiation to beam and diffuse solar radiations respectively can be obtained by pressing the "Process the Solar Radiation Data" pushbutton. The outcome of doing that is shown in Figure 5.12, where the amount of radiation received by a tilted surface is shown too. There are altogether 4 graphs plotted, the measured global solar radiation that strikes a horizontal surface, beam radiation, diffuse

radiation and solar radiation that strikes the tilted surface based on the tracking mode chosen. All these processed information are saved in a file, which will be used for evaluating the performance of the parabolic trough concentrator.

5.3.4 TRACKING MODE MODULE

This module complements the earlier meteorological data processing module that is used to determine the components of the measured solar radiation. The tracking modes are incorporated in the simulation itself, as the performance of the parabolic trough concentrators depend on the reflected solar radiation that is concentrated at the focus. The reflected solar radiation can only reach the focal line, if the parabolic trough can be aligned in such a way that the incoming solar rays are parallel to its principal axis. The best way to achieve this will be by using a 2-axis tracking mechanism that can track the sun continuously. Altogether there are five different tracking modes, that are classified based on their virtual tracking abilities, the equations used to differentiate these tracking modes are related to the angle of incidence θ. The menu requesting for the type of tracking modes is shown in Figure 5.11 and will be displayed before data can be processed. The tracking mode module is very important and the program designed to incorporate its effect is based on the tracking mode module flowchart, shown in Figure 5.13 and has been discussed thoroughly in section 3.4.4. The flowchart shown is used to obtain the ratio factor of beam radiation on a tilted surface to the radiation on a horizontal surface, R_b and the ratio factor of diffuse radiation on a tilted surface to diffuse radiation on a horizontal surface, R_d. The values obtained for R_b and R_d are used in the meteorological data processing module.

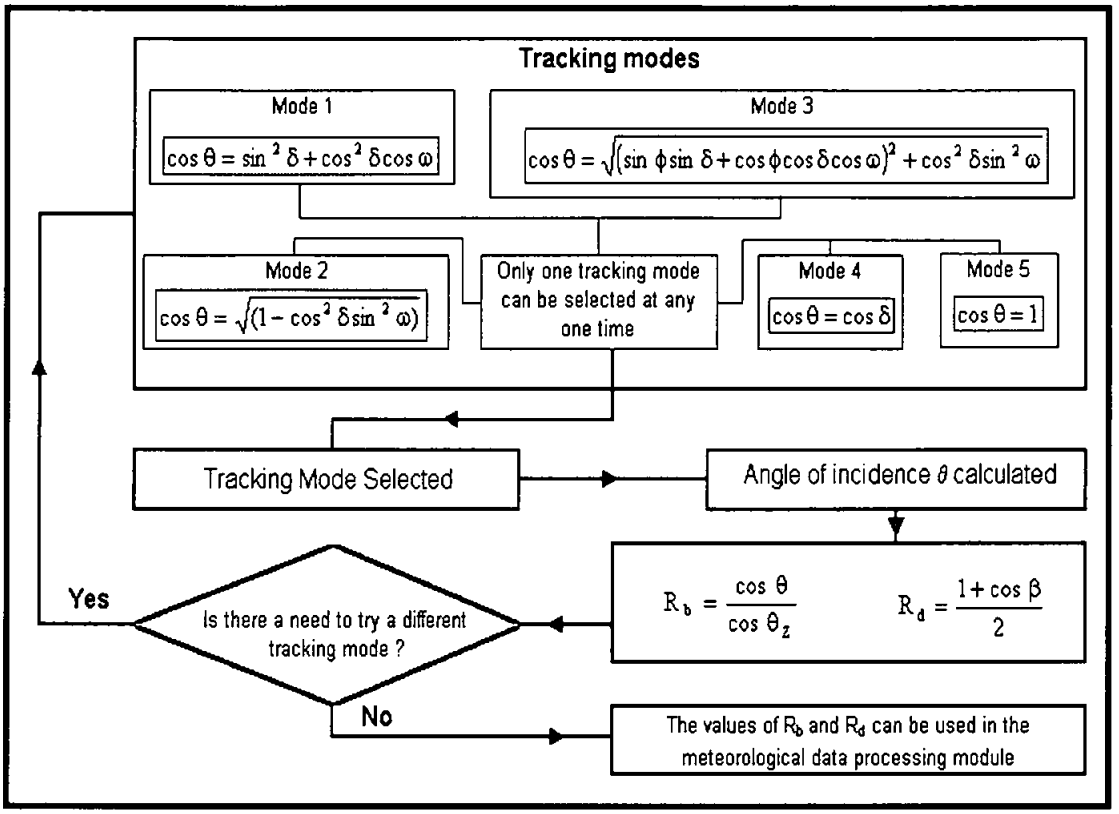

Figure 5.13 The tracking mode module flowchart that is used together with the meteorological data processing module.

5.3.5 THERMAL MODULE

The normal function of a concentrator is to reflect almost all the incidence solar radiation to concentrate at the focus point, or in this case the focus line. The thermal activities are usually associated with the heating up of the reflecting surface. The concentrator in this research work is made of iron, which is coated with an aluminised reflecting film. The main thermal module for the theoretical model developed in section 4.4 is given in Figure 5.14, and the output is the outlet temperature from the conduit tube of the receiver.

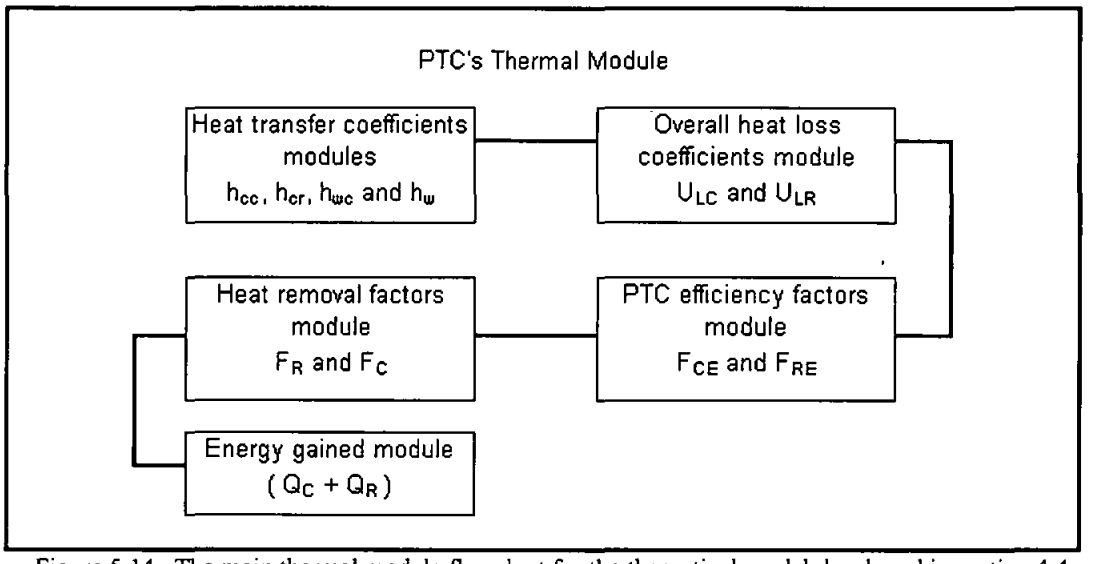

Figure 5.14 The main thermal module flowchart for the theoretical model developed in section 4.4.

5.3.6 OPTICAL MODULE

Optical module is considered an important module, as the main performance of a parabolic trough concentrator is related to the concentration of solar radiation to the focus line. The tracking mechanism is carefully monitored so that the parabolic trough will be facing the sun at all times. The module starts off with the proper design optics of the concentrator and the final result is related to a properly sized receiver that will be able to intercept most of the reflected rays. The optical module relies on the initial design module and a MATLAB program that incorporates its outcome is shown in Figure 5.15. It can be seen that once the width and depth data are input, at the push of "View My Design" tab, the graphical display of the parabolic trough concentrator is shown. Useful information pertaining to geometric concentration ratio, rim angle and efficiency are also given. These are considered as preliminary results as the actual simulation that incorporates all the information is not carried out yet. Therefore these results are useful for the optical analysis, as in the initial design module, no analysis of the concentration ratio is done. By using this design menu, all these information can be put together into the optical module.